1-1-2011

The process of autophagy in an in vitro model of myocardial ischemia-reperfusion injury

Kadija Abounit
Wayne State University,

THE PROCESS OF AUTOPHAGY IN AN *IN VITRO* MODEL OF MYOCARDIAL ISCHEMIA-REPERFUSION INJURY

by

KADIJA ABOUNIT

DISSERTATION

Submitted to the Graduate School

of Wayne State University,

Detroit, Michigan

in partial fulfillment of the requirements

for the degree of

DOCTOR OF PHILOSOPHY

2011

MAJOR: PHARMACOLOGY

Approved by:

_____

Advisor Date

_____

_____

_____

_____

DEDICATION

I dedicate this dissertation to my wonderful father and sisters. I am grateful to my father who taught me that hard work, commitment and patience always prevails. You all have been very supportive of me at all times. You gave the emotional strength and motivation to pursue this endeavor. I owe you all my achievements. Thank you so much and I love you with all my heart.

ACKNOWLEDGEMENTS

I would like to express my gratitude to my advisor and dear friend, Dr. Roy B. McCauley for his continued support, patience and encouragements. I will forever be grateful to him; he provided me with all the necessary tools to become a great scientist and the confidence to pursue my career goals. I feel very lucky and honored to have him as a mentor and friend. He has played a key role in my present success. I will always cherish the great moments I had with him and his wonderful wife.

I would like to thank Dr. Scarabelli for allowing me to complete my graduate studies in his laboratory, for that I am truly grateful.

I would like to thank the members of my dissertation committee: Drs. Stanley R. Terlecky, Raymond R. Mattingly and Paul M. Stemmer. Their advice, critiques and guidance allowed me to better myself and grow as a scientist. I would like to thank them for their continued support, understanding and kindness.

Sincere thanks to the Department of Pharmacology for their support (financial and other) and for making my journey so memorable. I feel really proud and lucky to have been part of this department as it has been, by far, the best environment I have worked in. I would like to thank the Graduate School; I could not have finished my dissertation work without their financial support.

Finally, thanks to my family and friends for their generous support and love.

TABLE OF CONTENTS

LIST OF FIGURES

CHAPTER 1 - INTRODUCTION

1.1. The Pathogenesis of Acute Myocardial Infarction

Acute myocardial infarction (AMI) results from a disruption of coronary blood flow to part of the heart, caused by the occlusion of a coronary artery. With an incidence of 935 in 100,000 persons leading to 141,462 deaths in 2006, AMI remains the principal cause of mortality in the United States. In addition, AMI is associated with a heavy financial burden. The American Heart Association estimates the cost of treating coronary heart disease related injuries at $165.4 billion for 2009 alone [1]. A prolonged ischemic event triggers several molecular and structural changes, which inevitably cause cardiac myocytes to be severely damaged or to die, further impairing myocardial function. Currently the treatment of AMI relies on reperfusion therapy based on inducing pharmacological (e.g. thrombolytics) and/or invasive reopening (e.g. angioplasty) of the occluded coronary artery. However, for the reperfusion therapy to be efficacious, it has to be started as soon as possible after the onset of ischemia [2]. If coronary flow is not re-established or is re-established after delay, post-ischemic cardiac cell loss and ventricular remodeling progress to heart failure in up to 40% of patients [3]. Paradoxically, the reintroduction of oxygen-rich blood to the ischemic tissue can have some deleterious effects, collectively referred to as “reperfusion injury”. Thus, the prevention of post-ischemic cardiac cell death may represent the best therapeutic modality to limit damage incurred by the myocardium.

During the past decades, extensive investigation has led to the development of cardioprotective therapeutic strategies against ischemia-reperfusion (I/R) injury. The description of ischemic pre-conditioning [4], where multiple brief periods of ischemia protect the myocardium from a subsequent sustained ischemic insult, had a major impact in the field of cardioprotection. This has led to the discovery of the phenomenon of ischemic post-conditioning,

where repetitive bouts of ischemia are applied at the onset of reperfusion, which was also shown to protect the heart from myocardial I/R injury [5]. Considerable advances have been made in identifying the molecular mechanisms that underlie the protection afforded by these strategies. This has opened new venues for the identification of novel therapeutic agents that mimic the cardioprotective effects of ischemic pre- and post-conditioning (pharmacological pre- and post-conditioning). In addition, pharmacological agents targeting key signaling effectors involved in the ischemic and reperfusion cascades have also been developed [6]. While the majority of these therapeutic strategies have proven to be efficient in protecting the heart against I/R injury in animal models, most of them have yielded disappointing results in clinical trials [7]. Despite these setbacks, new potential "druggable" targets for the clinical management of myocardial I/R injury keep emerging from the continued progress of our understanding of the pathogenesis of I/R injury.

At the clinical level, myocardial injury is characterized by myocardial stunning, arrhythmia, microvasculature dysfunction and myocardial cell death [8]. Myocardial cell death is governed by the complex biochemical cascades set in motion by both ischemia and reperfusion [9] (Figure 1). In cardiomycoytes, ischemia induces a rapid depletion of ATP, acidosis and a dysregulation of ion homeostasis (extracellular hyperkalemia, intracellular accumulation of Na^+, and cytosolic and mitochondrial build-up of Ca^{2+}). Depending on the severity of the ischemic insult and its duration, these events can lead to the disruption of the plasma membrane and irreversible injury. Reperfusion triggers multiple events in the ischemic myocardium. The restoration of blood flow aggravates the alterations of ionic fluxes induced by ischemia. The Ca^{2+} overload is exacerbated by the enhanced accumulation of Na^+. In addition, the reintroduction of oxygen triggers the production of reactive oxygen species (ROS).

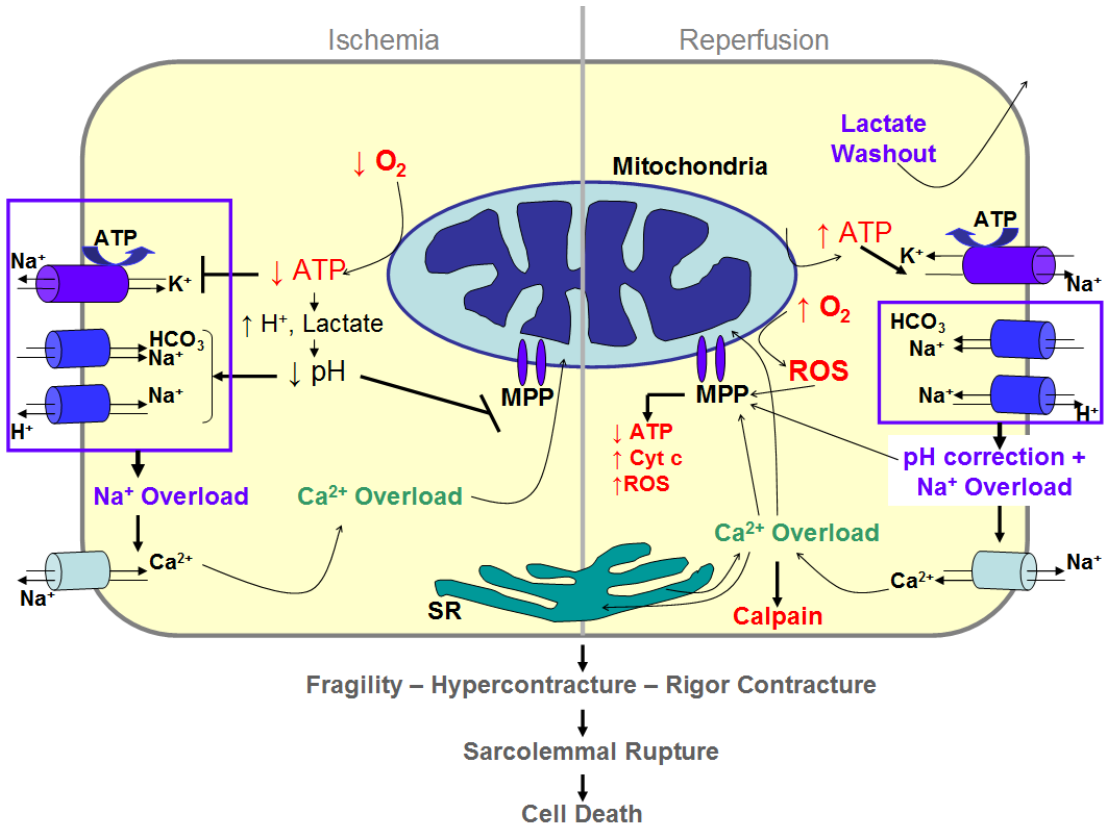

Figure 1: Cellular mechanisms of cardiac ischemia-reperfusion injury. The sequence of events elicited by ischemia include: ATP depletion, production of lactic acid, H^+ and CO_2 (anaerobic glycolysis) and acidification, overload of Na^+ (Na^+/H^+ exchanger and inhibition of the Na^+/K^+ ATPase pump), build-up of Ca^{2+} in the cytosol and mitochondria (reversal of Na^+/Ca^{2+} exchanger). In turn, reperfusion promotes the production of reactive oxygen species (ROS), restoration of a physiological pH (wash out of lactic acid, H^+ and activation of Na^+/H^+ exchanger and Na^+/HCO_3^- transporter), Ca^{2+} overload in cytosol, mitochondria and sarcoplasmic reticulum (reversal of Na^+/Ca^{2+} exchanger), restoration of ATP production and opening of the mitochondria permeability pore (MPP) (oxidative stress, normal pH, Ca^{2+} overload). The morphological changes induced by I/R include: (i) cytoskeleton fragility, caused by the degradation of α-fodrin mediated by Ca^{2+}-activated calpain, (ii) hypercontracture, which is caused by the ATP/cytosolic Ca^{2+} overload combination and can spread to adjacent cells, and (iii) rigor-contracture, which occurs when the ATP level is low (a slow ATP production recovery or damaged mitochondria). In addition, the opening of the MPP leads to loss of ATP, damage to the mitochondria, release of ROS and cytochrome c in the cytoplasm. Collectively, these events result in the physical disruption of the sarcolemma and cell death.

In parallel, oxidative stress, Ca^{2+} overload and the renormalization of the pH promote the opening of the mitochondrial permeability transition pore (MPP). This phenomenon results in the loss of the structural integrity and function of the mitochondria, ATP depletion, release of ROS and cytochrome c into the cytoplasm. The biochemical alterations elicited by ischemia-reperfusion have major repercussions on the morphology of cardiac cells [10]. The recovery of ATP production combined with an elevated intracellular level of Ca^{2+} provokes excessive myofibrillary contractility (hypercontracture). This mechanical stress was shown to propagate to adjacent myocytes through gap junctions and to contribute to the final size of the infarct [11]. In addition, hypercontracture is enhanced by the cell fragility caused by the calpain-mediated degradation of α-fodrin, a key constituent of the membrane cytoskeleton [12,13]. The activation of calpain proteases requires Ca^{2+} and is repressed by acidic pH. The excessive activation of calpains occurs primarily during reperfusion when the level of Ca^{2+} is abnormally elevated and the pH is renormalized. These morphological changes collectively lead to the disruption of the sarcolemma and cell death.

Myocardial injury can progress along two distinct cell death pathways - necrosis and apoptosis [14]. Necrosis develops in response to lethal exogenous stimuli under pathological conditions. Necrotic cell death is characterized by cell swelling, rupture of the cell membrane with release of cellular components (creatine kinase, troponin) and subsequent inflammation. In contrast, apoptosis (programmed cell death type I) can be triggered in response to physiological or pathological stimuli that are endogenous or exogenous to the cell. Apoptosis is an ATP-dependent process that progresses through a well-orchestrated series of molecular, biochemical, and morphological events that do not provoke an inflammatory response. The relative contribution of necrosis and apoptosis to the total cardiac cell loss following both ischemia and

reperfusion is not well established. The degree of ATP depletion appears to be a determinant factor in the mode of death that injured myocytes will undergo [15]. In the infarct core, which is completely deprived in oxygen and energy, myocytes die by necrosis. In contrast, in the peri-infarct penumbra which is hypoxic, myocardial cell death occurs via both apoptosis and necrosis [16]. Necrosis represents the predominant mechanism of myocyte death during ischemia. However, the occurrence of this process was also observed during the reperfusion phase. The presence of necrotic cells was detected in the infarct early following the restoration of blood flow but also 24 hours post-reperfusion. Also, apoptosis has been reported to occur in the majority of the injured rat cardiomyocytes during the first hours after coronary occlusion (i.e. ischemia) [17]. Conversely, Gottlieb and colleagues have observed the presence of apoptotic cells in reperfused but not in ischemic rabbit hearts [18]. Interestingly, evidence also pointed to a step-wise progression of the apoptotic program where apoptosis could be initiated during ischemia and completed during reperfusion [19-21]. The discrepancy in these findings may be due to the wide variety of experimental models. Each model has different technical limitations in its ability to estimate the incidence and timing of necrosis and apoptosis [22]. The picture of myocardial cell death was further complicated by the observation that autophagy is involved in the pathogenesis of myocardial I/R injury.

1.2. The Process of Autophagy and its Significance in the Heart

Macroautophagy (hereafter autophagy) is an evolutionarily conserved catabolic process that targets dysfunctional or damaged cytoplasmic constituents to the lysosome for degradation and recycling. Autophagy occurs constitutively in all eukaryotic cells where it operates as a metabolic homeostatic mechanism [23]. Autophagy can be further activated in response to various physiological and pathological stimuli to either promote cell survival (e.g. starvation,

oxidative stress [24]), or to act as a mode of cell death, type II programmed cell death (e.g. during development) [25]. Autophagy progresses through several steps orchestrated by a set of molecular effectors, the autophagy related genes (Atg) proteins (Figure 2). Upon induction, autophagy starts with the appearance of a small isolation membrane, the phagophore, which engulfs parts of the cytoplasm and elongates to form a double-membrane vesicle called the autophagosome. The latter undergoes a maturation process and ultimately fuses with a lysosome to form the autophagic vacuole (or autolysosome). The vesicular contents is degraded by lysosomal hydrolases, thereby providing the cell with a new source of amino acids, lipids and sugars for energy production. The formation of the autophagosome is initiated by the class III phosphoinositide 3-kinase (PI3-K) protein complex that includes Beclin 1 (Atg6) and involves two ubiquitin-like conjugation systems which result in the formation of Atg5-Atg12 and LC3-phosphatidylethanolamine (LC3-II) [26]. While the molecular mechanisms involved in each step of the autophagic process are well understood, a debate persists in the field over the origin of the phagophore. The endoplasmic reticulum (ER), the trans golgi network (TGN) and the mitochondria have been proposed as possible sources of autophagosomal membranes [27]. A recent study has provided strong evidence that in normal rat kidney cells, the autophagosomal membranes originate from the outer membrane of mitochondria during starvation but not under ER-stress conditions [28]. Whether this phenomenon can be observed in other cell types and under other stress conditions such as ischemia, awaits further studies. Nonetheless, this study has unraveled a new interplay between autophagy and the mitochondrion.

Autophagy is under the control of multiple signaling pathways [29] (Figure 3). The kinase mTOR (mammalian Target Of Rapamycin) is a key modulator of autophagy. mTOR is a sensor of nutrients and is repressed under conditions of nutrient deprivation and hypoxia.

Repression of mTOR promotes increased autophagic activity. mTOR receives multiple inputs from metabolic processes and growth factors. Under conditions of growth, mTOR activity is enhanced by factors that activate the class I PI3-K/Akt pathway, which inhibits TSC1/TSC2 and finally increases the activity of Rheb, a GTPase required for mTOR activity. The stimulation of this cascade results in the inhibition of autophagy. mTOR is also regulated by the adenosine monophosphate-activated protein kinase (AMPK), a sensor of the intracellular AMP/ATP ratio. AMPK is activated in response to elevated intracellular content of AMP caused by ATP hydrolysis. AMPK represses mTOR activity leading to activation of autophagy. Autophagy is modulated by other signaling pathways that are independent of mTOR. Zhang and colleagues have demonstrated that prolonged hypoxia induced mitophagy to promote mouse embryonic fibroblasts (MEF) survival. This process was mediated via activation of hypoxia inducible factor 1α (HIF-1α) and required the presence of BNIP3 and autophagy proteins including Beclin 1 and Atg5 [30]. A recent study has shown that under starvation conditions, the p110-β catalytic subunit of the Class I PI3-K could directly promote the stimulation of autophagy in MEF, in the liver and heart through its association with the Class III PI3-K initiation complex. This autophagy-promoting role of p110-β was independent of its kinase activity and Akt activation [31]. Depnding on the downstream target, the growth factor-mediated activation of the Ras signaling pathway either activates or inhibits autophagy. In NIH3T3 mouse fibroblasts, activation of the Class I PI3-K cascade by Ras results in inhibition of autophagy [32]. In contrast, the Ras-mediated activation of the Raf-1–MEK1/2–ERK1/2 signaling cascade in response to amino acid depletion promotes autophagy [33]. Finally, DAPk and DRP-1, two members of the Ca^{2+}/calmodulin-regulated Serine/Threonine death kinases family, were found to be necessary for the induction of autophagic programmed cell death (type II) in HeLa and MCF-7 cancer cells

subjected to multiple stimuli including amino acids depletion [34]. In a recent study, DAPk was shown to promote the initiation of autophagy by phosphorylating Beclin 1, which is subsequently released from the pro-apoptotic Bcl-2/Bcl-X_L complex [35,36].

Autophagy plays a crucial role in the heart [37]. The occurrence of autophagy in cardiac myocytes was reported for the first time in 1976 by Sybers and co-workers [38]. Because cardiac myocytes are terminally differentiated and unable to renew themselves, they rely on autophagy to maintain their viability and functionality. Cardiac myocytes have a high requirement in energy (ATP) which is reflected in an abundance of mitochondria. Mitophagy, a process responsible for the removal of damaged and dysfunctional mitochondria through autophagy, represents a key mechanism in the survival of cardiomyocytes. The presence of mitochondria in autophagosomes in cardiomyocytes exposed to various stress conditions was reported by several groups [38-40]. The significance of the autophagic process in the healthy heart has also been emphasized in several studies. A defect in the degradation phase of autophagy, resulting from a deficiency of LAMP2, a lysosomal membrane protein, induced severe cardiac dysfunction in patients and mice [41,42]. Most importantly, the deficiency in Atg5 expression in the heart of adult mice resulted in the development of cardiac hypertrophy, left ventricular dilation and contractile dysfunction [43]. Autophagy has been shown to be altered in various cardiac pathologies including myocardial hypertrophy, cardiomyopathies, and ischemic heart disease [44]. However, the role played by autophagy in the pathogenesis of these conditions is not clearly established.

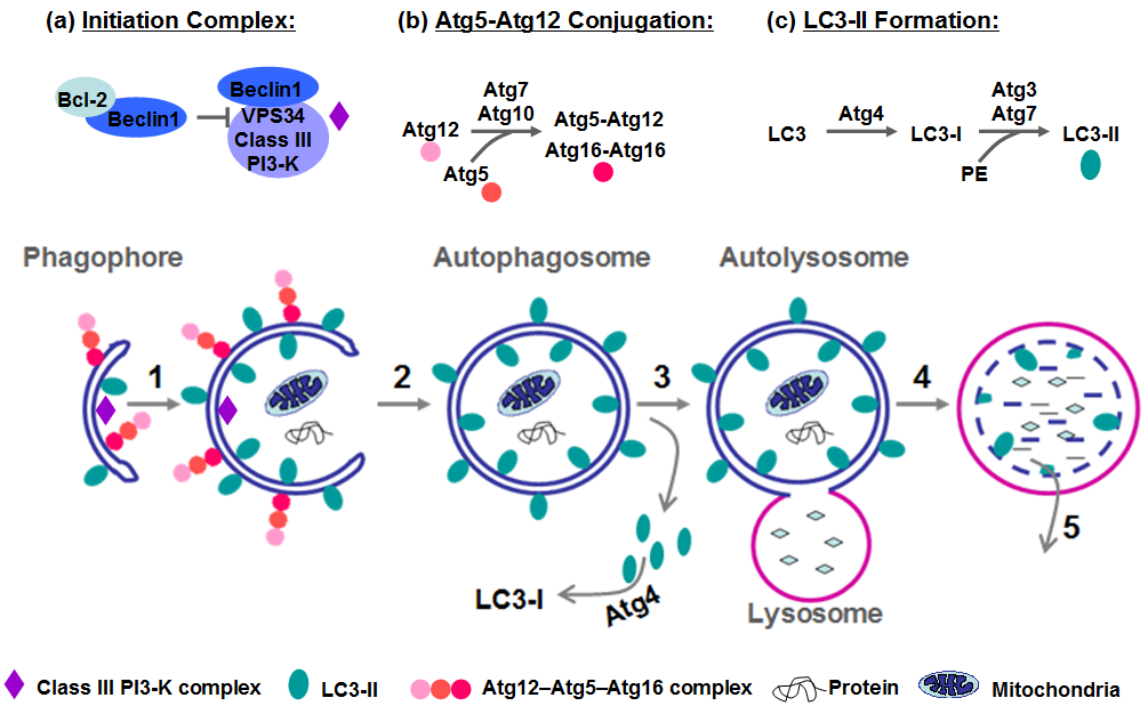

Figure 2: The process of autophagy. Autophagy is initiated with the formation of the phagophore, mediated by the class III PI3-K complex that includes Vps34, Vps15, Atg14 and Beclin 1 (**a**) and progresses through a succession of steps: (**1**) elongation of the phagophore and engulfment of cytoplasmic material targeted for degradation, (**2**) formation of the autophagosome, with delipidation of LC3-II by Atg4, (**3**) fusion of the autophagosome with the lysosome to form the autolysosome, (**4**) degradation of the vesicle content by lysosomal hydrolases and (**5**) recycling of the degradation products (amino acids, lipids and sugars) for ATP production. The autophagy machinery consists of two conjugation systems required for the elongation and extension of the phagophore: Atg5-Atg12, which subsequently oligomerizes with Atg16 (**b**), and LC3-phosphtidylethanolamine**,** LC3-II. LC3-II is formed as a result of the Atg4-mediated cleavage of cytosolic LC3. The resulting form of LC3, LC3-I is subsequently conjugated to a single phosphatidylethanolamine (PE) molecule to form LC3-II, a reaction mediated by Atg3 and Atg7 (**c**).

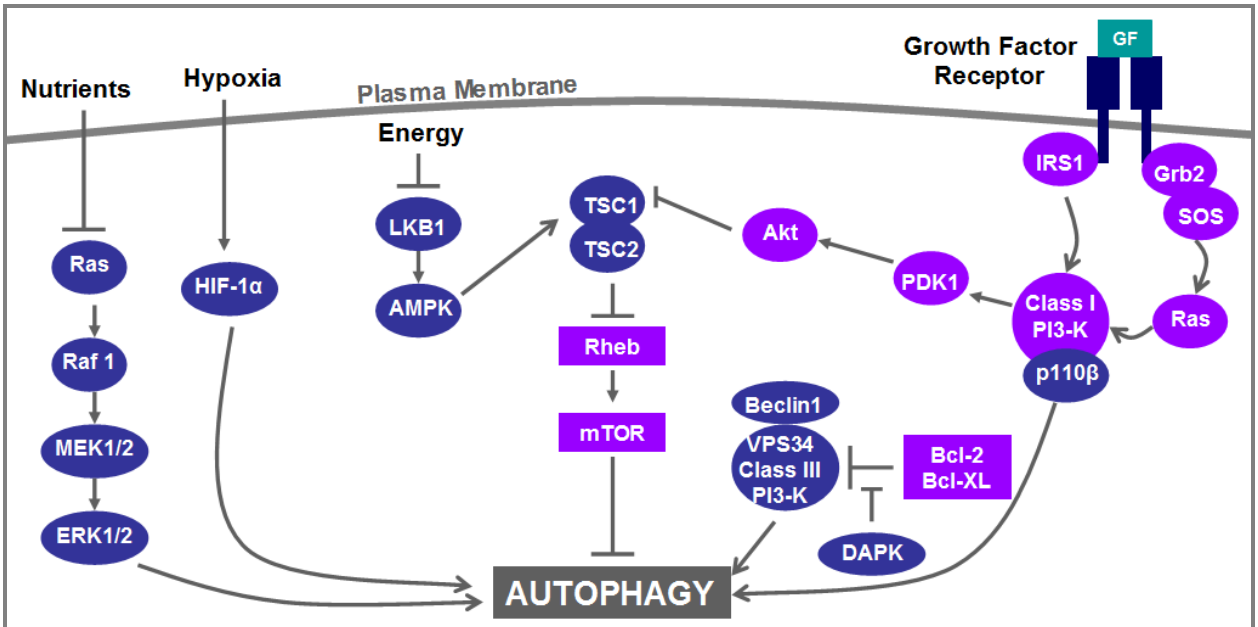

Figure 3: The regulation of autophagy Autophagy is regulated by multiple signaling pathways. In response to growth factors, mTOR is activated by the class I PI3-K and Akt, which inhibits TSC1/TSC2. The activation of this cascade leads to the inhibition of autophagy. mTOR activity is inhibited by AMPK, a kinase activated in response to elevated intracellular AMP/ATP ratio. In addition, the p110-β catalytic subunit of the class I PI3-K can directly stimulate autophagy during starvation, independently of Akt activation, through its association with the Class III PI3-K complex. The growth factor-mediated activation of Ras induces antagonistic effects on autophagy depending on its downstream target – while the activation of the Class I PI3-K cascade represses autophagy, the stimulation of the Raf-1–MEK1/2–ERK1/2 signaling cascade in response to amino acid depletion promotes autophagy. Hypoxia induces autophagy via activation of the hypoxia-inducible factor 1α (HIF-1α). Finally, autophagy is also regulated by the DAPk, which promotes the initiation of autophagy through the release of Beclin 1 from the Bcl-2/Bcl-X_L complex. The DAPk-related protein kinase 1 (DRP-1) was also found to be necessary for the induction of autophagy.

1.3. Autophagy in Myocardial Ischemia-Reperfusion Injury

The modulation and the role of autophagy during myocardial I/R injury have been extensively investigated. An increase in autophagosomes in cardiomyocytes following I/R injury has been reported by several groups and became a hallmark of myocardial I/R injury. However, the nature of the role of autophagy during myocardial I/R injury is highly controversial. Presently, autophagy is portrayed either as a cardioprotective mechanism or a contributor to cell death. The conflicting findings regarding the function of autophagy may stem from several experimental parameters. The process of autophagy has been investigated in multiple experimental models (*in vitro, ex vivo* and *in vivo*) and species (rat, pig, rabbit and mouse). As the degree of complexity of the model increases, it becomes virtually impossible to extrapolate results obtained from cultured cells to isolated hearts to the intact heart. Additional variables such as the intensity/duration of the ischemic insult and the methodology used to assess the occurrence and the function of autophagy may further complicate the picture.

A large array of data has been obtained from *in vivo* studies carried out in rodent and swine models of myocardial I/R injury. In a swine model of chronic myocardial stunning, Yan and co-workers [45] observed an increase in autophagy in the heart of pigs subjected to six episodes of ischemia and subsequent reperfusion. An inverse correlation between the occurrence of autophagy and apoptosis was reported. In their study, Matsui et al. [46] have reported an induction of autophagy in the hearts of mice subjected to 20 minutes of global ischemia. Furthermore, autophagy was enhanced after 20 minutes of reperfusion. The use of beclin $1^{+/-}$ mice allowed them to demonstrate that autophagy plays opposite roles during I/R injury. That is autophagy protected the heart during ischemia and promoted myocyte death during reperfusion and these effects were mediated by AMPK and Beclin 1, respectively. In the same line of

evidence, Noh and co-workers [47] have recently shown that autophagy was also enhanced in the hearts of rats subjected to 25 minutes of global ischemia followed by 24 hours of reperfusion. In this study, the administration of propofol, an intravenous anesthetic drug, during I/R reduced both the myocardial infarct size and the level of autophagy. This result suggested that autophagy was detrimental during myocardial I/ R injury. In most of the aforementioned studies, autophagy was found to be enhanced in the hearts of animals following both phases of I/R injury. In a recent study, French and colleagues [48] have reported the absence of autophagic structures in the infarcted zones of hearts from transgenic GFP-LC3 mice subjected to persistent ischemia (24 hours) or to ischemia (1, 4 hours) followed by 24 hours of reperfusion. In addition, the level of autophagosomes was reduced in the peri-infarct zones of ischemic hearts. The reduction in autophagy was further evidenced by a decrease in the LC3-II/LC3-I ratio and an up-regulation of mTOR activity in myocytes. To gain some insights into the role played by autophagy during myocardial I/R injury, the investigators used drugs that mimic the protective action of pre-conditioning such as hydrogen sulfide (an endogenous gasotransmitter) and chloramphenicol succinate (an inhibitor of cytochrome P450 monooxygenase**,** mitochondrial protein synthesis, and a bacteriostatic antimicrobial). The data derived from these studies were inconsistent. The infusion of hydrogen sulfide during I/R reduced the myocardial infarct size in pigs. This effect was accompanied by a decrease in mTOR activation and Beclin 1 expression in myocytes [49]. The administration of chloramphenicol succinate as a pre-treatment or during reperfusion protected the pig heart from I/R injury. In contrast, the cardioprotective effect of chloramphenicol succinate was associated with an increase in the expression of LC3-II and Beclin 1 [50].

Autophagy has also been studied in isolated hearts. In 1980, Decker and colleagues reported an induction of autophagy in Langendorff perfused rabbit hearts subjected to both ischemia and reperfusion. The majority of cardiac myocytes from rabbit hearts subjected to 1 hour of ischemia and 1 hour of reperfusion was irreversibly injured and contained non-functional lysosomes. On the other hand, shorter periods of ischemia (20 and 40 minutes) followed by 1 hour of reperfusion resulted in an improved contractility of cardiac myocytes concomitant with an increased presence of autophagic vacuoles. In this study, the increase in autophagy correlated with functional recovery and salvage of the myocardium after I/R, suggesting a cardioprotective role of autophagy against I/R injury [39,51]. The effect of cardioprotective drugs on the autophagic response elicited by I/R in isolated hearts was also investigated. For example, sulphaphenazole (an inhibitor of cytochrome P450 monooxygenase and an antimicrobial agent) pre-treatment of rat hearts subjected to 30 minutes of ischemia and 2 hours of reperfusion reduced the infarct size and increased autophagy. Using the same model, several groups have shown that pre-treatment with small doses of resveratrol alone or in combination with γ-tocotrienol, or Longevinex (a modified resveratrol) protected the heart against I/R injury. The cardioprotection afforded by these treatments was associated with an up-regulation of autophagy [52-54].

A large body of experimental work demonstrating the involvement of autophagy in the pathogenesis of I/R injury has been carried out in cultured cardiac cells. These efforts have been directed towards the development of experimental conditions that recapitulate the changes (extra- and intra-cellular) elicited in the heart by ischemia. Thus, the model of simulated ischemia-reperfusion (sI/R) has been used by several groups and it has been valuable in identifying key biochemical and cellular events underlying the pathogenesis of myocardial I/R

injury. According to the experimental context, this basic model can differ in several aspects: the use and formulation of the “ischemia buffer”, the level of oxygen (anoxia, hypoxia), the duration of ischemia and reperfusion, and the cellular model (primary cultures of isolated neonatal or adult cardiac myocytes, immortalized cardiac cell lines such as HL-1). Valentim et al. have reported that autophagy can contribute to the demise of cardiac cells following sI/R injury. They observed an increase in autophagosomes (acidic vacuoles positively marked for monodansylcadaverine or lysotracker) in primary cultures of both neonatal and adult rat cardiomyocytes exposed to 4 hours of simulated ischemia (2.0% O_2) followed by 16 hours of reperfusion. Inhibition of autophagy achieved by treatment with 3-methyladenine (3-MA) an inhibitor of autophagy by inhibition of PI3 kinases [55] or down-regulation of Beclin 1 reduced both the percentage of myocytes undergoing autophagy and cell death after sI/R [56]. In contrast, Hamacher-Brady and colleagues have examined the effect of sI/R on autophagy and shown its cardioprotective effect against sI/R on several occasions [57,58]. They have demonstrated that HL-1 cells exposed to 2 hours of simulated ischemia, achieved by incubating HL-1 cells in an “ischemia buffer” in the absence of oxygen, exhibited a low level of autophagy. The subsequent reperfusion of ischemic cardiac cells induced a partial reactivation of the autophagic process evidenced by the increase in autophagosomes after 1.5 and 3 hours. Treatments with either 3-MA or wortmannin, down-regulation of Beclin 1 or over-expression of $Atg5^{K130R}$ (a dominant negative mutant of Atg5) sensitized HL-1 cardiac cells to sI/R-induced apoptotic cell death. In addition, 2-chloro-*N*(6)-cyclopentyl adenosine (CCPA), a selective agonist of the adenosine receptor A1 that has cardioprotective properties, attenuated sI/R-induced cell death**,** presumably, through induction of autophagy.

1.4. Sildenafil and Myocardial Ischemia-Reperfusion Injury

Numerous studies carried out in animal models of I/R injury have demonstrated the cardioprotective action of sildenafil citrate. Sildenafil (Viagra) is a potent and selective inhibitor of cGMP specific phosphodiesterase-5 (PDE5) and is currently licensed for the treatment of erectile dysfunction and pulmonary hypertension. PDE5 catalyzes the degradation of cyclic guanosine monophosphate (cGMP) and its inhibition by sildenafil enhances cGMP accumulation, which, in turn, causes vasodilatation in the corpus cavernosum. PDE5 is highly expressed in a large variety of tissues including platelets and smooth muscle of the systemic vasculature [59]. Although the expression of PDE5 in canine and mouse hearts has been reported, it is not clear whether PDE5 is present in human cardiomyocytes. Several studies have documented potent, acute and delayed cardioprotection afforded by sildenafil in *in vitro*, *ex vivo* and *in vivo* models of myocardial I/R injury [60]. This PDE5 inhibitor was shown to attenuate cardiac I/R injury through several mechanisms (Figure 4) including: (i) enhancement of nitric oxide (NO) generation resulting from increased expression of endothelial/inducible nitric oxide synthase (eNOS/iNOS) [61], (ii) activation of protein kinase C (PKC) which is translocated from the cytosol to the plasma membrane [62], (iii) opening of mitochondrial K_{ATP} channels [63], (iv) preservation of the mitochondrial membrane potential and NO-dependent up-regulation of Bcl2/Bax ratio [64], and (v) activation of cGMP-dependent protein kinase G (PKG) [65]. Sildenafil has also been shown to mediate its cardioprotective effect via up-regulation of ERK1/2 phosphorylation, which was shown to occur in a PKG-dependent manner. Moreover, it has been reported that ERK1/2 mediates sildenafil-induced up-regulation of iNOS/eNOS, Bcl-2 and inactivation of glycogen synthase kinase 3β (GSK3β) [66]. In addition, a recent study has shown that the administration of sildenafil during the first 10 minutes of reperfusion after 30 minutes of

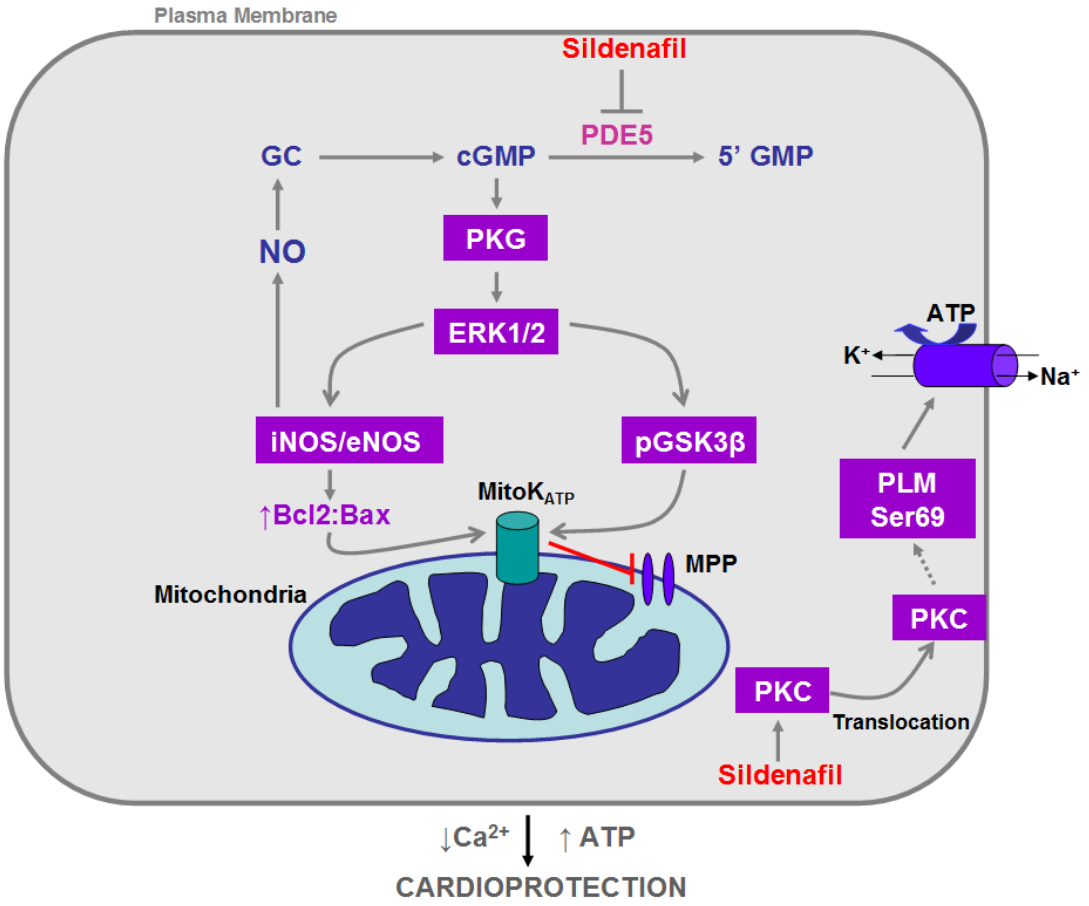

Figure 4: Mechanisms of cardioprotection by sildenafil. Sildenafil inhibits the phosphodiesterase-5 (PDE5), which catalyzes the degradation of cyclic guanosine monophosphate (cGMP), resulting in the accumulation of cGMP in the cell. The cardioprotection afforded by sildenafil against I/R injury is mediated by several mechanisms. The activation of cGMP-dependent protein kinase G (PKG) mediates the upregulation of ERK1/2 activity, which in turn can lead to the upregulation of iNOS/eNOS, Bcl-2 and inactivation of glycogen synthase kinase 3β (GSK3β). The activation of the mitochondrial K_{ATP} channels mediated by Bcl-2 and GSK3β can prevent the opening of the mitochondrial permeability transition pore (MPP), thereby preserving the mitochondrial membrane potential. In parallel, sildenafil can induce the activation of protein kinase C (PKC) which is translocated from the cytosol to the plasma membrane. In addition, sildenafil triggers the phosphorylation of phospholemman (PLM) at position Ser69, which leads to the activation of its downstream target, the Na^+/K^+-ATPase in a PKC-dependent manner. These effects limit the ATP depletion and the influx of calcium in the cell, two major contributors of cell injury.

global ischemia protected isolated mouse hearts against infarction. This effect was shown to be mediated by the phosphorylation of phospholemman (PLM), a type 1 transmembrane protein, at position serine 69, which leads to the activation of its downstream target, the Na^+/K^+-ATPase in a PKC-dependent manner [67]. While sildenafil has been previously shown to reduce necrotic and apoptotic cardiac cell death induced by I/R, its effect on autophagy and the associated underlying signaling mechanism have never been investigated.

1.5. Specific Aims

The experiments described in this dissertation were designed to clearly establish the relationship between autophagy and myocardial injury. The central hypothesis is that autophagy is a beneficial process in cardiomyocytes and that the paucity of ATP may limit its occurrence during I/R. To test this hypothesis, it was necessary to develop a valid *in vitro* model of myocardial I/R injury, referred to as Hypoxia-Reoxygenation. In our model, ischemia ("hypoxia") was mimicked by incubating murine atrial-derived HL-1 myocytes [68] in an ischemia buffer in presence of two different concentrations of oxygen – 0.5% and 2.0%. Reperfusion ("reoxygenation") was achieved by restoring normal conditions of growth. Thus, our primary objective was to determine whether our model recapitulated the cellular events encountered in the ischemic myocardium. Consistent with this, we have focused on establishing the bioenergetic status of HL-1 cells following both ischemia and reperfusion. ATP depletion is a key feature of ischemia and is caused by the inhibition of the mitochondrial metabolic processes (oxidative phosphorylation and glycolysis) owing to the lack of oxygen. Although, reperfusion reactivates the production of ATP in the ischemic myocyte, the replenishment of ATP stores can be hampered by damage to the mitochondria elicited during reperfusion. In addition, the degree of ATP depletion is a determining factor in the mode of cell death that injured myocytes will

undergo. Accordingly, it was also essential to estimate cell death as an index of the validity of our model. The second objective of this project was to study the modulation and role of autophagy in HL-1 cardiomyocytes during ischemia alone or followed by reperfusion. Finally, this model was used to test the effect of sildenafil citrate, a cardioprotective agent, on the alterations of autophagy elicited by both I/R.

CHAPTER 2 – MATERIALS AND EXPERIMENTAL METHODS

2.1. Materials

The Claycomb medium, fibronectin, fetal bovine serum (FBS), norepinephrine, 2-deoxyglucose, 3-methyladenine, aprotinin, phenylmethylsulfonyl fluoride (PMSF), bovine serum albumin and all of the chemicals not otherwise stated were from Sigma-Aldrich. L-glutamine, antibiotics, trypsin, 1X phosphate-buffered Saline (PBS) and 0.4% Trypan blue were obtained from Invitrogen. Okadaic acid, pepstatin, leupeptin, E64d, bafilomycin A1, pepstatin A methyl ester and cell-permeant E64d (EST) were all purchased from Calbiochem. Sildenafil citrate was kindly provided by Pfizer. The bicinchoninic acid (BCA) protein assay kit and the West-Pico chemiluminescence detection system were purchased from Pierce. The ATPlite assay kit was acquired from PerkinElmer Life Sciences. The Trans-Blot pure nitrocellulose membrane, 30% acrylamide/bisacrylamide solution, 10X Tris Buffered Saline (TBS), 10X Tris-Glycine-SDS, 10X Tris-Glycine electrophoresis buffers and the precision plus protein kaleidoscope standards were all purchased from Bio-Rad Laboratories.

The following antibodies were used for western blot analysis: rabbit anti-LC3 (1:2,500) was a gift of Dr. David Kessel (Wayne State University); rabbit anti-pan Akt (1:3,000), rabbit anti-phospho-Akt Ser473 (1:2,000), rabbit anti-mTOR (1:2,000), rabbit anti-phospho-mTOR Ser2448 (1:500), rabbit anti-AMPKα (1:1,000), rabbit anti-phospho-AMPKα Thr172 (1:2,000) were all purchased from Cell Signaling Technology; goat anti-actin (1:500), rabbit anti-ERK1 (1:1,000), mouse anti-phospho ERK (1:1,000), rabbit anti-beclin 1 (1:2,000), rabbit anti-PDE5a (1:1,000) and the horseradish peroxidase (HRP)-labeled goat anti-rabbit (1:2,000), goat anti-mouse (1:1,000) and donkey anti-goat (1:2,000) secondary antibodies were all purchased from

Santa Cruz Biotechnologies, Inc. All antibodies used for Western blot analyses were characterized for their specificity and optimal concentration.

2.2. HL-1 Cell Culture Conditions

The immortalized murine atrial derived-HL-1 cardiac cell line was a gift of Dr. Claycomb (Louisiana State University) [68]. The cells were maintained in Claycomb medium supplemented with 10% fetal bovine serum (FBS), 0.1 mM norepinephrine, 2 mM L-glutamine and 100 units/mL penicillin/streptomycin. Cell cultures were maintained in a humidified incubator at 37°C in an atmosphere of 5% CO_2/95% air and sub-cultured (1:3 ratio) every 3 days. Flasks and Petri dishes used for HL-1 cell culture were pre-coated overnight at 37°C with sterilized 0.02% gelatin and 0.1% fibronectin (200:1)

2.3. Hypoxia-Reoxygenation Model

For simulation of ischemia, the medium of HL-1 cardiomyocytes was replaced with the ischemia buffer (118 mM NaCl, 1 mM NaH_2PO_4, 16 mM KCl, 2.5 mM $CaCl{\bullet}2H_2O$, 24 mM $NaHCO_3$, 20 mM HEPES, 10 mM 2-deoxyglucose, and 20 mM sodium lactate, pH 6.8). This buffer was derived from the Esumi ischemia buffer [69] and was formulated to mimic the extracellular environment and the reduced intracellular energy state that occur in ischemic myocardium *in vivo*. The buffer contains 2-deoxyglucose, a glucose analogue unable to undergo glycolysis, which ultimately inhibits cellular metabolism. In addition, the buffer contains a high concentration of potassium (mimicking extracellular hyperkalemia) and has an acidic pH. To induce hypoxia, the cells were transferred to a sealed chamber placed in humidified incubator at 37 °C in an atmosphere of 0.5% or 2.0% O_2, 5% CO_2 balanced with N_2 for the time indicated.

The levels of O_2 and CO_2 present in the chamber were controlled by the OxyCycler (model C-40, BioSpherix, Ltd.) which sits outside the incubator and is attached to the chamber by umbilicals with actuator pods on the ends. The OxyCycler remotely senses the O_2 concentration in the chamber and infuses N_2 to lower concentration to reach the setpoint.

After completion of the ischemic treatment, HL-1 cells were washed twice with PBS and complete growth medium was added to the cells. The ischemic cardiac cultures were returned to a humidified incubator at 37°C in an atmosphere of 5% CO_2/95% air for the indicated period of reoxygenation to simulate reperfusion.

2.4. Preparation of Cellular Extracts

HL-1 cells were washed twice with ice-cold PBS and scraped while the dish was held on ice into RIPA buffer (50 mM Tris, 150 mM NaCl, 1 mM EDTA, 1% NP-40 and 0.25% sodium deoxycholate, pH 7.4) containing inhibitors of phosphatases and proteases (1 mM PMSF, 1 mM sodium orthovanadate, 1 mM sodium fluoride, 50 nM okadaic acid, 10 µg/mL aprotinin, 5 µg/mL pepstatin, 10 µg/mL leupeptin and 5 µg/mL E64d). The cell suspension was incubated for 15 min on ice. Insoluble material was removed by centrifugation at 14,000 rpm for 10 min. The resulting whole cell lysate was transferred to fresh tubes and kept on ice for immediate use or placed at -80°C for longer storage. Protein concentrations were determined using the BCA protein assay.

2.5. Western Blot Analysis

Sodium Dodecyl Sulfate (SDS) loading buffer was added to 40 µg of HL-1 cellular extract. The samples were heated for 5 min at 95°C and resolved by SDS-polyacrylamide gel

electrophoresis (PAGE). The profile of LC3 processing was determined by SDS-18% PAGE. The detection of mTOR (total and phosphorylated form) was performed with 7% gels. SDS-10% polyacrylamide gels were used to detect all other proteins. The fractionated proteins were transferred to nitrocellulose membrane in 25 mM Tris-HCl, 192 mM glycine and 20% methanol at 100V for 40 min to 105 min. Nonspecific binding sites were blocked with 5 % non-fat dry milk in TBS-T (20 mM Tris-HCl, pH 7.5, 500 mM NaCl, and 0.1% (v/v) Tween-20) for 1 hour at room temperature or overnight at 4°C. The membrane was washed twice with TBS-T and incubated with the primary antibody diluted in TBS-T for 1 hour at room temperature with shaking. The excess antibody was removed by washing the membrane with TBS-T three times for 5 min at room temperature. The immunoblot was incubated with the appropriate horseradish peroxidase labeled secondary antibody, diluted in TBS-T containing 5% non-fat dry milk, for 1 hour at room temperature with shaking. The membrane was then washed three times for 5 min at room temperature. The West-Pico chemiluminescence detection system was used to visualize the immunoreactive bands by autoradiography, according to the manufacturer's instructions. The autoradiographic films were scanned using an Epson photoscanner and protein band intensities were analyzed by densitometry and quantified using the free open source software ImageJ (http://rsb.info.nih.gov//ij/). The level of expression of the protein of interest was normalized to the level of actin or β-tubulin (loading control).

2.6. Autophagy Assessment

Autophagy was assessed by measuring the endogenous level of LC3-II by Western blotting. In higher eukaryotes, LC3-II is the only known protein that specifically associates with autophagosomes and autolysosomes and is therefore commonly used as a marker of autophagy

[70]. Upon activation of autophagy, LC3 is cleaved at its C-terminus by Atg4 to yield LC3-I, which is subsequently conjugated to a single phosphatidylethanolamine (PE) lipid molecule to form LC3-II. The latter is relocated to the membrane of the autophagosomes that fuse with the lysosomes. LC3-II is found at the luminal and cytosolic surfaces of autophagosomes. While the luminal pool is degraded after fusion with the lysosome, cytosolic LC3-II can be delipidated and recycled. Although both forms of LC3 have almost the same molecular weight, their electrophoretic properties differ. LC3-II (apparent 14 kDa) exhibits faster mobility than LC3-I (apparent 16 kDa) on SDS-PAGE. LC3 forms I and II can be differentially recognized by the LC3 antibodies. Thus, the endogenous levels of LC3-II (relative to a loading control rather than to LC3-I) measured by Western blotting reflects the number of autophagosomes in the cells at a given time. However, as LC3-II is degraded after the autophagosome fuses with the lysosome, the net level of LC3-II will not reflect the level of autophagy. This issue can be circumvented by preventing the lysosomal degradation of LC3-II, so that it accumulates in the cells [71]. This can be achieved by either (1) neutralizing the lysosomal pH with bafilomycin A1 (Baf A1), a proton pump inhibitor, or (2) inhibiting the lysosomal proteases with E64D and pepstatin A methyl ester or (3) a combination of both. In the course of our studies, it was found that the incorporation of a lysosomal inhibitor cocktail (LIC) containing 100 nM Baf A1, 5 μg/mL E64D (inhibitor of cysteine proteases including cathepsin B) and 5 μg/mL pepstatin A methyl ester (cathepsin D inhibitor) into HL-1 cardiac cultures for 2 hours was efficient in preventing the degradation of LC3-II as assessed by Western blotting. However, the LIC or the corresponding concentration of DMSO (vehicle, 0.2%) induced a significant increase in the level of cell death measured by flow cytometric analysis of Annexin V and propidium iodide (PI) stained cells (Figure 5), indicating that the LIC was highly cytototoxic. Therefore, we have examined the optimal conditions of Baf

A1 treatment that resulted in a maximal accumulation of LC3-II without inducing any cytotoxicity. The dose-response study indicated that the incubation of HL-1 cells for 2 hours with 25 nM Baf A1 resulted in a maximal accumulation of LC3-II detected by Western blotting. Interestingly, higher doses of Baf A1 reduced the level of LC3-II accumulation in HL-1 cells. This effect was in part due to the elevated concentration of the vehicle, as HL-1 cells treated for 2 hours with increasing doses of DMSO alone exhibited lower levels of LC3-II. These results suggested that DMSO either countered the action of Baf A1 or inhibited autophagy. In addition, Baf A1 (25 nM) and the corresponding concentration of DMSO (vehicle, 0.025%) had no effect on the levels of necrotic or apoptotic cells measured by flow cytometry analysis of Annexin V and PI labeled cells (Figure 5). Thus, in our studies the degradation of LC3-II was prevented by adding 25 nM Baf A1 (in 0.025% DMSO) to the cardiac cultures for a maximum period of 2 hours. The autophagic flux is commonly determined by comparing the LC3-II levels in the presence (cumulative LC3-II) and absence (instantaneous LC3-II) of lysosomal degradation. However, this approach requires that autophagy is under steady-state (i.e. LC3-II synthesis and degradation are equal at the beginning and end of the Baf A1 treatment period) [72]. Since the kinetics of LC3-II synthesis and degradation have not been established in our model, the level of autophagy in HL-1 cells was determined by comparing the level of cumulative LC3-II between samples.

The role of autophagy was assessed by inhibiting the initiation step of autophagy with 3-methyaldenine (3-MA), a Class III PI3-K inhibitor. The dose-response study of 3-MA (dissolved in sterile water) indicated that the administration of 10 mM in cardiac cultures for 2 hours induced a decrease in the level of LC3-II as assessed by Western blotting. The 3-MA-mediated inhibition of autophagy resulted in little cytotoxicity as measured by flow cytometric

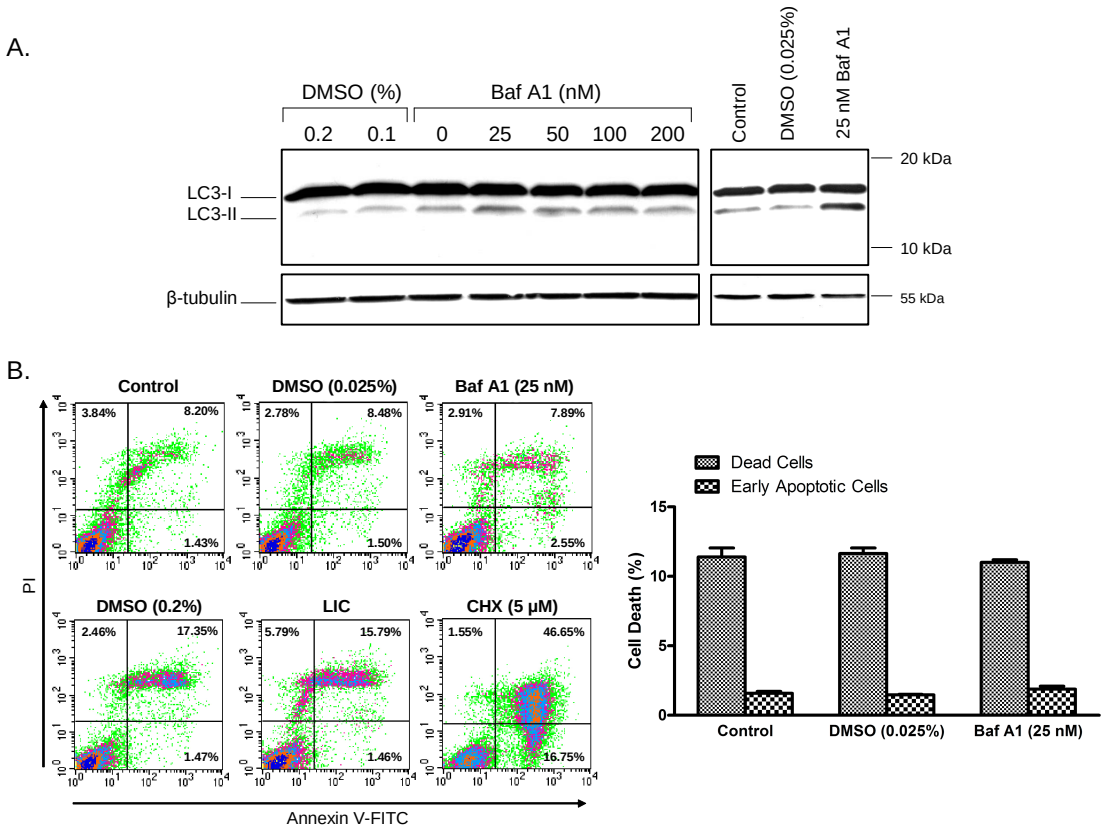

Figure 5: Effect of bafilomycin A1 on autophagy and viability of HL-1 cardiac cells.
A. Profile of LC3 processing in HL-1 cells incubated with increasing concentrations of bafilomycin A1 (Baf A1, 0-200 nM), with DMSO (vehicle) or with the lysosomal inhibitors cocktail (LIC, 100 nM Baf A1, 5 μg/mL E64D, 5 μg/mL pepstatin A methyl ester) for 2 hours assessed by Western blotting. β-tubulin was used as a loading control. **B.** Flow cytometric analysis of HL-1 cells incubated for 2 hours with Baf A1 (25 nM) or LIC and labeled with AnnexinV-FITC and propidium iodide (PI). Control samples include HL-1 cells that were untreated (Control), treated with vehicle alone (DMSO: 0.025% or 0.2%, for Baf A1 or LIC, respectively) or treated with 5 μM of cycloheximide (CHX) for 24 hours. The percentages of dead cells (Annexin $V^{+/-}$-PI^{+}) and early apoptotic cells (Annexin V^{+}-PI^{-}) were expressed as mean ± SEM from two independent experiments and represented graphically.

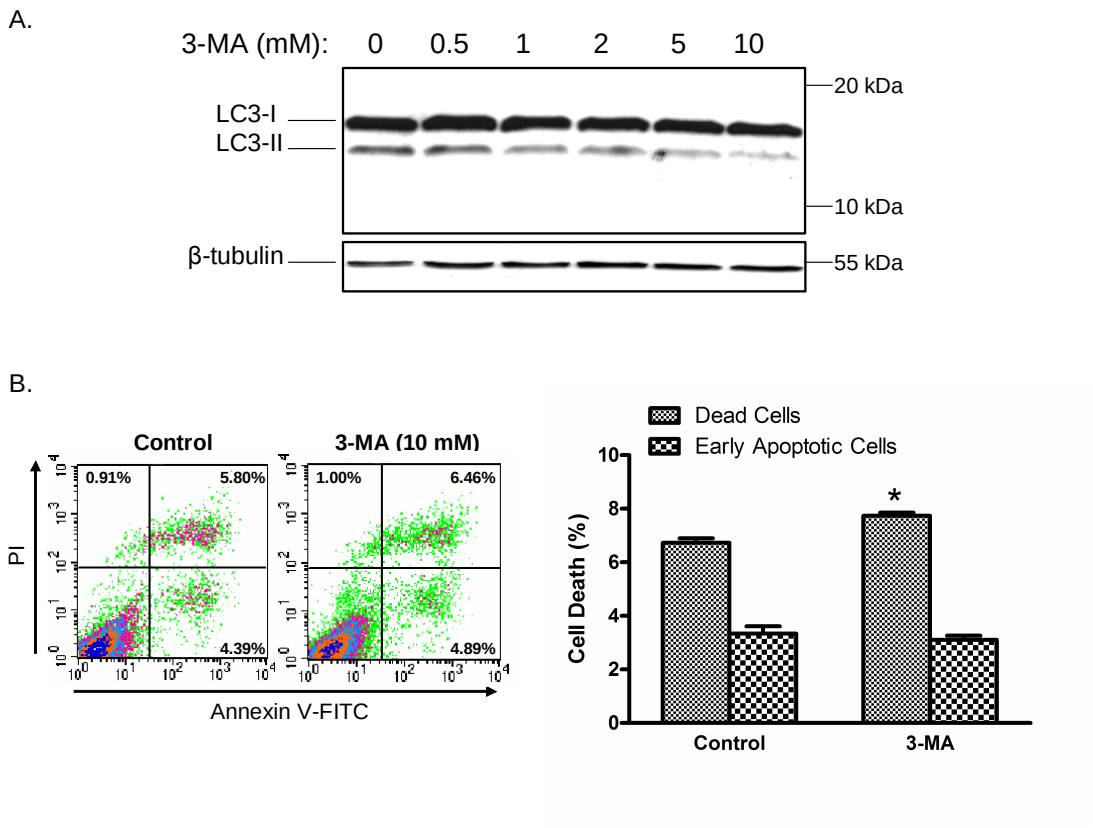

<u>Figure 6</u>: Effect of 3-methyladenine on autophagy and viability of HL-1 cardiac cells. A. Profile of LC3 processing in HL-1 cells incubated for 2 hours with increasing concentrations of 3-methyladenine (3-MA) as analyzed by Western blotting. β-tubulin was used as a loading control. **B.** Flow cytometry analysis of HL-1 cells that were untreated (Control) or treated with 3-MA (10 mM) for 2 hours and labeled with AnnexinV-FITC and propidium iodide (PI). The percentages of dead cells (Annexin $V^{+/-}$-PI^{+}) and early apoptotic cells (Annexin V^{+}-PI^{-}) were expressed as mean ± SEM from five independent experiments and represented graphically. $^{*}p<0.01$ (vs. Control) by One-Way ANOVA.

analysis of Annexin V-PI double stained cells (Figure 6). Based on these results, the inhibition of autophagy was achieved by incubating HL-1 cells with 10 mM 3-MA for a maximal period of 2 hours.

2.7. Measurement of ATP Levels

ATP levels were measured by a biochemiluminescent-based assay that relies on the property of the firefly luciferase to oxidize the substrate D-luciferin in an ATP-dependent process generating chemiluninescence. The light intensity is a direct measure of ATP concentration. This assay was performed using the ATPlite assay kit, according to the instructions of the manufacturer. Briefly, HL-1 cells were plated (in triplicate for each treatment group) in a black 96-well plate with a density of 15,000 cells/100 µL per well. Cells were allowed to attach overnight and subsequently subjected to the indicated treatment. The release of intracellular ATP was achieved by adding 50 µL of Mammalian Lysis Buffer to the cells. Cells were shaken at 700 rpm for 5 min and 50 µL of a solution containing D-luciferin (substrate) and luciferase (enzyme) was added to the cells. Cell lysates were shaken at 700 rpm for 5 min and incubated for 10 min in the dark. The luminescence was analyzed after a 1-sec delay with a 10-msec integration on an Infinite M200 microplate reader (Tecan Group Ltd., Switzerland). A standard curve was generated from known concentrations of ATP (0-24 µM) and used to calculate the concentration of ATP in each sample. Luminescence increased linearly with the negative log of the ATP concentration in the samples over the range of concentrations measured. The ATP level (pmoles of ATP in 15,000 cells) of each sample was normalized to the ATP level measured in control cells before their exposure to hypoxia (2.2 nmoles of ATP/15,000 cells) and graphically represented as mean ± SEM in relation to control from at least three experiments. To

determine whether compounds present in the ischemia buffer or standard cell culture media interfered with reagents of the ATP assay kit, the following control experiment was performed. HL-1 cardiac cells were subjected to 2 hours of hypoxia (0.5% O_2) alone or followed by 2 hours of reoxygenation (H2/R2). Control groups included HL-1 cells incubated under normal conditions of growth for the periods of time that corresponded to those of the experimental groups. At the end of the treatment period, cells were lysed and 10 μM of purified ATP was added to the cell lysates. Following the addition of the substrate solution, the luminescence was read. As documented in Figure 7, following hypoxia alone and H/R, the ATP content of HL-1 cells was significantly decreased in comparison to healthy cells. The addition of extracellular ATP resulted in an enhancement of the luminescence measured in the samples (control and treatment) that was proportional to the amount of ATP added. These data suggest that the low ATP contents measured in hypoxic cardiac cultures and HL-1 cells exposed to H/R did not result from a technical artifact.

2.8. Trypan Blue Exclusion Assay

Following the indicated treatment, cardiac cultures were washed with PBS, incubated for 2 min in 0.25 mg/mL trypsin in versene (0.2 g/L EDTA•4Na in PBS) and then neutralized by the addition of FBS. Cells were centrifuged (1,500 rpm for 2 min). The supernatant was aspirated and the cells were resuspended in a suitable volume of PBS (0.5 mL). Following addition of an equal volume of 0.4% Trypan blue, the cells (adherent and floating) were counted in a hemocytometer. The number of dead cells with disrupted membranes (blue cells) in a total of 200 cells was counted in duplicate, for each dish of plated cells. The level of cell death (percentage of blue cells/total cells) of each treatment group was normalized to the basal level of

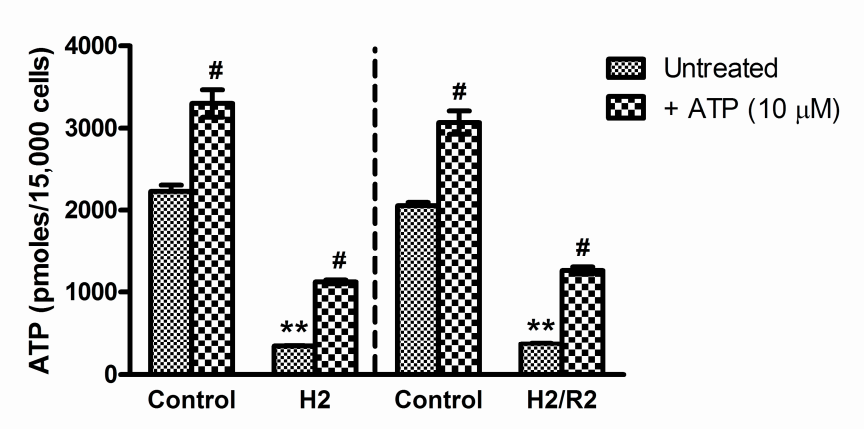

Figure 7: Effect of extracellular ATP on ATP levels measured in HL-1 cardiac cells exposed to hypoxia-reoxygenation. HL-1 cells were untreated (Control) or exposed to 2 hours of hypoxia (0.5% O_2) alone (H2) or followed by 2 hours of reoxygenation (H2/R2). ATP levels were measured in absence (untreated) or presence of 10 μM ATP and represented graphically as mean ± SEM from three independent experiments. **$p<0.0001$ (vs. Control) and $^{\#}p<0.0001$ (vs. untreated) by One-Way ANOVA.

cell death measured under control conditions (3-5%) and was graphically represented as the mean ± SEM in relation to controls from at least three experiments.

2.9. Measurement of Phosphatidylserine Exposure by Annexin V Binding

The adherent cells were rinsed twice with PBS before harvesting by incubating them for 2 min in 0.25 mg/mL trypsin in versene. The trypsin was neutralized through addition of FBS. Floating and adherent cells were washed twice with ice cold PBS and resuspended in 1X Binding buffer to a final concentration of 1 x 10^6 cells/mL. Cells (1 x 10^5) were incubated for 15 minutes at room temperature in the dark with 5 μL FITC-Annexin V and 5 μL Propidium Iodide (PI) according to the manufacturer's instructions. At the end of the incubation period, 1X Binding buffer (400 μL) was added to the cells. HL-1 cells were analyzed by flow cytometry. Control samples included unstained cells, cells stained with FITC-Annexin V alone and cells stained with PI alone. For each sample, 2 x 10^4 cells were analyzed on a LSR II flow cytometer (Becton Dickinson). Annexin V-FITC and PI signals were excited using a 488-nm laser light and emissions were captured using bandpass filters set at 530 ± 30 and 613 ± 20 nm, respectively. Cell Quest Acquisition and Analysis software (BD Bioscience, CA) was used to acquire and quantify fluorescence signal intensities and draw bivariate dot-density plots. Numbers in the lower left (LL), the upper right (UR), the lower right (LR) and upper left (UL) quadrants denote percentages of viable cells (Annexin V^-/PI^-), necrotic or late apoptotic cells (Annexin V^+/PI^+), early apoptotic cells (Annexin V^+/PI^-), and non viable cells (Annexin V^-/PI^+), respectively. The percentages of dead cells (UL+UR - Annexin $V^{+/-}/PI^+$) and early apoptotic cells (LR - Annexin V^+/PI^-) relative to control levels were expressed as mean ± SEM from at least three independent experiments and represented graphically.

2.10. Statistical Analysis

For all of the outcomes collected in this project, descriptive statistics for each experimental group were performed. These statistics included means, medians, standard deviations, ranges and confidence intervals. The data were expressed as means ± SEMs and represented graphically to provide visualization of the group trends. All experiments were repeated at least three times. Statistical analysis between two groups was performed by Student's t test. In most of the following studies involving more than two groups, single-factor one way analysis of variance (ANOVA) was performed for each group of treatments. When a significant experimental effect was detected ($p<0.05$), pairwise comparisons of the different levels of the factor were performed using the Bonferonni post-test. The interaction between various factors was analyzed by the two factor ANOVAs. When a significant interaction was detected, further analyses were done to assess the effect of one factor within each level of the other factor and vice versa.

CHAPTER 3 – RESULTS

3.1. Validation of the *In Vitro* Model of Cardiac Ischemia-Reperfusion Injury

For our *in vitro* model of I/R injury (hypoxia-reoxygenation, H/R), the murine atrial-derived HL-1 cell line was used as a cellular model because of the multiple advantages it offers. Primary cultures of isolated cardiac myocytes can be contaminated with other cell types (endothelial cells, fibroblasts and leucocytes) and can undergo spontaneous deterioration. In contrast, HL-1 cells constitute a homogeneous cell population that can continuously divide while retaining many features of mature cardiomyocytes [68]. These characteristics ensure not only that the changes in a process can be attributed to a single cell type, but a greater reproducibility of the results as well. The HL-1 cell line represents an excellent tool for studying normal and pathophysiological cardiomyocyte functions. [73].

In our model, ischemia (hereafter referred to as hypoxia) was induced by replacing the standard medium with an "ischemia buffer" and placing HL-1 cardiac cultures in a hypoxic atmosphere. The "ischemia buffer" was formulated to mimic the extracellular environment and the reduced energy state that cardiomyocytes are exposed to during ischemia *in vivo*. The "ischemia buffer" contains 2-deoxyglucose, a glucose analogue unable to undergo glycolysis, which ultimately inhibits cellular metabolism. In addition, the buffer contains a high concentration of potassium (hyperkalemia) and has an acidic pH (6.8). The use of this model has been successful in identifying key biochemical and cellular events involved in triggering cardiac cell death following H/R [40,57,58]. In contrast to other studies carried out in the model of simulated I/R injury, our model is unique in the sense that two different concentrations of O_2 – 0.5% and 2.0% were used to achieve different degrees of ischemia. This approach allowed us to

get closer to the situation encountered in patients suffering from myocardial infarction. In these patients, although the occlusion of the coronary artery induces nearly complete ischemia in the risk area with subsequent irreversible damage, the peri-infarct penumbra of the myocardium maintains a low level of oxygen by diffusion from adjacent areas. Finally, the "reperfusion" (hereafter referred to as reoxygenation) was achieved by restoring the normal culture conditions.

3.1.1. The bioenergetic status of HL-1 cells during hypoxia-reoxygenation

The primary focus was to determine whether the experimental conditions used to mimic ischemia in cultured HL-1 cardiac cells triggered the same metabolic changes encountered in the ischemic cardiomyocytes *in vivo*. To do so, HL-1 cardiac cultures were incubated in the ischemia buffer in presence of 0.5% or 2.0% O_2 for increasing periods of time (30, 60 and 120 minutes) and the ATP levels were measured at the end of each hypoxic period. As shown in Figure 8A, the ATP content of HL-1 cells dropped significantly following 30 minutes of hypoxic exposure to reach 15% of control levels by 2 hours of hypoxia induced with both 0.5% and 2.0% O_2. Interestingly, the degree of hypoxia had a differential effect on the rate of ATP depletion during the first 30 minutes. HL-1 cells exposed to 2.0% O_2 maintained a slightly, though significantly, higher ATP content than cells exposed to 0.5% O_2, ATP reached 32% and 24% of control levels, respectively ($p<0.001$ by two-way ANOVA). These results indicate that the experimental approach used to simulate ischemia in HL-1 cardiac cultures induced a dramatic ATP depletion, a pathological hallmark of myocardial infarction. To determine whether the restoration of normal conditions promoted the replenishment of intracellular ATP stores, the ATP level was measured in HL-1 cells subjected to 2 hours of hypoxia (0.5% or 2.0% O_2) followed by 1, 2 and 4 hours of reoxygenation. The results shown in Figure 8B indicate that reoxygenation elicited a progressive

restoration of ATP production in myocytes. However, the ATP levels remained remarkably lower than control at all time points during reoxygenation. Importantly, the degree of hypoxia significantly influenced the rate of ATP replenishment elicited by reoxygenation. Following 4 hours of reoxygenation, HL-1 cells previously exposed to 2.0% O_2 had a higher ATP content than cells pre-exposed to 0.5% O_2. The ATP levels reached 30% and 23% of control, respectively. These data indicate that reoxygenation promoted a partial re-energization of hypoxic cardiomyocytes. Other events triggered by either hypoxia or reoxygenation such as oxidative stress and mitochondrial damage may prevent the complete recovery of the myocyte bioenergetic state.

To further assess the changes in the bioenergetic status of HL-1 cells induced by hypoxia and H/R, the activation of AMPK was used as an alternative indicator. AMPK senses the changes of the intracellular AMP/ATP ratio. In response to elevated AMP cellular content, AMPK is activated through phosphorylation of the catalytic α subunit at threonine 172 (Thr172) by the upstream AMPK kinases (AMPKKs). As a result, the utilization of ATP is reduced and ATP production is facilitated (e.g. by fatty acid oxidation) [74]. As shown in Figure 9A, the degree of AMPKα phosphorylation at Thr172 in HL-1 cells was significantly enhanced at all time points during hypoxia (0.5% or 2.0% O_2) with respect to control conditions. These levels remained constant throughout the 2 hour-period in healthy HL-1 cells. In addition, the expression levels of AMPKα were apparently, but not significantly elevated at all time points during hypoxia (0.5% and 2.0% O_2) compared to control cells. It is noteworthy that the band corresponding to AMPKα is slightly shifted up in the hypoxic samples, suggesting that AMPK is fully phosphorylated/activated during hypoxia. These results were consistent with the low energetic status of hypoxic cells.

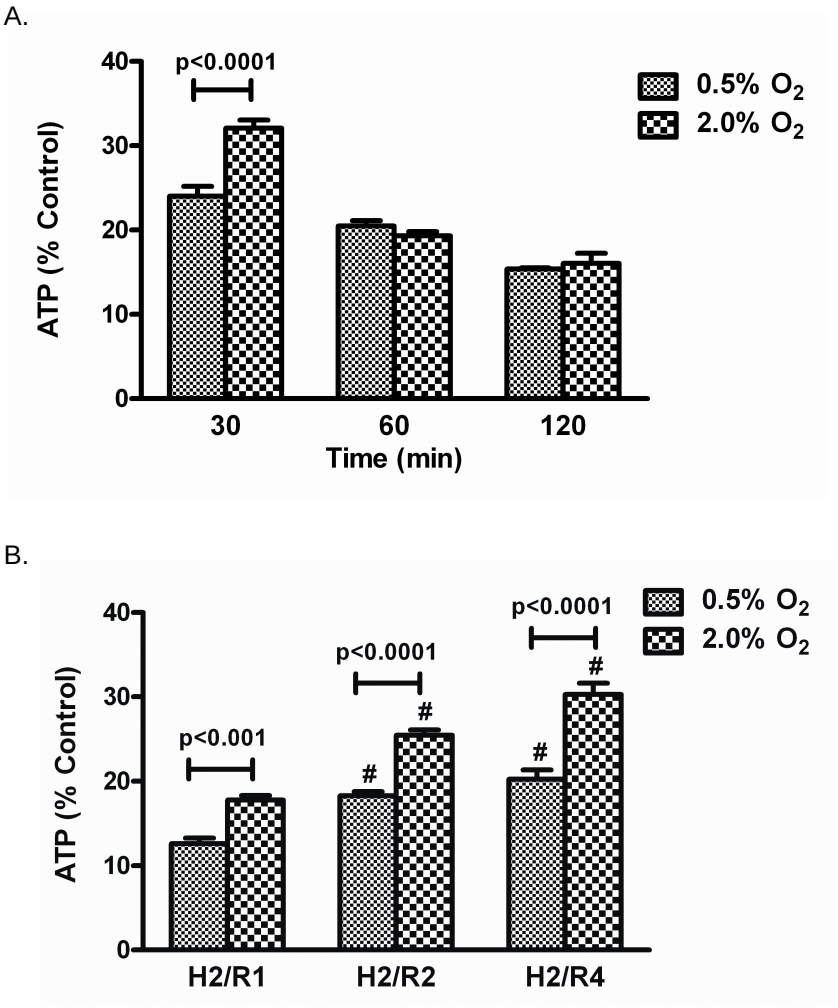

<u>Figure 8</u>: The bioenergetic status of HL-1 cells exposed to hypoxia-reoxygenation. A. HL-1 cells were exposed to hypoxia (0.5% or 2.0% O_2) for 30, 60 and 120 minutes. **B.** HL-1 cells were exposed to 2 hours of hypoxia (0.5% or 2.0% O_2) followed by 1, 2 and 4 hours of reoxygenation (H2/R1, H2/R2 and H2/R4). The levels of ATP were measured and expressed as percentages relative to controls. ATP levels were represented as mean ± SEM from three independent experiments. $^{\#}p<0.005$ (vs. H2/R1) by One-Way ANOVA. The comparison between the oxygen concentrations (0.5% and 2.0%) was performed by Two-Way ANOVA.

To test whether the partial recovery of ATP production occurring during reoxygenation was associated with a down-regulation of AMPKα activity, the levels of expression and activation of AMPKα were assessed in HL-1 cells subjected to 2 hours of hypoxia (0.5% or 2.0% O_2) followed by 1, 2 and 4 hours of reoxygenation by Western blotting. The results shown in Figure 9B indicate that reoxygenation induced a partial dephosphorylation of AMPKα in previously hypoxic HL-1 cells. The levels of phosphorylated AMPKα in HL-1 cells pre-exposed to 0.5% or 2.0% O_2 were significantly enhanced following 4 hours of reoxygenation in comparison to healthy cells ($p<0.05$ by one-way ANOVA). Although, the levels of AMPKα activation were also found to be significantly elevated following 2 hours of reoxygenation by Student's t-Test. Importantly, reoxygenation had no effect on the abundance of AMPKα in myocytes, this level remained constant throughout the reoxygenation period in comparison to healthy cells. These results suggest that the partial recovery of ATP production in reoxygenating HL-1 cells was accompanied by a concomitant and incomplete dephosphorylation of AMPKα. Altogether, these data support the validity of our *in vitro* model of myocardial ischemia as it recapitulated the low energetic state of cardiomyocytes induced by ischemia and a partial recovery of ATP production during reperfusion.

3.1.2. HL-1 cell viability following hypoxia-reoxygenation

We then sought to establish the extent of cell injury elicited by both hypoxia and H/R. We have examined the level of cardiac cell death induced by 2 hours of hypoxia (0.5% or 2.0% O_2). Cell viability was measured by assessing the ability of myocytes to exclude Trypan blue, a vital dye that penetrates dead cells through their damaged membrane. Hypoxia significantly increased cell death in comparison to control conditions (Figure 10A). Importantly, cells exposed to 0.5%

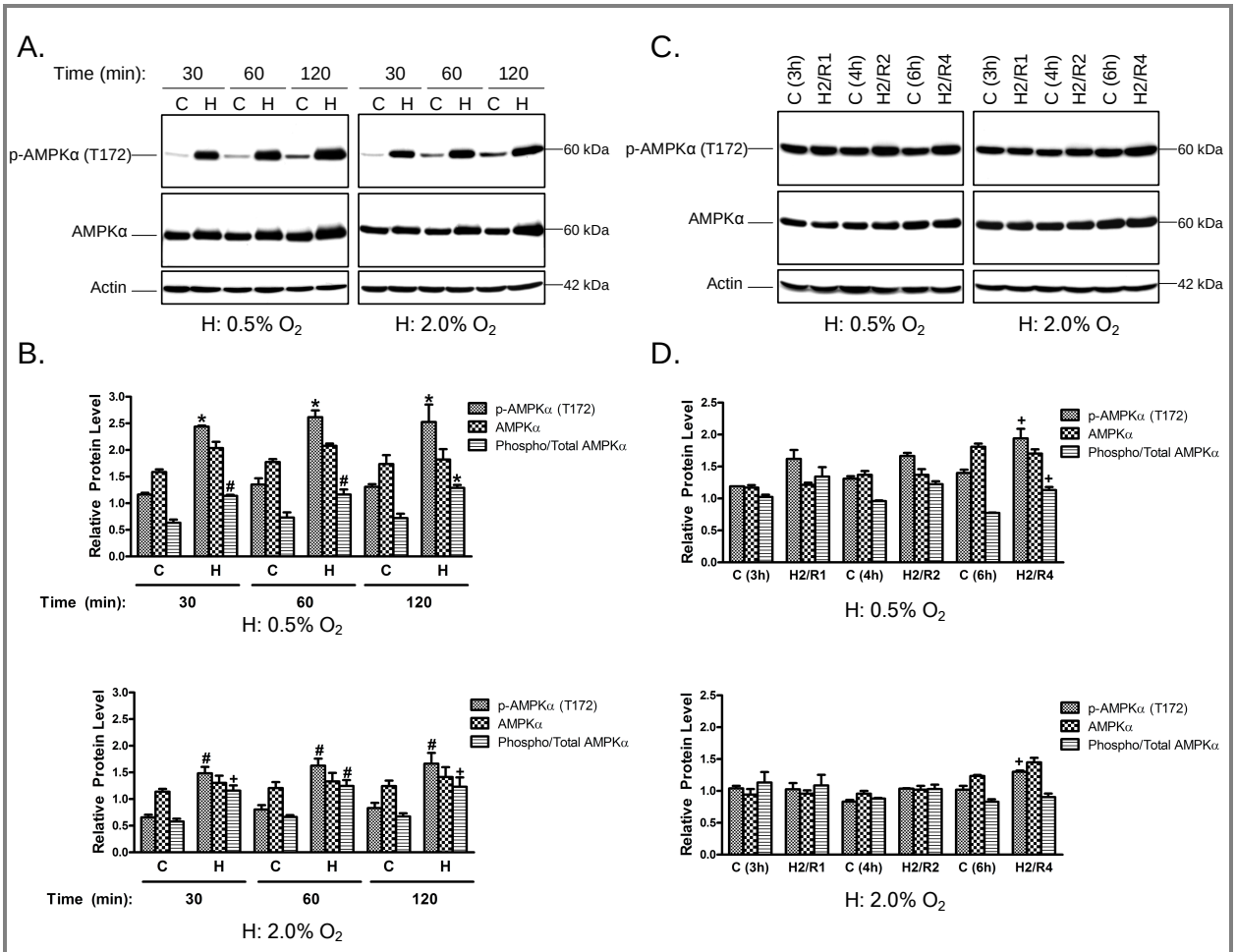

<u>Figure 9</u>: Time course of AMPKα expression and phosphorylation in HL-1 cells exposed to hypoxia-reoxygenation. A, B. HL-1 cells were exposed to hypoxia (0.5% or 2.0% O_2) for 30, 60 and 120 minutes. **C, D.** HL-1 cells were exposed to 2 hours of hypoxia (0.5% or 2.0% O_2) followed by 1, 2 and 4 hours of reoxygenation (H2/R1, H2/R2 and H2/R4). Control cells were incubated under normal conditions for the same periods of time (C). The levels of expression and phosphorylation of AMPKα were assessed by Western botting. The levels of phosphorylated and total AMPKα were measured by densitometry analysis of the immunoreactive bands and normalized to actin. Results were graphically represented as mean ± SEM from four independent experiments. $^{*}p<0.001$, $^{\#}p<0.005$, $^{+}p<0.05$ (vs. C) by One-Way ANOVA.

O_2 were more susceptible as the number of dead cells reached 358% of control (vs. 321% of controls in the case of 2.0% O_2, $p<0.0001$ by one-way ANOVA). These results suggest that the degree of hypoxia dictates the extent of cardiac injury. Since the occurrence of apoptosis has also been reported in the ischemic myocardium, we have monitored the activation of apoptosis in HL-1 cells exposed to 2 hours of hypoxia with 0.5% or 2.0% O_2. The translocation of phosphatidylserine (PS) residues from the inner to the outer leaflet of the cell membrane is an early event of the apoptotic program and was therefore used as a marker of early apoptosis. Thus, HL-1 cells were stained with fluorescein-labeled Annexin V (a calcium-dependent phospholipid-binding protein that exhibits a high binding affinity for accessible PS) and propidium iodide (PI, a fluorescent DNA intercalating dye that penetrates dead or damaged cells) and analyzed by flow cytometry. This technique is not suitable to discriminate between cells that are necrotic and late apoptotic. Indeed, during the late stage of apoptosis, apoptotic bodies are formed and are phagocytosed by macrophages. However, in cells in culture, the removal of apoptotic cells by phagocytes is not possible and thus these cells inevitably die by necrosis. In addition, Annexin V is able to insinuate through the disrupted membranes of necrotic cells, and bind to their internally located PS residues. Consistent with this, flow cytometric analysis of Annexin V-PI stained cells revealed three cell populations (i) viable cells (Annexin V^- and PI^-), (ii) early apoptotic cells (Annexin V^+ and PI^-) and (iii) dead cells (Annexin $V^{+/-}$ and PI^+). Our results show that hypoxia induced a significant increase in cell death that was more pronounced with 0.5% than 2.0% O_2; the percentages of dead cells reached 284% and 250% of control levels, respectively ($p<0.0001$ by one-way ANOVA) (Figure 10B, C). These results were in agreement with the level of hypoxic cell death measured by Trypan blue staining. Importantly, the level of cells undergoing early apoptosis following hypoxia remained similar to controls. Altogether, these data indicate

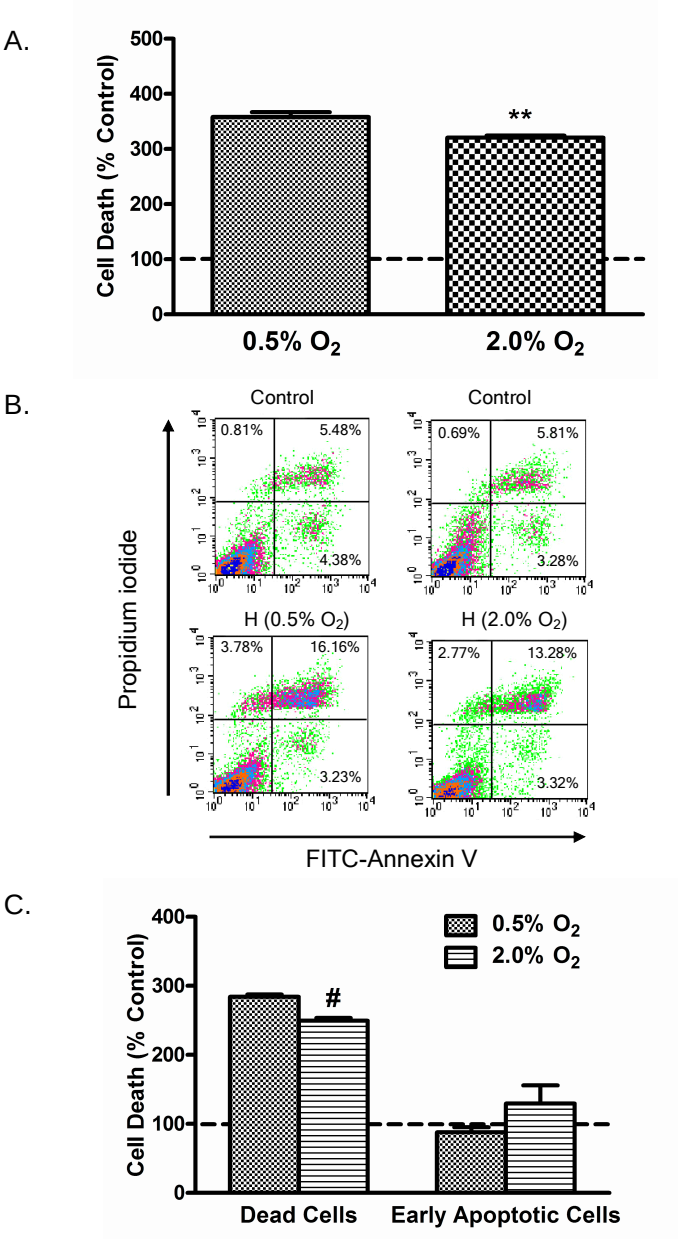

<u>Figure 10</u>: Effect of hypoxia on HL-1 cell viability. HL-1 cells were incubated under normal conditions (Control) or exposed to hypoxia (H) with 0.5% or 2.0% O_2 for 2 hours. **A**. Cell death was evaluated by Trypan blue staining. The percentages of dead cells (Trypan Blue positive/total cells) relative to controls were represented graphically as mean ± SEM from three independent experiments. $^{**}p<0.0001$ (vs. 0.5% O_2) by One-Way ANOVA. **B, C**. Flow cytometric analysis of HL-1 cells labeled with FITC-Annexin V and Propidium Iodide (PI). The percentages of dead cells (Annexin $V^{+/-}$-PI^{+}) and early apoptotic cells (Annexin V^{+}-PI^{-}) relative to controls were expressed as mean ± SEM from three independent experiments and graphically represented. $^{\#}p<0.001$ (vs. 0.5% O_2) by One-Way ANOVA.

that the viability of HL-1 cells was significantly and differentially affected by the degree of hypoxia.

Next, we determined whether reoxygenation exacerbated or limited cardiac cell injury induced by hypoxia. HL-1 cells were exposed to 2 hours of hypoxia followed by increasing periods of reoxygenation (2 and 4 hours) and cell death was assessed by Trypan blue exclusion. The results indicate that the level of cell death remained elevated during the 4-hour period of reoxygenation compared to control conditions (Figure 11A). However, the number of cells accumulating the dye was significantly decreased after 4 hours of reoxygenation. In addition, myocytes exposed to 2.0% O_2 were significantly less prone to death during the first 2 hours of reoxygenation than cells exposed to 0.5% O_2. The apparent decrease in cardiac cell death observed during reoxygenation may be due to cells that have lysed and therefore not counted.

We have assessed the occurrence of apoptosis in HL-1 cells subjected to 2 hours of hypoxia followed by 2, 4, 9 and 16 hours of reoxygenation by Annexin V-FITC and PI staining and flow cytometry. Following hypoxia, cell death was reduced by half following 2 hours of reoxygenation (Figure 11B). Importantly, cardiomyocyte death occurred to a similar extent during reoxygenation and normal conditions. In contrast, reoxygenation triggered the activation of the apoptotic program in hypoxic cardiomyocytes. Although the level of early apoptosis was elevated at all time points during reoxygenation in comparison to control conditions, the temporal profile of apoptosis activation differed depending on the degree of hypoxia. In the case of 0.5% O_2, the percentage of early apoptotic myocytes increased to 143% of control during the first 2 hours of reoxygenation, peaked by 4 hours to reach 217% of control level, and progressively decreased thereafter to reach 161% of control level by 16 hours. In contrast, when hypoxia was induced with 2.0% O_2, the level of early apoptotic cells increased to reach a peak by

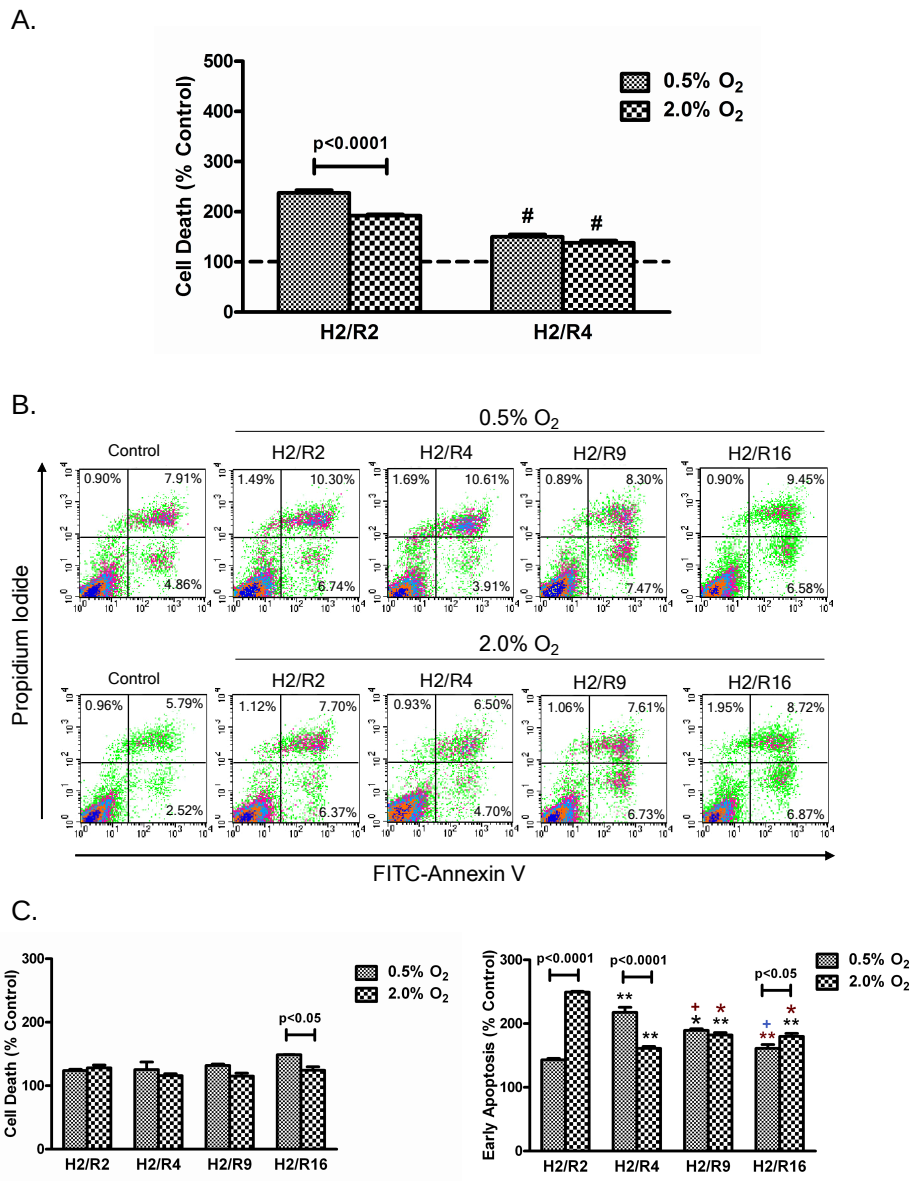

Figure 11: Cardiac cell death following hypoxia-reoxygenation. A. HL-1 cells were exposed to 2 hours of hypoxia (0.5% or 2.0% O_2) followed by 2 and 4 hours of reoxygenation (H2/Rs) and cell death was evaluated by Trypan blue exclusion. The percentages of dead cells relative to healthy controls were represented graphically as mean ± SEM from three independent experiments. $^{+}p<0.05$ (vs. H2/R2) by One-Way ANOVA. **B, C**. Flow cytometric analysis of Annexin V and Propidium Iodide labeling of HL-1 cells that were healthy (Control) or subjected to 2 hours of hypoxia (0.5% or 2.0% O_2) followed by 2, 4, 9 and 16 hours of reoxygenation (H2/Rs). The percentages of dead cells (Annexin $V^{+/-}/PI^{+}$) and early apoptotic cells (Annexin V^{+}/PI^{-}) relative to control levels were expressed as mean ± SEM from three independent experiments and represented graphically. $^{**}p<0.0001$, $^{*}p<0.005$ (vs. H2/R2); $^{**}p<0.0001$, $^{\#}p<0.01$, $^{*}p<0.005$, $^{+}p<0.05$ (vs. H2/R4); $^{+}p<0.05$ (vs. H2/R9) by One-Way ANOVA.

2 hours of rexoygenation (249% of control) and decreased to attain 180% of control level by 16 hours of reoxygenation. These results indicate that reoxygenation triggered

In summary, we have validated our model of myocardial ischemia as we have found that hypoxia triggered a drastic depletion of ATP in HL-1 cells, a hallmark of ischemia. This effect was accompanied by an increase in cell death that was more pronounced when cardiac cultures were exposed to 2 hours of hypoxia induced with 0.5% than with 2.0% O_2. In turn, reoxygenation promoted a partial bioenergetic recovery of hypoxic HL-1 cells. This effect was accompanied by an activation of the apoptotic program. These data suggest that the low ATP levels present in reoxygenating myocytes were sufficient to trigger apoptosis. However, the status of biochemical markers of later stages of apoptosis have not been examined, therefore it is unknown whether these ATP levels would be sufficient for the completion of the apoptotic program.

3.2. Modulation and Role of Autophagy during Hypoxia-Reoxygenation

3.2.1. Autophagy in HL-1 cells exposed to hypoxia-reoxygenation

As we have demonstrated that our system was a suitable model of myocardial I/R injury, the next objective of this project was to study autophagy. First, we have established the temporal profile of autophagy in HL-1 cardiomyocytes exposed to hypoxia induced with 0.5% or 2.0% O_2. The induction of autophagy was monitored by assessing the intracellular level of LC3-II, the specific marker of the autophagosome, by western blotting. An increase in the intracellular level of LC3-II can result from two distinct phenomena, an up-regulation of the autophagic process or a blockade of its lysosomal degradation phase. Thus, to discriminate between these possibilities,

it was essential to block the lysosomal degradation of LC3-II, which, in turn, leads to a time-dependent accumulation of LC3-II. This was achieved by incubating HL-1 cardiac cultures with 25 nM Baf A1, an inhibitor of the autophagosome-lysosome fusion. The level of autophagy was estimated by comparing the LC3-II levels in the presence of Baf A1 (cumulative LC3-II) between the samples. As depicted in Figure 12, the hypoxic treatment had no effect on the level of LC3-I in HL-1 cells. In addition, the autophagic response of HL-1 cells was not altered following 1 hour of hypoxia induced with either 0.5% or 2.0% O_2. However, a prolonged period of hypoxia (2 hours) induced a differential effect on autophagy, depending on the level of oxygen. HL-1 cells exposed to 0.5% O_2 exhibited a lower level of autophagy as judged by the significant decrease in LC3-II accumulation when compared to healthy HL-1 cells (Figure 12A). In contrast, the level of autophagy in cardiac cultures exposed to a hypoxic atmosphere containing a higher concentration of oxygen (2.0% O_2) remained similar to control cells (Figure 12B). These results suggest that the degree of hypoxia is a determining factor in the autophagic response elicited in HL-1 cells. To determine how reoxygenation affected this outcome, we have assessed the level of autophagy in HL-1 cells exposed to 2 hours of hypoxia (0.5% or 2.0% O_2) followed by 1, 2 and 4 hours of reoxygenation (H2/R1, H2/R2 and H2/R4). As previously described, the level of autophagy was assessed by comparing the levels of LC3-II measured in presence of 25 nM Baf A1 by western blotting, present in healthy myocytes and HL-1 cells exposed to H/R. The incubation period with Baf A1 was limited to 2 hours to prevent non-specific effects mediated by the long-term blockade of autophagy. Thus, Baf A1 was present throughout (H2/R1, H2/R2) or during the last 2 hours of the reoxygenation period (H2/R4). In parallel, healthy cultures were incubated under normal conditions and subjected to the same Baf

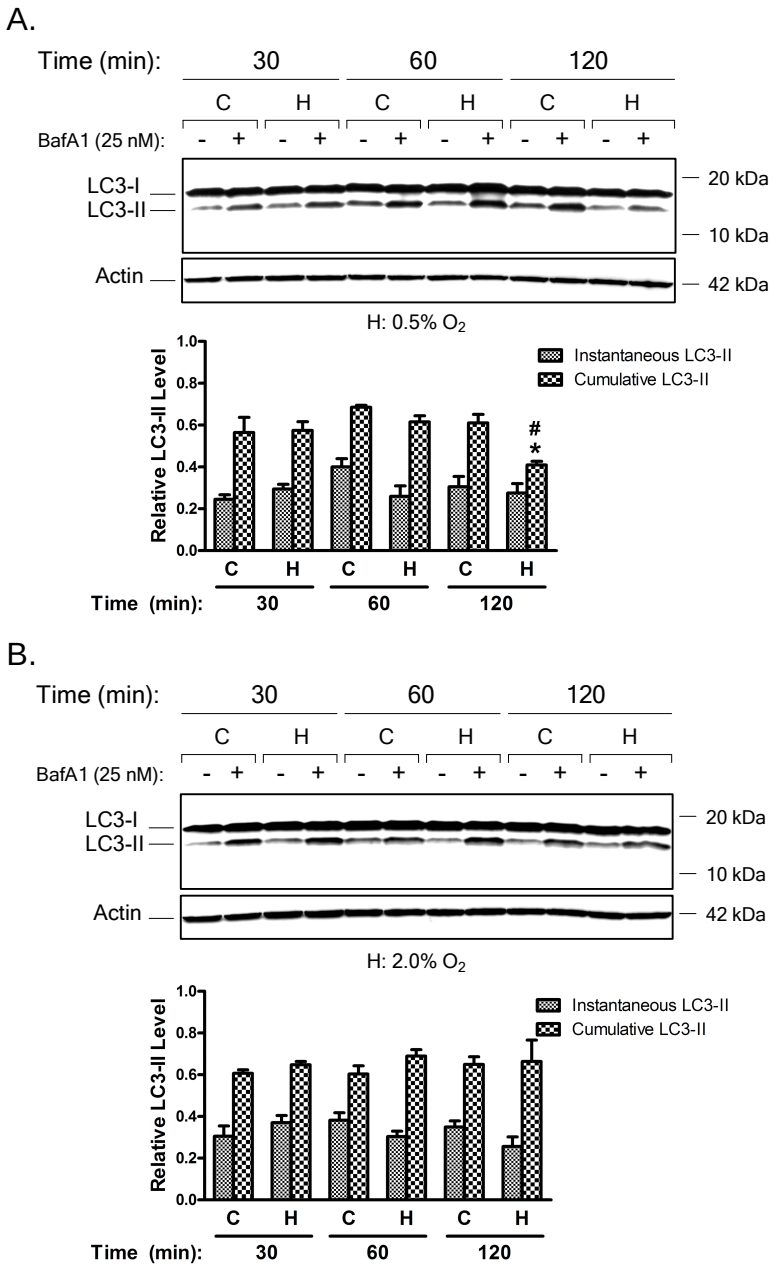

Figure 12: Temporal profile of autophagy in hypoxic HL-1 cardiomyocytes. HL-1 cells were exposed to increasing periods of hypoxia (H) with **A**. 0.5% O_2 or **B**. 2.0% O_2. Bafilomycin A1 (25 nM) was absent (-) or present (+) during the hypoxic period. Cell lysates were analyzed by Western blotting for LC3. Actin was used as a loading control. Control samples (C) include HL-1 cells grown under normal conditions for the same time periods in the absence or presence of Baf A1. The ratio LC3-II/Actin were determined by densitometry analysis of the immunoreactive bands and represented graphically as mean ± SEM from five independent experiments. $^{*}p<0.01$ (vs. C 120 min), $^{\#}p<0.001$ (vs. H 60 min) by One-Way ANOVA.

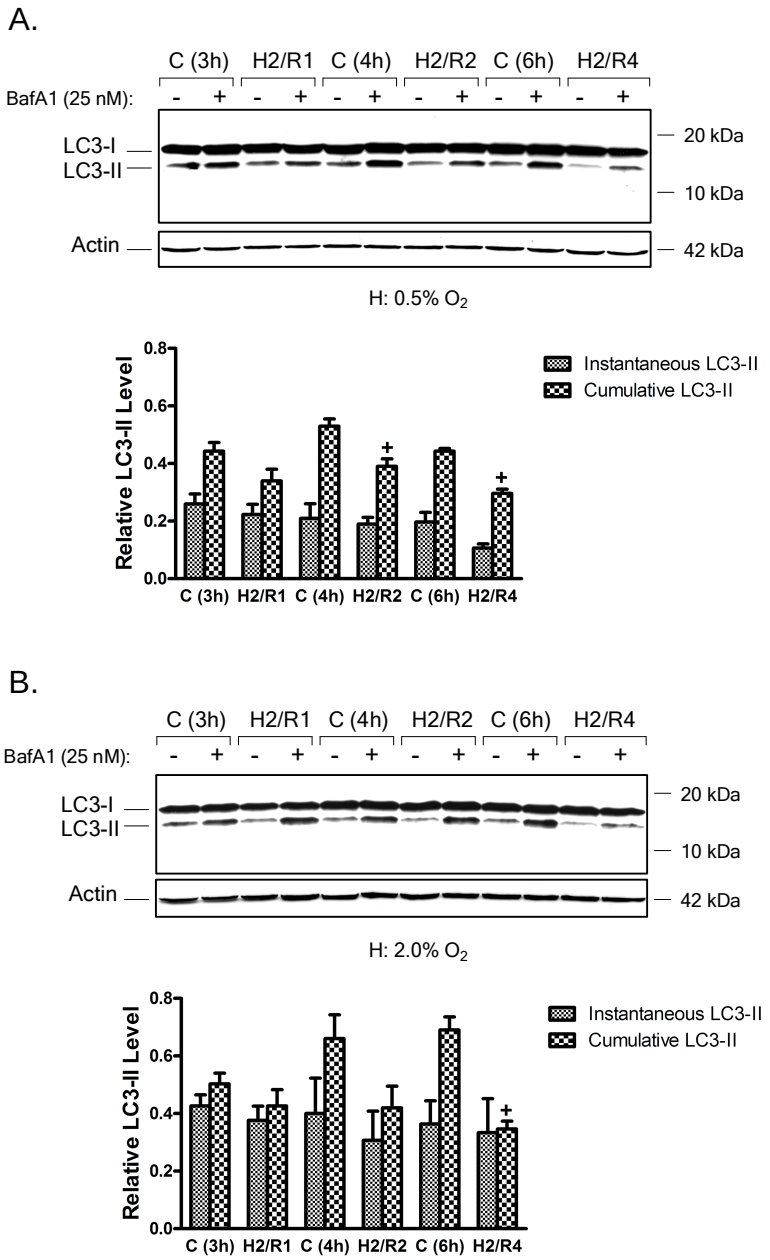

<u>Figure 13</u>: The modulation of autophagy during hypoxia-reoxygenation. HL-1 cells were exposed to 2 hours of hypoxia with 0.5% O_2 (**A**) or 2.0% O_2 (**B**) followed by 1, 2 and 4 hours of reoxygenation (H2/Rs). Bafilomycin A1 (Baf A1, 25 nM) was absent (-) or present (+) throughout the reoxygenation period (H2/R1, H2/R2) or during the last 2 hours of reoxygenation (H2/R4). Cell lystaes were prepared and analyzed by Western blotting for LC3. Actin was used as a loading control. Control samples (C) include HL-1 cells grown under normal conditions for the same periods in the absence or presence of Baf A1. The ratio LC3-II/Actin were determined by densitometry analysis of the immunoreactive bands and represented graphically as mean ± SEM from three independent experiments. $^{+}p<0.05$ (vs. C) by One-Way ANOVA.

A1 treatment for identical periods. Our results indicate that the levels of LC3-I in HL-1 cells were not altered by the reoxygenation process. In addition, cardiomyocytes exposed to H/R exhibited different temporal profiles of autophagy depending on the degree of hypoxia. Following 2 and 4 hours of reoxygenation, the cumulative levels of LC3-II in myocytes exposed to 0.5% O_2 were significantly lower compared to healthy cells (Figure 13A). In contrast, the level of autophagy in HL-1 cells pre-exposed to hypoxic conditions of 2.0% O_2 was similar to controls during the first 2 hours of reoxygenation but was significantly attenuated by 4 hours of reoxygenation compared to healthy cells (Figure 13B). These results suggest that the process of autophagy was compromised in HL-1 cells during H/R with a timing that was oxygen-dependent.

3.2.2. Mode of regulation of autophagy in HL-1 cells during hypoxia-reoxygenation

We next sought to investigate the molecular mechanisms underlying the autophagic response elicited by H/R. Our previous results showed that hypoxia (2 hours), according to its degree, had a differential effect on the level of autophagy in HL-1 myocytes. The level of autophagy was either unchanged (2.0% O_2) or partially inhibited (0.5% O_2) compared to healthy cells (Figure 12). ATP is required for the successful completion of autophagy. Thus, it is likely that the low ATP content of hypoxic cells limited their autophagic response. To test this possibility, HL-1 cells were incubated in the ischemia buffer containing glucose instead of 2-deoxyglucose (2-DG, an inhibitor of glycolysis) and exposed to 0.5% or 2.0% O_2 for 60 and 120 minutes. The bioenergetic status of cardiac cells was subsequently assessed by measuring ATP levels and analyzing the expression and phosphorylation profiles of AMPKα by Western blotting. As documented in Figure 14A, HL-1 cells exposed to 60 and 120 minutes of hypoxia in presence of glucose exhibited lower ATP contents in comparison to controls. Interestingly, the

decrease in ATP was dependent on the level of oxygen present during hypoxia. Indeed, the ATP levels of myocytes exposed to 0.5% and 2.0% O_2 reached 40% and 50% of controls, respectively. However, these levels remained 2 to 3-fold higher than the levels of ATP of cells exposed to hypoxia in presence of 2-DG. These results suggest that the drastic ATP depletion induced by hypoxia was in part mediated by 2-DG and additional factors including oxygen may contribute to that effect. The levels of AMPKα phosphorylation in myocytes exposed to hypoxia in presence of glucose appeared to be slightly increased in comparison to healthy cells (Figure 14B). However, a statistical difference was observed only for myocytes exposed to 2 hours of hypoxia induced with 0.5% O_2. HL-1 cells exposed to hypoxia in presence of 2-DG exhibited significantly elevated levels of phosphorylated AMPKα. The abundance of AMPK was not significantly affected by hypoxia. Next, we sought to determine whether the levels of ATP present in HL-1 cells exposed to hypoxia in presence of glucose could promote autophagy. We found that autophagy was significantly enhanced in cells exposed to 60 and 120 minutes of hypoxia (0.5% and 2.0% O_2) in presence of glucose in comparison to cells that were healthy or subjected to hypoxia in presence of 2-DG (Figure 15). In addition, the level of autophagy was increased to a similar extent in cells exposed to 0.5% and 2.0% O_2 in presence of glucose. These results confirm that energy is a limiting factor in the hypoxia-induced autophagic response of HL-1 myocytes. However, the attenuation of autophagy in hypoxic myocytes exposed to 0.5% O_2 appeared to be oxygen-dependent. Our results previously showed that the reintroduction of glucose (i.e. restoration of standard culture medium) in hypoxic cardiac cultures during reoxygenation did not enhance autophagy. Thus, the modulation of autophagy in HL-1 cells during hypoxia and reoxygenation may involve distinct mechanisms.

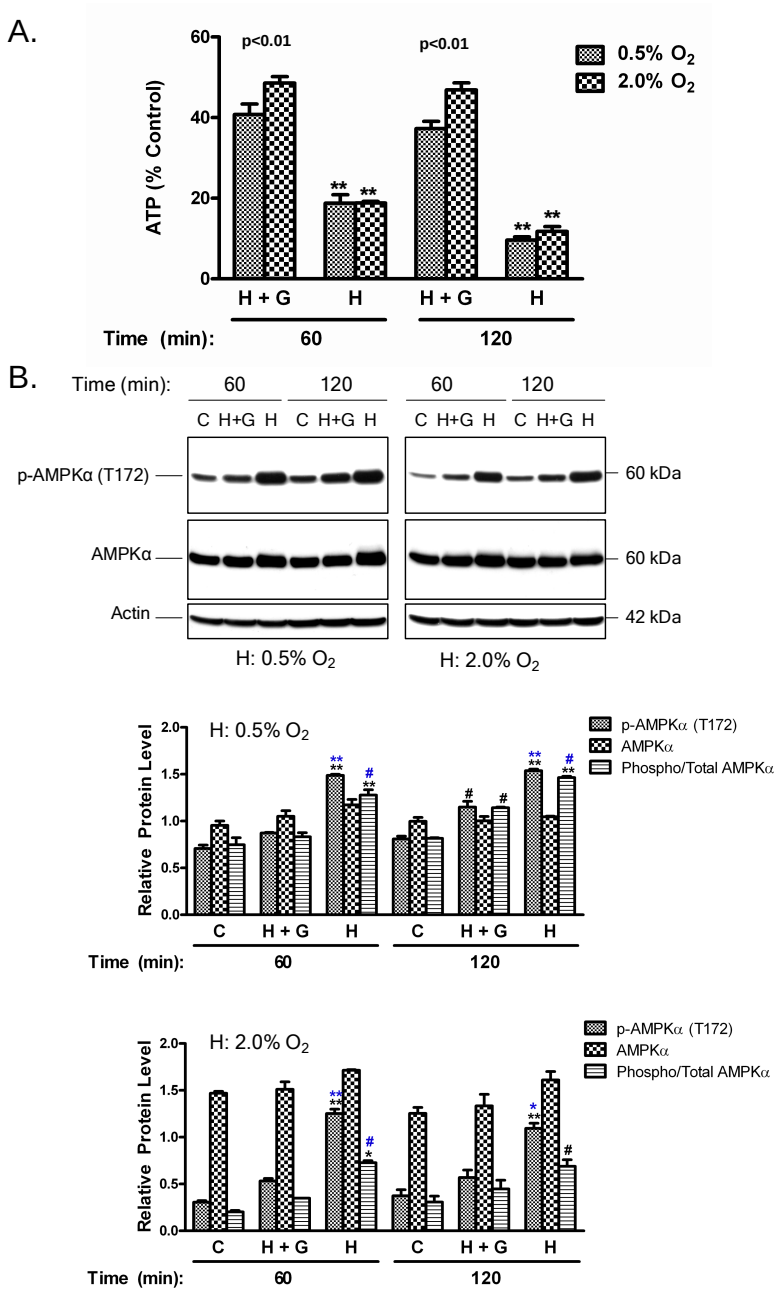

<u>Figure 14</u>: The bioenergetic status of HL-1 cells exposed to hypoxia in presence of glucose. HL-1 cells were exposed to 60 or 120 minutes of hypoxia (0.5% and 2.0% O_2) in presence of 20 mM Glucose (H+G) or 10 mM 2-deoxyglucose (H). Control cells were grown in normal conditions for identical periods of time (C). **A.** The ATP contents were measured and represented as mean ± SEM relative to healthy cells (% Control) of three independent experiments. $^{**}p<0.0001$ (vs. H+G) by One-Way ANOVA and $p<0.01$ (vs. 0.5% O_2) by Two-Way ANOVA. **B.** AMPKα expression and phosphorylation profiles in HL-1 cells subjected to the aforementioned treatments were analyzed by Western blotting. The protein levels were normalized to actin (loading control). The results were graphically represented as mean ± SEM of three independent experiments. $^{**}p<0.0001$, $^{*}p<0.001$, $^{\#}p<0.01$ (vs. C), and $^{**}p<0.0001$, $^{*}p<0.001$, $^{\#}p<0.01$ (vs. H+G) by One-Way ANOVA.

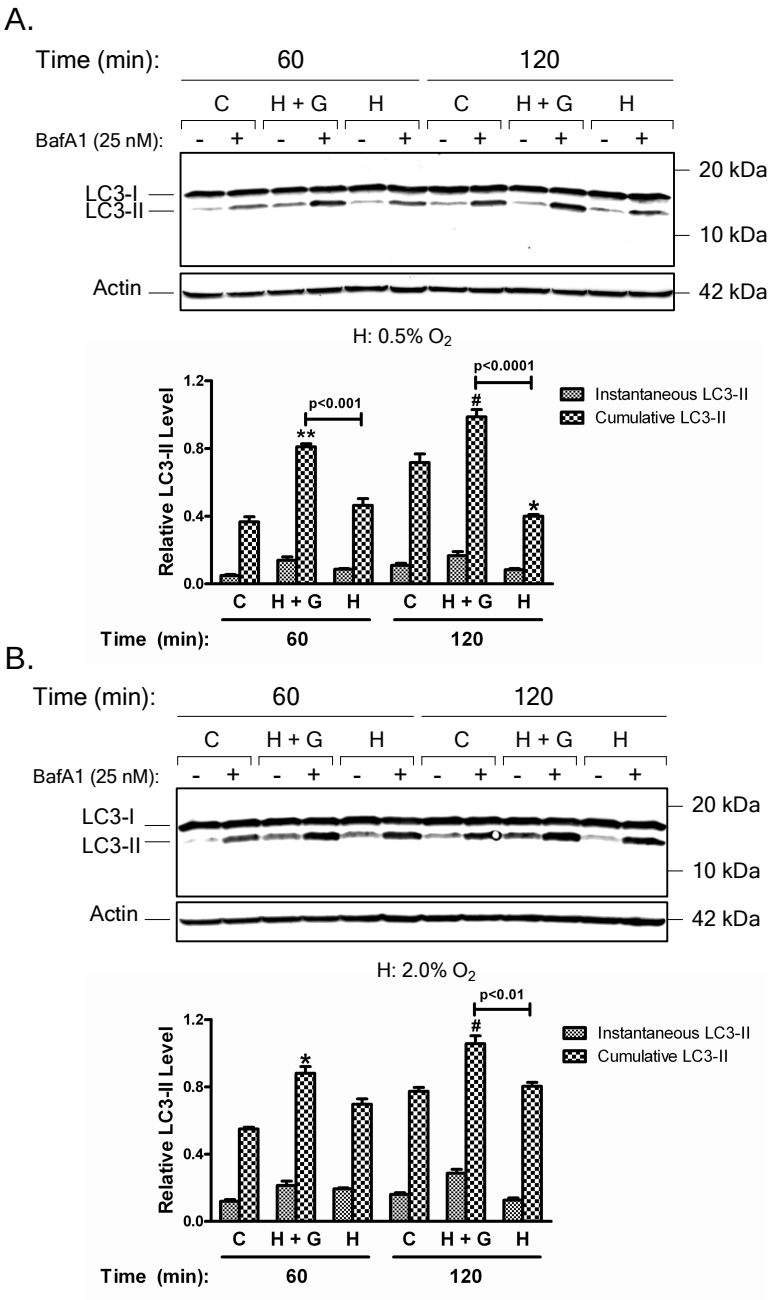

Figure 15: Autophagy in HL-1 cells exposed to hypoxia in presence of glucose. HL-1 cells were exposed to 60 or 120 minutes of hypoxia with 0.5% O_2 (**A**) or 2.0% O_2 (**B**) in presence of 20 mM Glucose (H+G) or 10 mM 2-deoxyglucose (H). Control cells were grown in normal conditions for the corresponding period of time (C). Baf A1 (25 nM) was absent (-) or present (+) throughout hypoxia. Autophagy was assessed by LC3 Western blotting and actin was used as a loading control. The ratio LC3-II/Actin were determined by densitometry analysis of the immunoreactive bands and represented graphically as mean ± SEM from three independent experiments. $^{**}p<0.0001$, $^{*}p<0.001$, $^{\#}p<0.01$ (vs. C) by One-Way ANOVA.

To further investigate the molecular mechanisms that control autophagy in HL-1 cells during H/R, we have explored the activation profiles of signaling pathways known to modulate this process (Figure 3). Under conditions of nutrient and energy depletion, autophagy is stimulated through inactivation of mTOR, a negative modulator of autophagy. mTOR inhibition can result from (i) the repression of the PI3-K/Akt pathway or from (ii) the activation of AMPK in response to low ATP levels. In addition, autophagy was shown to be activated by the Raf-1-MEK1/2-ERK1/2 signaling cascade in response to amino acid depletion [32]. Thus, we have first examined the expression and phosphorylation (indicative of kinase activity) profiles of Akt, mTOR and ERK1/2 in healthy cells and HL-1 cells exposed to 30, 60 and 120 minutes of hypoxia (0.5% and 2.0% O_2) by Western blotting (Figures 16a and 16b). Under normal conditions, the levels of expression and activation of Akt, ERK1/2 and mTOR remained constant throughout the 2-hour period. In contrast, hypoxia, whether induced with 0.5% or 2.0% O_2, severely impaired the activation of Akt, ERK1/2 and mTOR in HL-1 cells. Interestingly, the kinetics of deactivation of these kinases differed markedly. The phosphorylation of ERK1/2 was dramatically reduced after 30 minutes and almost completely disappeared after 60 and 120 minutes of hypoxia. The phosphorylation of mTOR at Ser2448, which was shown to correlate with the activation by growth factors [75], progressively decreased to reach 53%, 28% and 20% of control levels after 30, 60 and 120 minutes of hypoxia, respectively. In contrast, the phosphorylative activation of Akt declined at a slower rate as the level of Ser473-phosphorylated Akt reached 62% of control levels by 30 minutes of hypoxia. This level was sustained during the first hour of hypoxia and decreased to be barely detectable after 120 minutes of hypoxia. These results suggest that the deactivation of ERK1/2 was an early event during hypoxia and was followed by the consecutive dephosphorylation of mTOR and Akt. Importantly, the abundance

of ERK1/2, Akt and mTOR in HL-1 cells exposed to 2.0% O_2 remained unchanged in comparison to healthy cells. However, hypoxia (0.5% O_2) had a significant effect on the total expression levels of mTOR and Akt. While the expression level of mTOR was significantly elevated at all time points during hypoxia, Akt expression was enhanced by 60 minutes of hypoxia (0.5% O_2) only. As described earlier, hypoxia induced a dramatic activation of the pro-autophagic kinase, AMPKα without affecting its overall expression levels. Finally, we have established the expression profile of Beclin 1, which is involved, along with the class III PI3-K, in the autophagosome formation. The abundance of Beclin 1 in HL-1 cells was unaffected by hypoxia. Altogether, these results indicate that hypoxia significantly influenced the activation status of modulators of autophagy. While the inactivation of the Akt/mTOR pathway and the activation of AMPKα are consistent with a stimulation of autophagy, the inactivation of ERK1/2 exerts an inhibitory action on autophagy. However, our previous results indicate that autophagy not only was not enhanced in hypoxic myocytes but also was partially repressed after 2 hours of hypoxia (0.5% O_2). These results suggest the existence of a mechanism that may act in parallel to thwart the action of mTOR, thereby limiting the occurrence of autophagy. Alternatively, hypoxia may lead to a dysregulation of these pathways, presumably caused by the shortage in ATP.

Next, we sought to determine the effect of reoxygenation on the hypoxia-mediated inactivation of Akt, ERK1/2 and mTOR. To this end, HL-1 cardiac cultures were subjected to 2 hours of hypoxia (0.5% or 2.0% O_2) followed by 1, 2 and 4 hours of reoxygenation. The temporal profiles of expression and phosphorylation/activation of Akt, ERK1/2, mTOR and Beclin 1 during H/R were analyzed by western blotting. As shown in Figure 17a and 17b, the levels of expression of Akt, ERK1/2, mTOR and Beclin 1 in HL-1 cells were similar to controls throughout the reoxygenation period. However, H/R induced a reactivation of Akt, ERK1/2 and

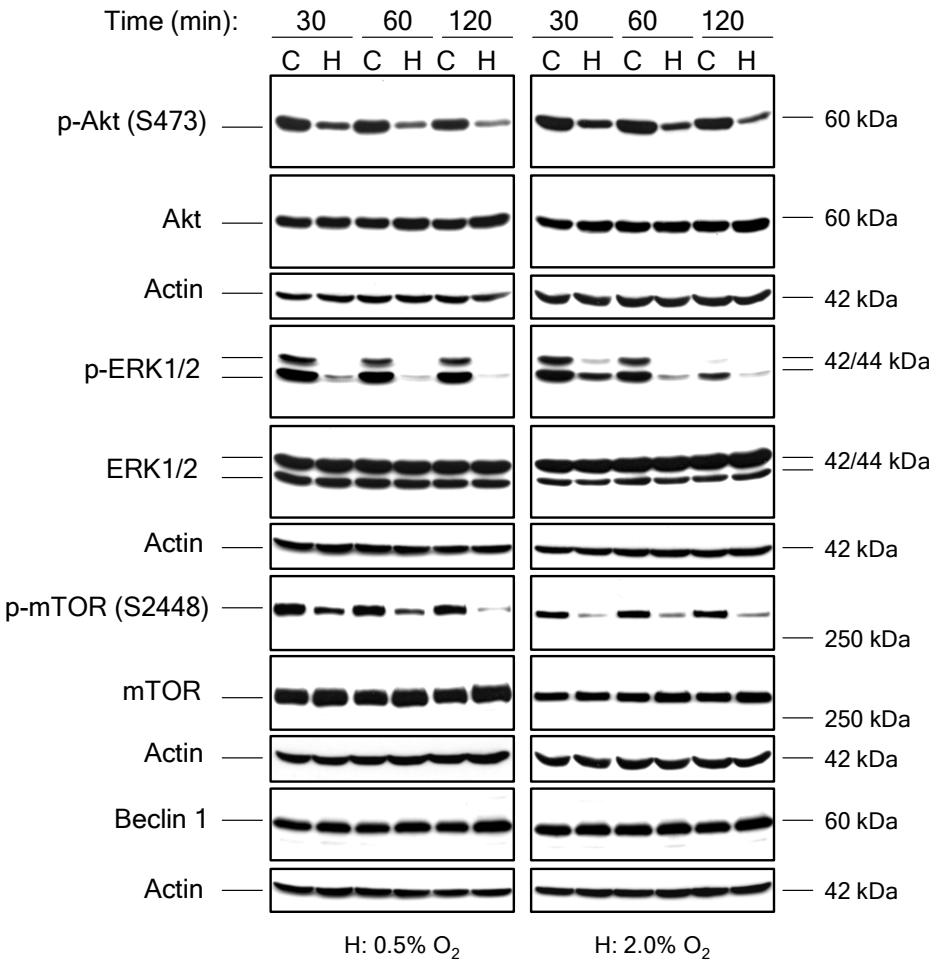

Figure 16a: Effect of hypoxia on modulators of autophagy. HL-1 cells were exposed to increasing periods of hypoxia (H) with 0.5% (left panel) or 2.0% (right panel) O_2. The temporal profiles of expression and activation of modulators of autophagy (Akt, ERK1/2, mTOR and Beclin 1) were analyzed by immunoblotting. Actin was used as a loading control in all Western blots. Control cells were grown in normal conditions for periods of time corresponding to the treatment groups (C). Blots shown are representative of at least three independent experiments. The quantifications are shown in Figure 16b.

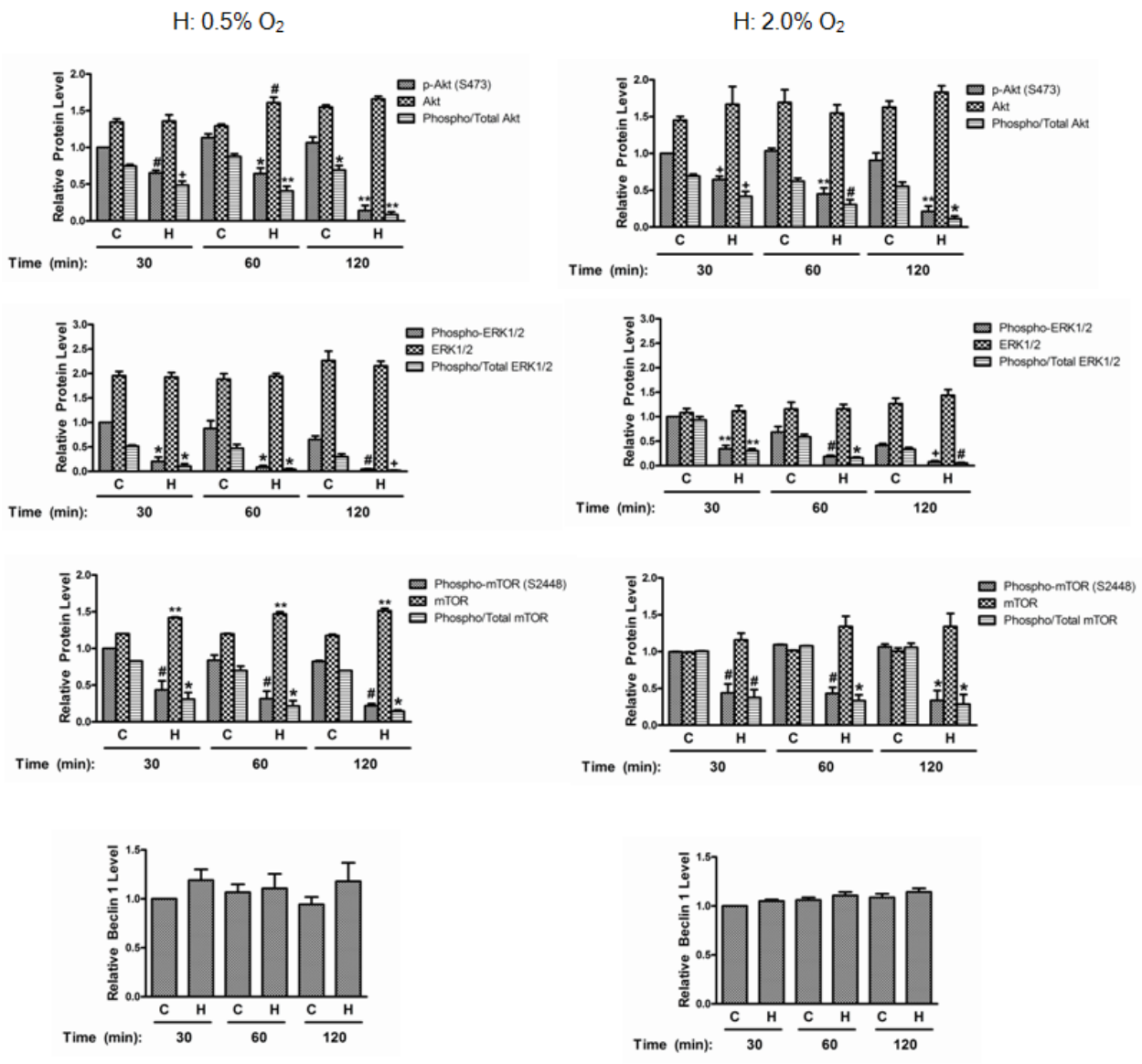

<u>Figure 16b</u>: Effect of hypoxia on modulators of autophagy. Quantifications of Akt, ERK1/2, mTOR and Beclin 1 expression and activation levels in HL-1 cells exposed to increasing periods of hypoxia (H) with 0.5% (left panel) or 2.0% (right panel) O_2. The levels of expression of Akt, ERK1/2, mTOR and Beclin 1 were determined in relation to actin. The levels of phosphorylated Akt, ERK1/2 and mTOR were determined in relation to both, actin and the total protein level. The ratio were determined by densitometry analysis of the immunoreactive bands and represented graphically as mean ± SEM from at least three independent experiments. $^{**}p<0.0001$, $^{*}p<0.001$, $^{\#}p<0.01$, $^{+}p<0.05$ (vs. C) by One-Way ANOVA.

mTOR in HL-1 cells. Akt phosporylation at Ser473 was significantly enhanced after 1 and 2 hours of reoxygenation and declined to reach control levels by 4 hours of reoxygenation. In contrast, ERK1/2 exhibited distinct kinetics of reactivation. In comparison to healthy controls, ERK1/2 phosphorylation was significantly increased by 1 hour of reoxygenation and progressively declined to reach levels significantly lower than controls after 4 hours of reoxygenation. Interestingly, HL-1 cells exposed to H/R exhibited, to some extent, the same profile of mTOR phosphorylation as healthy cells. Myocytes exposed to 0.5% or 2.0% O_2 displayed similar profiles of phosphorylation of Akt, ERK1/2 and mTOR. In addition, we have previously shown that AMPKα phosphorylation was enhanced in HL-1cells following 4 hours of reoxygenation compared to healthy cells and that the protein levels were not affected by H/R. While the status of activation of Akt and mTOR might maintain basal levels of autophagy in HL-1 cells exposed to H/R, the concomitant activation of AMPKα and inactivation of ERK1/2 were consistent with an enhanced autophagic activity. However, we observed that autophagy was repressed in HL-1 cells following 4 hours of reoxygenation. This effect may result from other cellular events triggered by H/R.

3.2.3. The role of autophagy during cardiac hypoxia-reoxygenation

To investigate whether autophagy is protective or detrimental to cardiac cells during hypoxia, we have employed a pharmacological approach to block autophagy at its initiation level. The class III PI3-K is involved in the sequestration step of autophagy and 3-methyladenine (3-MA) is commonly used to inhibit its activity [55]. Thus, HL-1 cells were exposed to 2 hours of hypoxia (0.5% or 2.0% O_2) in presence or absence of 10 mM 3-MA. To verify the effect on the autophagic response, HL-1 cells were co-incubated with 25 nM Baf A1 and the LC3-II levels

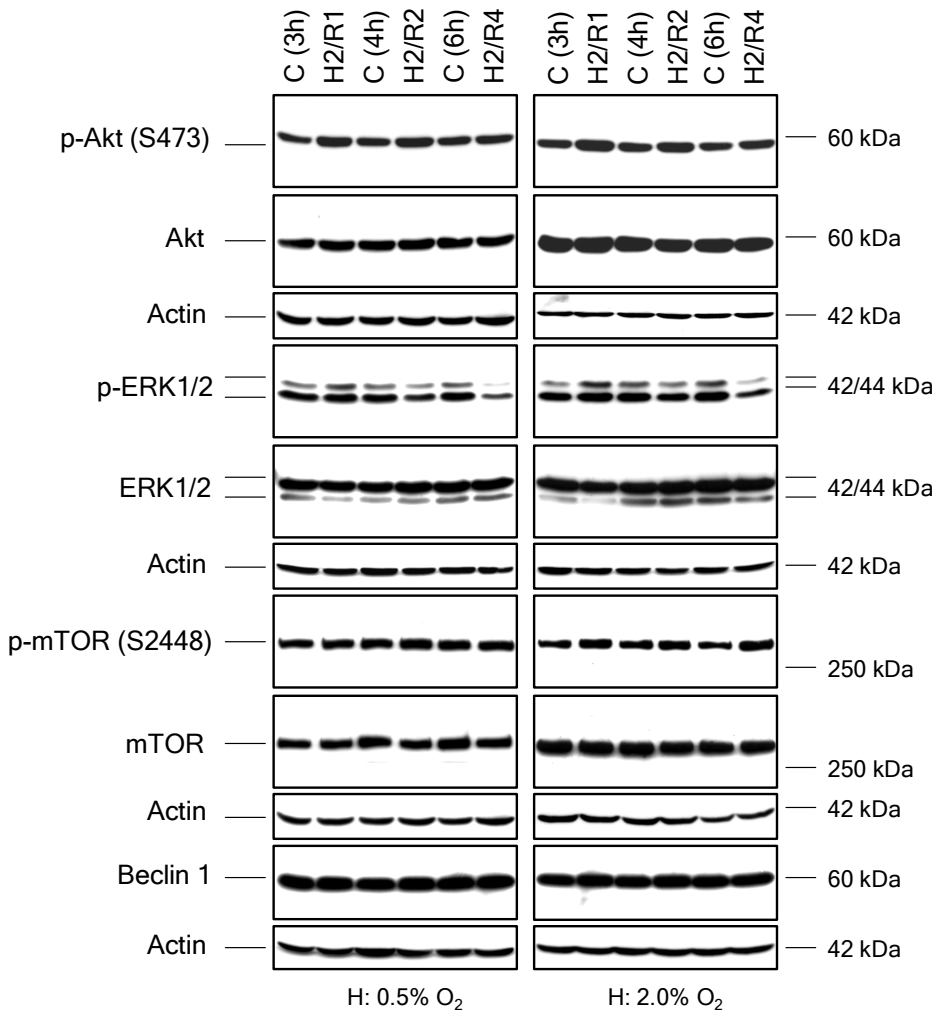

<u>Figure 17a</u>: Effect of hypoxia-reoxygenation on modulators of autophagy. HL-1 cells were exposed to 2 hours of hypoxia with 0.5% (left panel) or 2.0% (right panel) O_2 followed by 1, 2 and 4 hours of reoxygenation (H2/Rs). The temporal profiles of expression and activation of Akt, ERK1/2, mTOR and Beclin 1 were analyzed by Western blotting. Actin was used as a loading control. Control cells were grown in normal conditions for the corresponding period of time (C). Results shown are representative of at least three independent experiments. The quantifications are shown in Figure 17b.

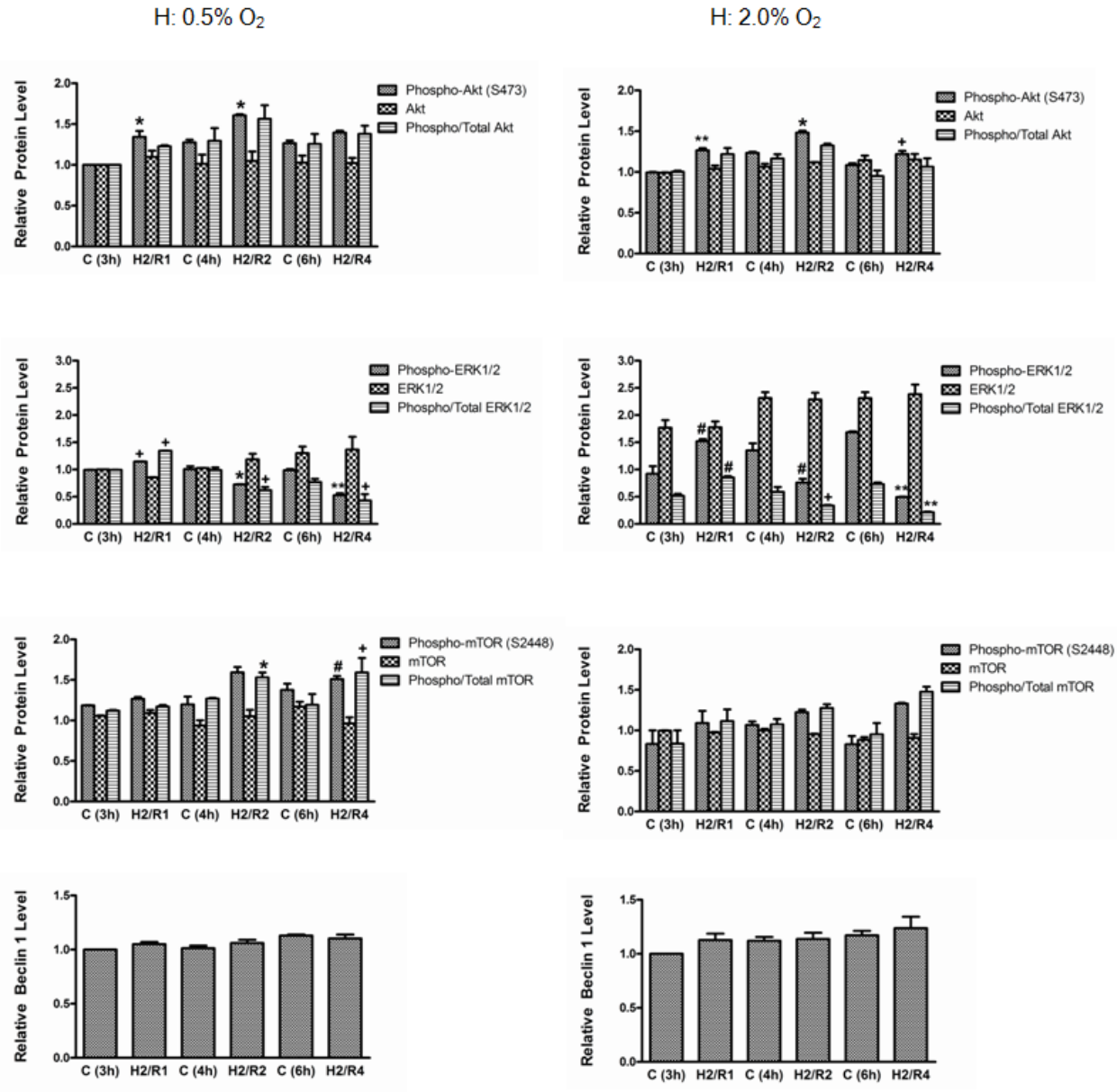

<u>Figure 17b</u>: Effect of hypoxia-reoxygenation on modulators of autophagy. Quantifications of Akt, ERK1/2, mTOR and Beclin 1 expression and activation levels in HL-1 cells exposed to 2 hours of hypoxia with 0.5% (left panel) or 2.0% (right panel) O_2 followed by 1, 2 and 4 hours of reoxygenation (H2/Rs). The levels of expression of Akt, ERK1/2, mTOR and Beclin 1 were determined in relation to actin. The levels of phosphorylated Akt, ERK1/2 and mTOR were determined in relation to both, actin and the total protein level. Ratio were determined by densitometry analysis of the immunoreactive bands and represented graphically as mean ± SEM from at least three independent experiments. $^{**}p<0.0001$, $^{*}p<0.001$, $^{\#}p<0.01$, $^{+}p<0.05$ in comparison to the corresponding control (C) by One-Way ANOVA.

were assessed by western blot analysis. 3-MA reduced autophagy in healthy and hypoxic cells as judged by the dramatic decrease in LC3-II cumulative levels (Figure 18). This result indicated that 3-MA treatment efficiently inhibited autophagy in hypoxic cardiac cultures.

To investigate the association of autophagy with cardiac cell death during hypoxia, HL-1 cells were exposed to 2 hours of hypoxia (0.5% or 2.0% O_2) in presence of 10 mM 3-MA and cell death was assessed by both Trypan blue exclusion and flow cytomteric analysis of Annexin V-PI stained myocytes. Under normal conditions, 3-MA slightly increased the basal level of cell death. The presence of 3-MA during the hypoxic period significantly enhanced hypoxia-mediated cell death. The levels of dead (Trypan blue positive) cells exposed to 0.5 % and 2.0% O_2 increased by 1.7- and 1.5-fold, respectively (Figure 19A). The same effect of 3-MA on cell death following hypoxia was observed by flow cytometric analysis, but to a lesser extent (Figure 19B). The inhibition of autophagy did not affect the level of hypoxic cells undergoing apoptosis. These results suggest that autophagy promotes the survival of HL-1 cardiomyocytes during hypoxia. This finding was further confirmed by establishing the association between autophagy stimulation and hypoxia-induced cell death. Our previous results indicated that the substitution of glucose for 2-DG in the ischemia buffer caused an up-regulation of autophagy in HL-1 cells exposed to hypoxia (0.5% and 2.0% O_2). Thus, we sought to determine whether this effect protected cardiac cells against the injurious effects of hypoxia. As shown in Figure 20, the presence of glucose during 2 hours of hypoxia induced a significant decrease in the percentage of Trypan blue positive cardiomyocytes. Interestingly, the cardioprotection afforded by glucose was slightly greater for hypoxic myocytes exposed to 0.5% O_2 than 2.0% O_2 as the number of dead

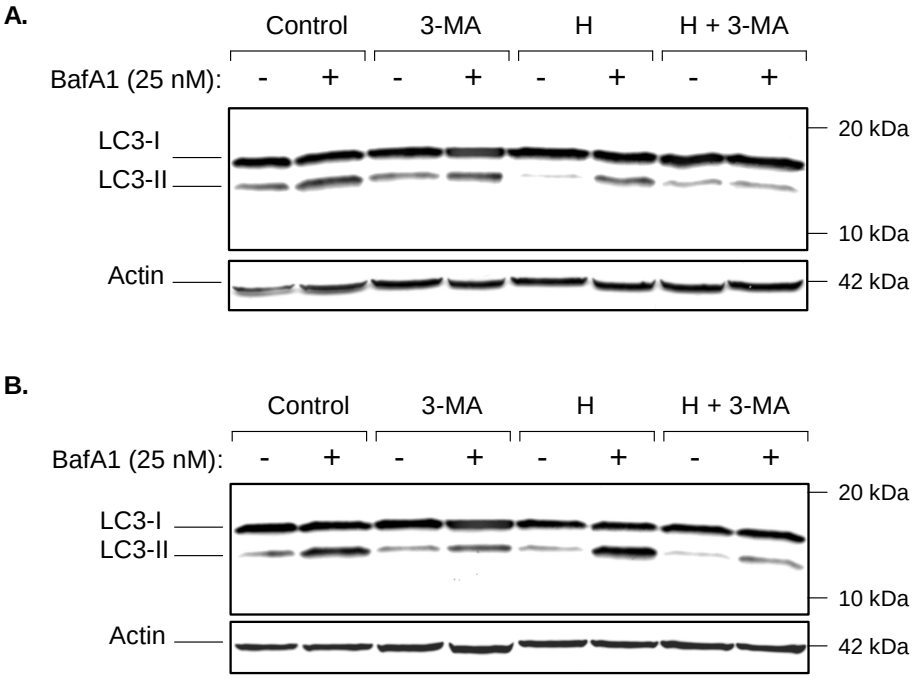

Figure 18: Effect of 3-methyladenine on autophagy in hypoxic cardiomyocytes. HL-1 cells were exposed to 2 hours of hypoxia (H) with **A**. 0.5% O_2 or **B**. 2.0% O_2 and treated with 10 nM 3-MA (H + 3-MA). Baf A1 (25 nM) was absent (-) or present (+) throughout hypoxia. Control samples include HL-1 cells incubated under normal conditions (Control) and subjected to the same drug treatments. Actin was used as a loading control. Results are representative of two independent experiments.

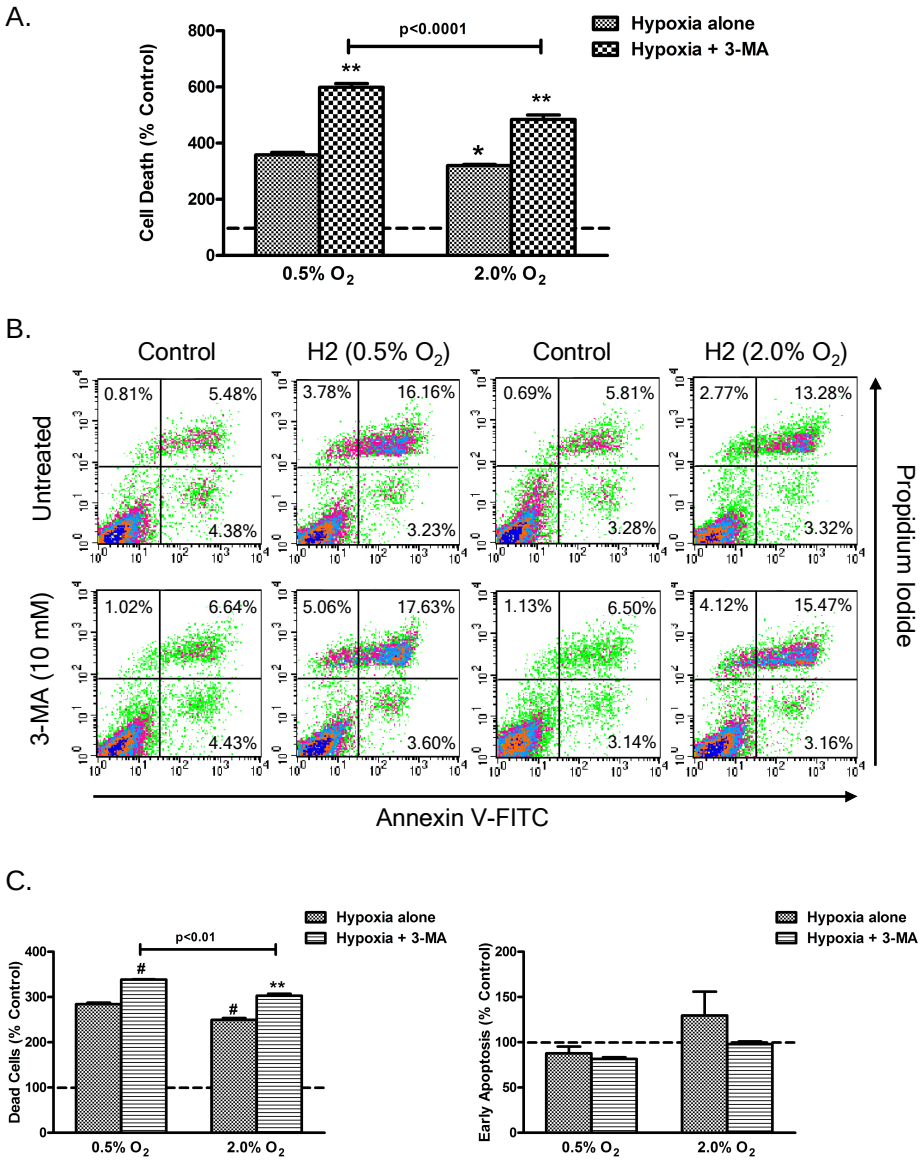

Figure 19: Effect of 3-methyladenine on hypoxia-induced cardiac cell death. HL-1 cells were exposed to 2 hours of hypoxia (H2) with 0.5% or 2.0% O_2 in presence of 10 mM 3-MA. **A**. Cell death was assessed by Trypan blue exclusion. The percentages of cell death in relation to controls (healthy cells) were represented graphically as mean ± SEM from three independent experiments. $^{**}p<0.0001$ (vs. Hypoxic alone) by One-Way ANOVA, $p<0.0001$ (vs. 0.5% O_2) by Two-Way ANOVA. **B, C**. Flow cytometric analysis of AnnexinV-PI stained cells. The percentages of dead cells (Annexin $V^{+/-}$-PI^{+}) and early apoptotic cells (Annexin V^{+}-PI^{-}) relative to control levels expressed as mean ± SEM from three independent experiments and represented graphically. $^{**}p<0.0001$, $^{\#}p<0.001$ (vs. Hypoxia alone) by One-Way ANOVA and $p<0.01$ (vs. 0.5% O_2) by Two-Way ANOVA.

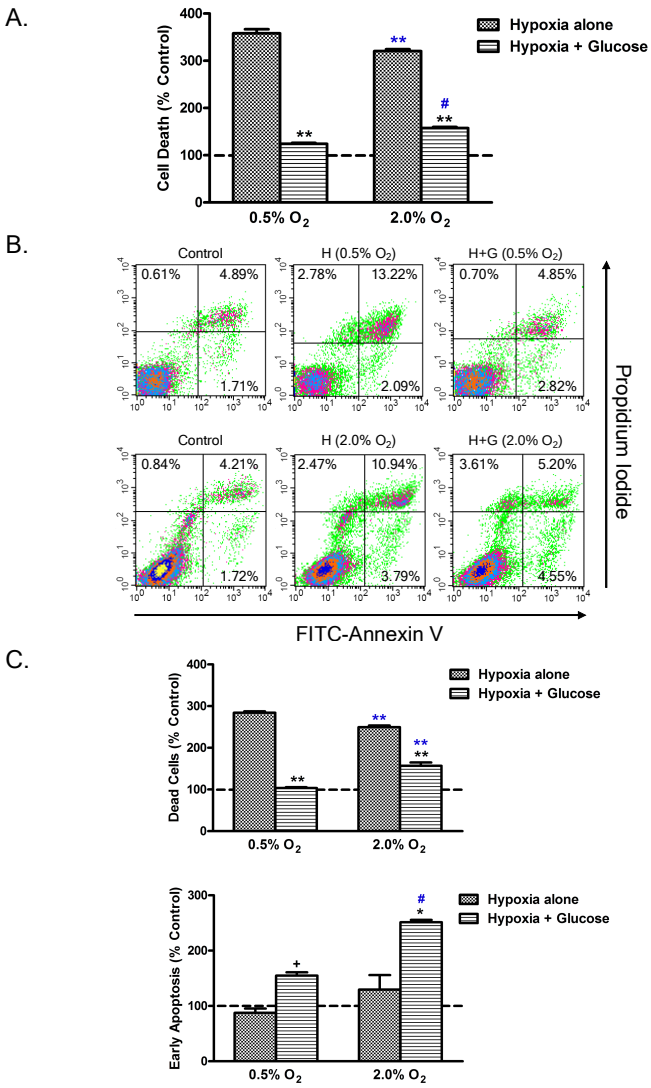

<u>Figure 20</u>: Cardiac cell death following hypoxia induced in presence of glucose. HL-1 cells were exposed to 2 hours of hypoxia with 0.5% or 2.0% O_2 in presence of 10 mM 2-deoxyglucose (hypoxia alone) or 20 mM glucose (hypoxia + glucose). **A**. Necrotic cell death was assessed by Trypan blue exclusion. The percentages of cell death in relation to controls (healthy cells) were represented graphically as mean ± SEM from three independent experiments. $^{**}p<0.0001$ (vs. hypoxia alone) by One-Way ANOVA, $^{**}p<0.0001$ and $^{\#}p<0.001$ (vs. 0.5% O_2) by Two-Way ANOVA. **B, C**. Flow cytometric analysis of AnnexinV-PI stained cells. The percentages of dead cells (UL+UR) and early apoptotic cells relative to control levels were represented graphically and expressed as mean ± SEM from three independent experiments. $^{**}p<0.0001$, $^{+}p<0.01$ $^{*}p<0.05$ (vs. hypoxia alone) by One-Way ANOVA and $^{**}p<0.0001$ and $^{\#}p<0.001$ (vs. 0.5% O_2) by Two-Way ANOVA.

cells reached 120% and 160% of controls, respectively ($p<0.001$ by two-way ANOVA). Similar results were obtained by flow cytometric analysis of Annexin-V/PI stained hypoxic cells (Figure 20B, C). In addition, the reduction in cell death was accompanied by a concomitant increase in early apoptosis. Indeed, the presence of glucose during hypoxia resulted in a significant increase in the percentage of early apoptotic cells, which reached 118% and 251% of controls when hypoxia was induced with 0.5% and 2.0% O_2, respectively ($p<0.001$ by two way ANOVA). These results suggest that the events triggered by glucose during hypoxia are oxygen-dependent. These findings further evidenced a cardioprotective role of autophagy during hypoxia.

To define the role played by autophagy during reoxygenation, HL-1 cells were exposed to 2 hours of hypoxia (0.5% or 2.0% O_2) followed by 2 and 4 hours of reoxygenation. Autophagy was inhibited during reoxygenation only, as 10 mM 3-MA was present throughout the reoxygenation period (H2/R2) or during the last 2 hours of reoxygenation (H2/R4). The successful inhibition of autophagy was verified by examining the levels of LC3-II in presence of 25 nM Baf A1 in HL-1 cells exposed to H/R by Western blotting. As shown in Figure 21, 3-MA significantly reduced the levels of accumulation of LC3-II in both, healthy cells and myocytes exposed to H/R. To determine whether the inhibition of autophagy exacerbates or reduces cell death following H/R, cell death was measured in HL-1 cells exposed to H2/R2 and H2/R4. 3-MA was present throughout reoxygenation (H2/R2) or added during the last two hours of reoxygenation (H2/R4). As shown in Figure 22A, 3-MA treatment significantly increased the percentage of cells accumulating Trypan blue during the 4-hour period of reoxygenation. In agreement with this, the level of dead cells (Annexin $V^{+/-}$-PI^{+}) was significantly increased when autophagy was inhibited during the reoxygenation period as analyzed by flow cytomtery (Figure 22B). These results indicate that 3-MA exacerbated cardiac cell death during reoxygenation. The

findings concerning apoptosis were more complicated. Interestingly, 3-MA had opposite effects on early apoptosis depending on the degree of hypoxia. When hypoxia was induced with 0.5% O_2, 3-MA increased the number of cells undergoing early apoptosis during the last two hours of reoxygenation (H2/R4). Conversely, the inhibition of autophagy during reoxygenation attenuated the level of early apoptosis in cardiac cultures pre-exposed to 2.0% O_2. One possible explanation for these results is that 3-MA may accelerate the apoptotic program in HL-1 cells. In the case of 0.5% O_2, 3-MA enhanced the level of cells undergoing early apoptosis. In contrast to severe hypoxia, cells that have been previously exposed to hypoxic conditions of 2.0% O_2 exhibited higher level of early apoptosis following 2 hours of reoxygenation and it is likely that 3-MA induced a rapid progression from early to late apoptosis, resulting in a decrease in early apoptotic cells. This possibility can be tested by evaluating the levels of late apoptosis. Nevertheless, these data indicated that 3-MA enhanced both necrosis and early apoptosis during reoxygenation and provided evidence that despite its low level, autophagy plays a protective role during H/R.

In summary, we have shown that hypoxia (2 hours), depending on its degree, either partially repressed autophagy in the case of 0.5% O_2 or did not affect this process in HL-1 cells exposed to 2.0% O_2. As we explored the molecular mechanisms underlying the autophagic response elicited by H/R, we demonstrated that energy limited autophagy in hypoxic cells and highlighted a disconnect between autophagy and the activation status of its key modulators. Indeed, the inhibition of mTOR mediated by AMPK and/or Akt did not lead to a stimulation of autophagy in hypoxic cardiomyocytes. In addition, the process of autophagy was significantly impaired in reoxygenating HL-1 cells with a timing that was oxygen-dependent. Reoxygenation induced a renormalization of the activation levels of Akt and mTOR suggesting that these

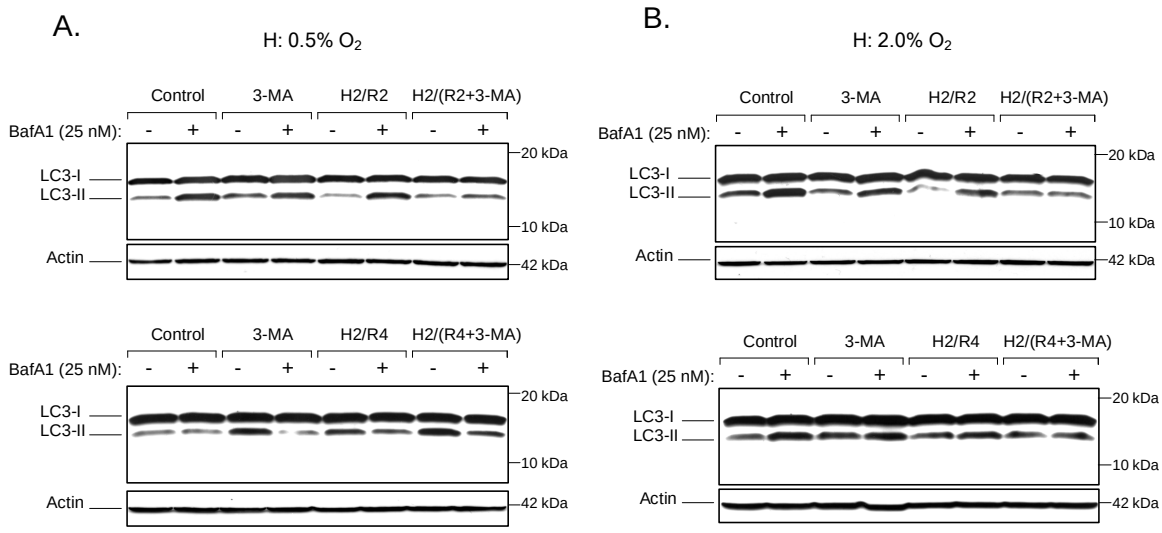

<u>Figure 21</u>: Effect of 3-methyladenine on autophagy in cardiomyocytes exposed to hypoxia-reoxygenation. HL-1 cells were exposed to 2 hours of hypoxia with **A**. 0.5% O_2 or **B**. 2.0% O_2 followed by 2 or 4 hours of reoxygenation. 3-MA (10 mM) was absent (H2/R2, H2/R4), present either throughout reoxygenation (H2/(R2 + 3-MA)) or during the last two hours of reoxygenation (H2/(R4 + 3-MA)). Baf A1 (25 nM) was absent (-) or present (+) throughout reoxygenation (H2/R2) or the last two hours of reoxygenation (H2/R4). Control samples include HL-1 cells incubated under normal conditions and subjected to the same drug treatments (Control, 3-MA). Autophagy was assessed by LC3 Western blotting and actin was used as a loading control. Results are representative of two independent experiments.

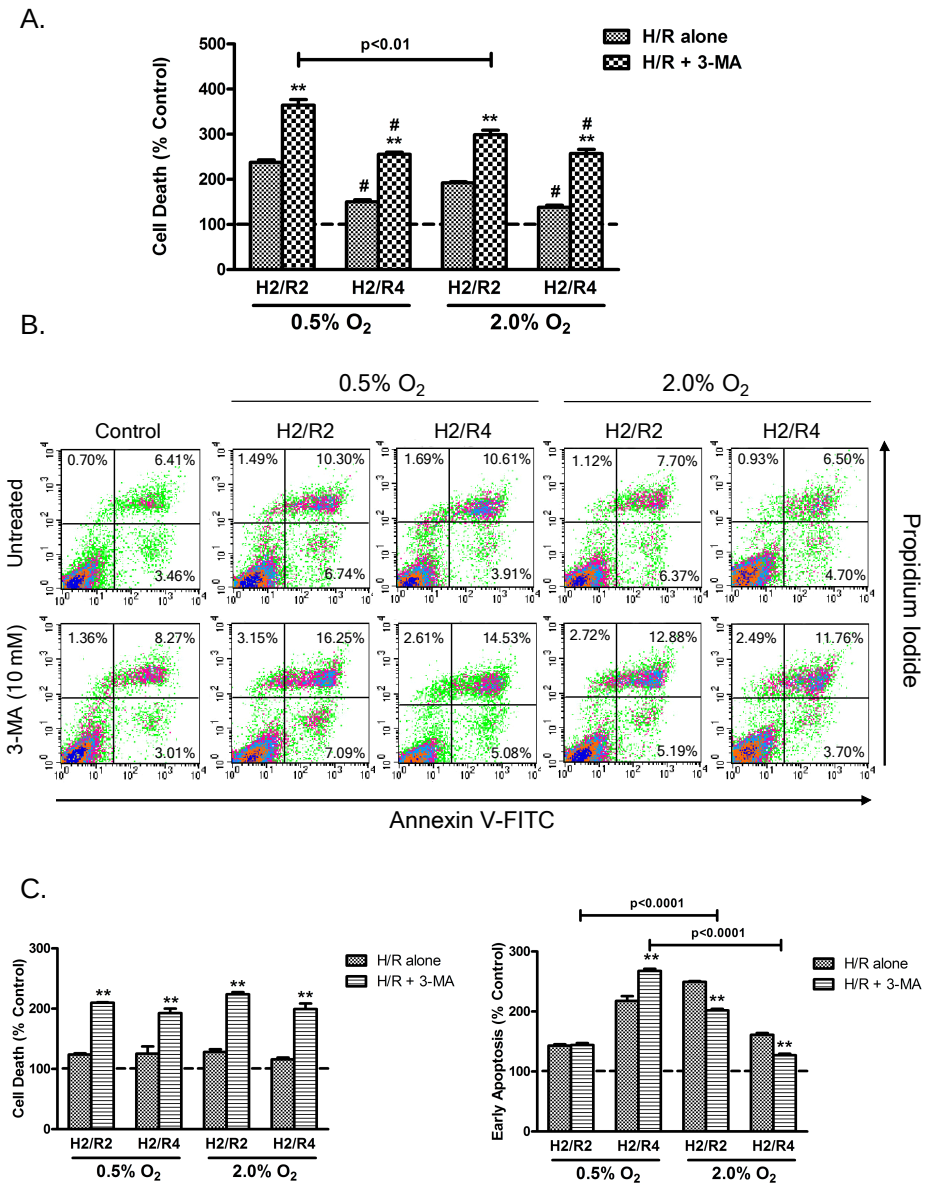

<u>Figure 22</u>: Effect of autophagy inhibition on hypoxia-reoxygenation-mediated HL-1 cell death. HL-1 cells were exposed to 2 hours of hypoxia (0.5% or 2.0% O_2) followed by 2 and 4 hours of reoxygenation (H2/Rs). 3-MA (10 mM) was present throughout the rexoygenation period (H2/R2) or during the last 2 hours of reoxygenation (H2/R4). **A**. Cell death was assessed by Trypan blue exclusion. The percentages of cell death in relation to controls were represented graphically as mean ± SEM from three independent experiments. $^{**}p<0.0001$ (vs. H/R alone by One-Way ANOVA and $p<0.01$ in comparison to Hypoxia (0.5% O_2) by Two-Way ANOVA. **B, C**. Flow cytometric analysis of AnnexinV-PI stained cells. The percentages of dead cells (Annexin $V^{+/-}/PI^-$) and early apoptotic cells (Annexin V^+/PI^-) relative to control levels are expressed as mean ± SEM from three independent experiments and represented graphically. $^{**}p<0.0001$ (vs. H/R alone) by One-Way ANOVA and $p<0.0001$ in comparison to Hypoxia (0.5% O_2) by Two-Way ANOVA.

pathways may not be responsible for the repression of autophagic activity. In contrast the dephosphorylation of ERK1/2 and enhanced activation of AMPKα failed to increase autophagy during reoxygenation, suggesting the existence of other cellular events that limit autophagy. Finally, we have shown that autophagy serves as a protective mechanism during both hypoxia and reoxygenation. The stimulation of autophagy mediated by glucose and the inhibition of autophagy mediated by 3-MA, attenuated and enhanced cell death induced by hypoxia, respectively. The presence of 3-MA in reoxygenated cardiomyocytes exacerbated cell death following H/R.

3.3. Effect of Sildenafil in HL-1 Cardiomyocytes Exposed to Hypoxia-Reoxygenation

3.3.1. Cardioprotective effect of sildenafil during hypoxia-reoxygenation

Sildenafil citrate (SNF) is an inhibitor of phosphodiesterase 5 (PDE5) that was shown to exhibit cardioprotective properties in various models of I/R injury. The ultimate objective of this project was to determine the efficacy of SNF as a cardioprotectant in our model of I/R. To do so, we employed H/R conditions that induced a significant level of injury. This result was observed when HL-1 cells were exposed to 2 hours of hypoxia induced with 0.5% O_2 alone or followed by 2 hours of reoxygenation. Although PDE5 was shown to be expressed in isolated ventricular cardiomyocytes from mice [64], we have confirmed the expression of PDE5 in murine atrial HL-1 cardiomyocytes by western blotting (Figure 23A). To determine whether SNF can protect HL-1 cells against hypoxia induced injury, HL-1 cells were exposed to 2 hours of hypoxia in presence of graded concentrations of SNF (0, 1.5 and 15 μM). In parallel, control cells were

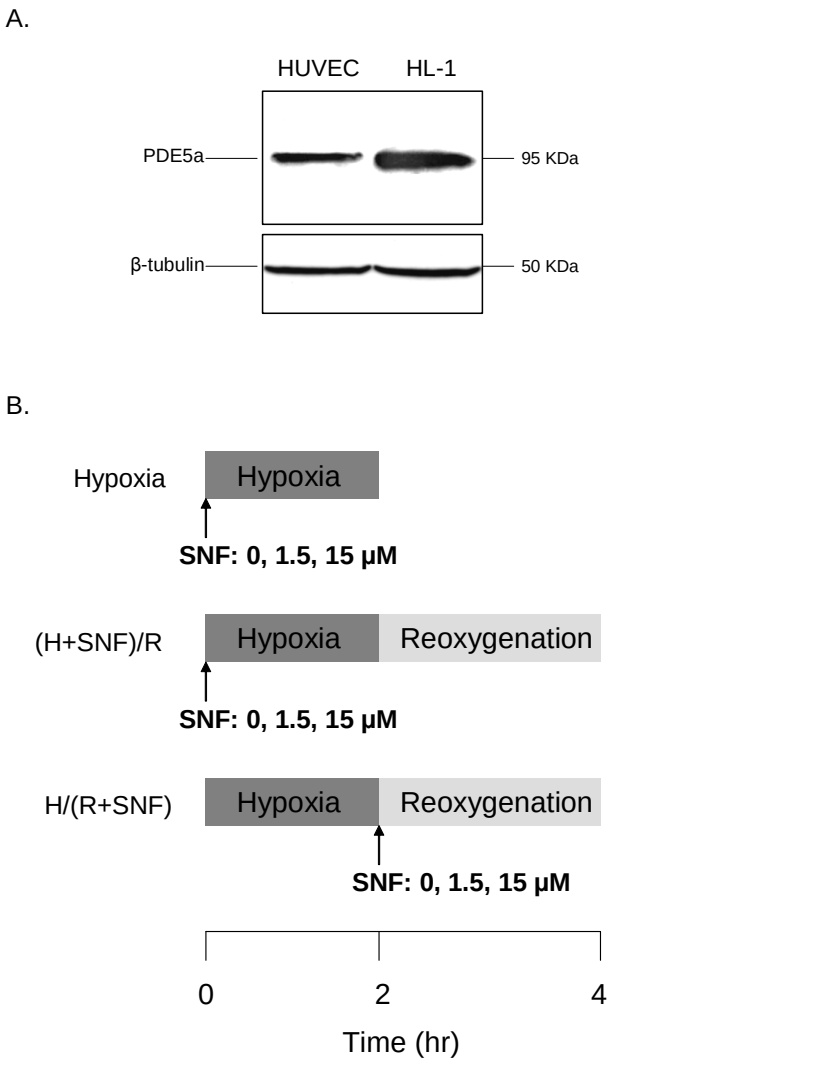

Figure 23: A. Expression of PDE5 in HL-1 cardiomyocytes. HL-1 cell lysate was analyzed by western blotting for the expression of PDE5, the target of sildenafil. Human Umbilical Vein Endothelial Cells (HUVEC) lysate was used as a positive control. β-Tubulin was used a loading control. **B. Experimental protocols for Sildenafil studies.** HL-1 cells were exposed to 2 hours of hypoxia (0.5% O_2) alone (Hypoxia) or followed by 2 hours of reoxygenation where sildenafil (SNF: 0, 1.5, 15 μM) was added at the onset of hypoxia ((H+SNF)/R) or reoxygenation (H/(R+SNF)).

treated with similar doses of SNF and grown under normal conditions for an identical period. As previously shown, hypoxia induced a 3.6-fold increase in the percentage of Trypan blue positive cardiomyocytes in comparison to control conditions (Figure 24A). The presence of 15 μM SNF during hypoxia significantly limited the occurrence of cell death as the number of dead cells was increased only by 2-fold compared to control. A lower dose of SNF (1.5 μM) had no effect on hypoxia-induced cell death. Interestingly, SNF had an opposite effect on the viability of cells grown under normal conditions as a dose of 15 μM induced a slight increase in cell death. These results suggest that high dose of SNF (15 μM) seems to be beneficial to hypoxic cardiac cells. The effect of SNF on apoptosis was also examined by flow cytometric analysis of Annexin V-PI labeled cells (Figure 24B). As previously shown, hypoxia induced an increase in cell death with no effect on the basal level of early apoptosis. These outcomes were not altered by the presence of SNF in hypoxic cultures. However, the percentage of early apoptotic cells in healthy cultures was significantly decreased by SNF treatment (15 μM). Altogether, these results suggest that high doses of SNF may be cardioprotective against hypoxia.

Next, we sought to determine whether SNF could protect cardiac cells against injury induced by 2 hours of hypoxia followed by 2 hours of reoxygenation. Two SNF treatment regimens were tested, SNF (0, 1.5, 15 μM) was applied at the onset of hypoxia or reperfusion. The rationale behind this approach is that an infarct-reducing agent can be applied at different times depending on the clinical situation I/R occurs. In patients undergoing cardiac surgery, the cardioprotective agent can be applied before or at the onset of the ischemic event (e.g. addition of the drug in the cardioplegic solution). In contrast, patients who suffer an acute myocardial infarction can only be treated by applying the drug at reperfusion. As previously shown, the level

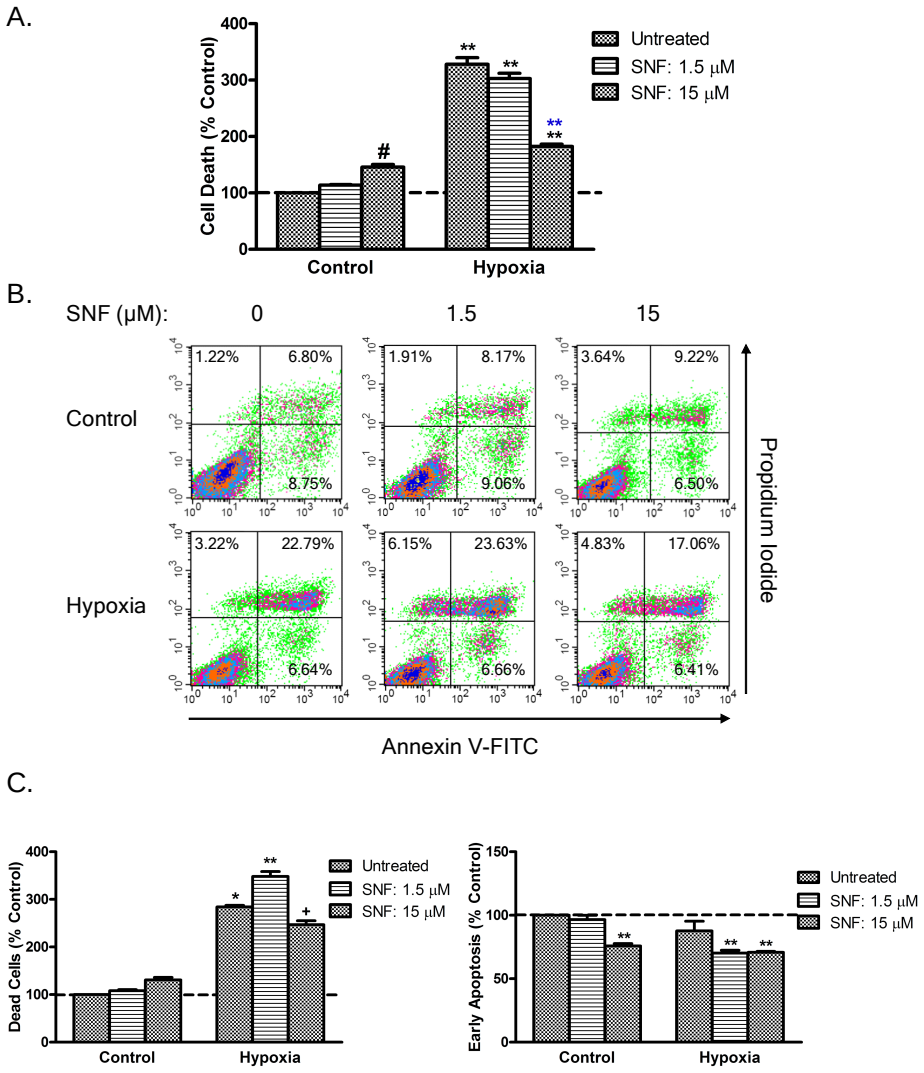

Figure 24: Effect of sidenafil on hypoxia-induced cardiac cell death. HL-1 cells were exposed to 2 hours of hypoxia (0.5% O_2) in presence of SNF (0, 1.5, 15 μM). Control cells were treated with similar concentrations of SNF and grown under normal conditions for an identical period of time. **A.** Trypan blue exclusion. The percentages of cell death in relation to controls (healthy cells) were represented graphically as mean ± SEM from three independent experiments. **p<0.0001, $^{\#}$p<0.01 (vs. Control) and **p<0.0001 (vs. untreated hypoxic cells) by One-Way ANOVA. **B.** Flow cytometric analysis of AnnexinV-PI stained cells. The percentages of dead cells (UL+UR) and early apoptotic cells relative to control levels were represented graphically and expressed as mean ± SEM from three independent experiments. **p<0.0001, *p<0.001, $^{+}$p<0.05 (vs. Untreated Control) by One-Way ANOVA.

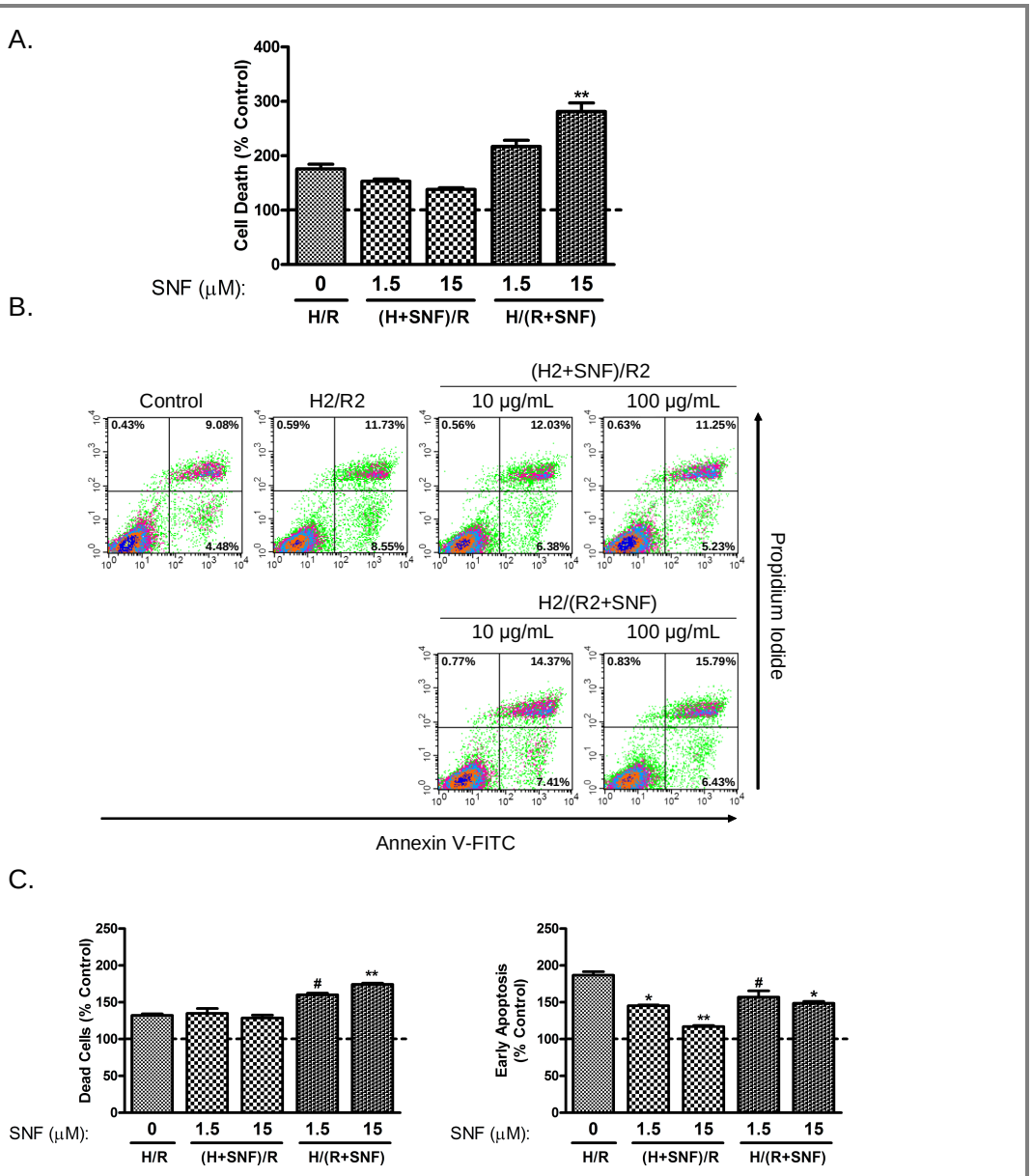

Figure 25: Effect of sildenafil on cardiac cell death elicited by hypoxia-reoxygenation. HL-1 cells were exposed to 2 hours of hypoxia (0.5% O_2) followed by 2 hours of reoxygenation (H/R). SNF (0, 1.5, 15 μM) was added at the onset of hypoxia [(H+SNF)/R] or reoxygenation [H/(R+SNF)]. Control cells were treated with similar concentrations of SNF and grown under normal conditions for an identical period of time. **A.** Trypan blue exclusion. The percentages of cell death in relation to controls (healthy cells) were represented graphically as mean ± SEM from three independent experiments. **p<0.0001 (vs. H/R) by One-Way ANOVA. **B.** Flow cytometric analysis of AnnexinV-PI stained cells. The percentages of dead cells (UL+UR) and early apoptotic cells relative to control levels were represented graphically and expressed as mean ± SEM from three independent experiments. **p<0.0001, *p<0.001, $^{\#}$p<0.01 (vs. H/R) by One-Way ANOVA.

of cell death induced by hypoxia was significantly reduced following 2 hours of reoxygenation as it reached ~180% of controls. This effect was accompanied by a 3-fold increase in the population of early apoptotic cells. The presence of SNF during hypoxia had no effect on the overall level of cell death following 2 hours of reoxygenation as assessed by both Trypan blue and PI staining (Figure 25). However, the level of early apoptosis was significantly decreased by SNF in a dose-dependent manner, indicating that the application of SNF at the onset of hypoxia limited the activation of apoptosis during the first two hours of reoxygenation. Conversely, the administration of SNF (1.5 and 15 μM) at the onset of reoxygenation resulted in a significant increase in cell death compared to untreated H/R cells (Figure 25). This effect was accompanied by a slight, though significant, decrease in the population of early apoptotic cells. This result suggests that SNF may accelerate the progression of early apoptotic cells to later stages of the apoptotic program. Thus, the application of SNF during reoxygenation may be detrimental to cardiac cells. Taken together, these results suggest that the presence of SNF during hypoxia may protect cardiac cells against hypoxia-induced cell death and decreases the occurrence of apoptosis during reoxygenation in a dose-dependent manner. A dose of 15 μM SNF was more effective in protecting cardiac myocytes against H/R-mediated injury. Conversely, the addition of SNF during reoxygenation exacerbated H/R-induced cardiac injury.

3.3.2. The modulation of autophagy by sildenafil during hypoxia-reoxygenation

The effect of SNF on autophagy during myocardial I/R injury has never been studied. Thus, we sought to determine how SNF could affect the autophagic response of HL-1 cells in our model. To this end, HL-1 cardiac cultures were exposed to 2 hours of hypoxia and simultaneously treated with increasing concentration of SNF (0, 1.5, 15 μM). We have examined

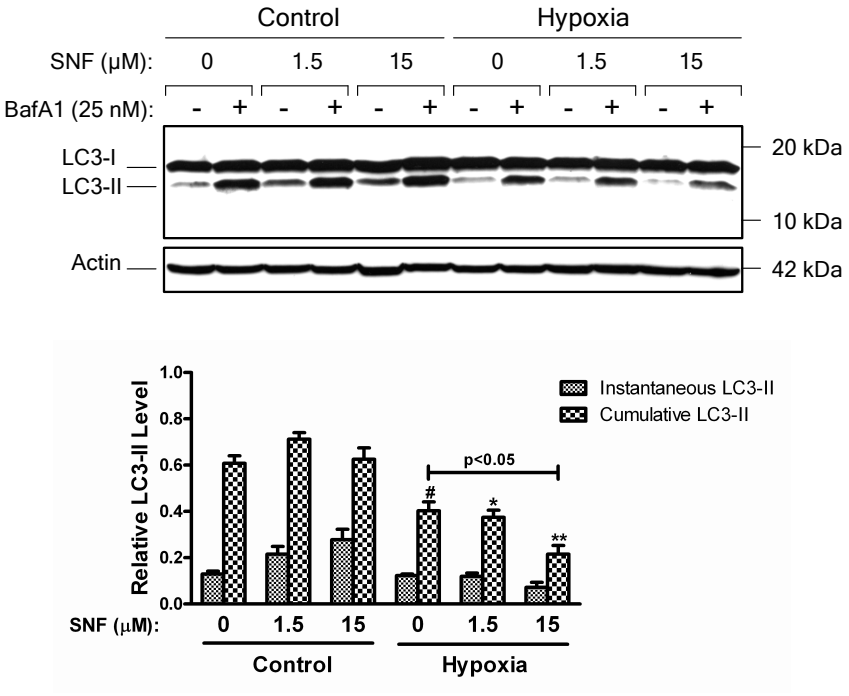

Figure 26: Effect of sildenafil on autophagy in hypoxic cardiac cells. HL-1 cells were exposed to 2 hours of hypoxia (Hypoxia, 0.5% O_2) in presence of SNF (0, 1.5, 15 μM). Control cells were treated with similar doses of SNF and grown in normal conditions for the identical period of time. Baf A1 (25 nM) was absent (-) or present (+) throughout hypoxia. Autophagy was assessed by LC3 Western blotting and actin was used as a loading control. The ratio LC3-II/Actin were determined by densitometry analysis of the immunoreactive bands and represented graphically as mean ± SEM from four independent experiments. $^{**}p<0.0001$, $^{*}p<0.001$, $^{\#}p<0.01$ (vs. Untreated Control) and $p<0.05$ (vs. Untreated Hypoxia) by One-Way ANOVA.

the profiles of LC3 processing in the absence and presence of 25 nM Baf A1. As documented in Figure 26, SNF had no significant effect on the basal level of autophagy in healthy HL-1 cells. As previously shown, hypoxia induced a partial inhibition of autophagy in HL-1 cells as judged by the decrease in LC3-II accumulation in comparison to control conditions. This effect was enhanced when SNF (15 μM) was present during hypoxia, suggesting that SNF limited autophagy in hypoxic cells. Next, we investigated the effect of SNF on autophagy in HL-1 cells exposed to 2 hours of hypoxia followed by 2 hours of reoxygenation. SNF (0, 1.5, 15 μM) was added either at the onset of hypoxia or reoxygenation. The results shown in Figure 27A indicate that under normal conditions, SNF significantly increased the level of LC3-II accumulation in a dose-dependent manner, suggesting that SNF induced autophagy in HL-1 cells. The exposure of HL-1 cells to 2 hours of hypoxia followed by 2 hours of reoxygenation markedly reduced the accumulation of LC3-II associated with the reoxygenation period. These observations are in line with the results obtained from the reoxygenation time course experiment. The presence of SNF throughout hypoxia induced a significant increase in the accumulation of LC3-II during reoxygenation in comparison to untreated H/R cells. This effect was more pronounced with SNF at a dose of 1.5 μM. However, the SNF-induced increase in LC3-II accumulation remained lower than control cells. These results suggest that SNF limited the inhibition of autophagy induced by H/R in cardiac cells. The addition of SNF at the onset of reoxygenation resulted in a different profile of autophagy in cardiomyocytes exposed to H/R. As seen in Figure 27B, the level of LC3-II accumulation in HL-1 cardiac cells exposed to H/R was not altered by the presence of SNF during reoxygenation. However, both concentrations of SNF induced a significant increase in the instantaneous level of LC3-II. Since Baf A1 treatment did not enhance the accumulation of LC3-II, these results suggest that SNF, when present during reoxygenation, caused an inhibition

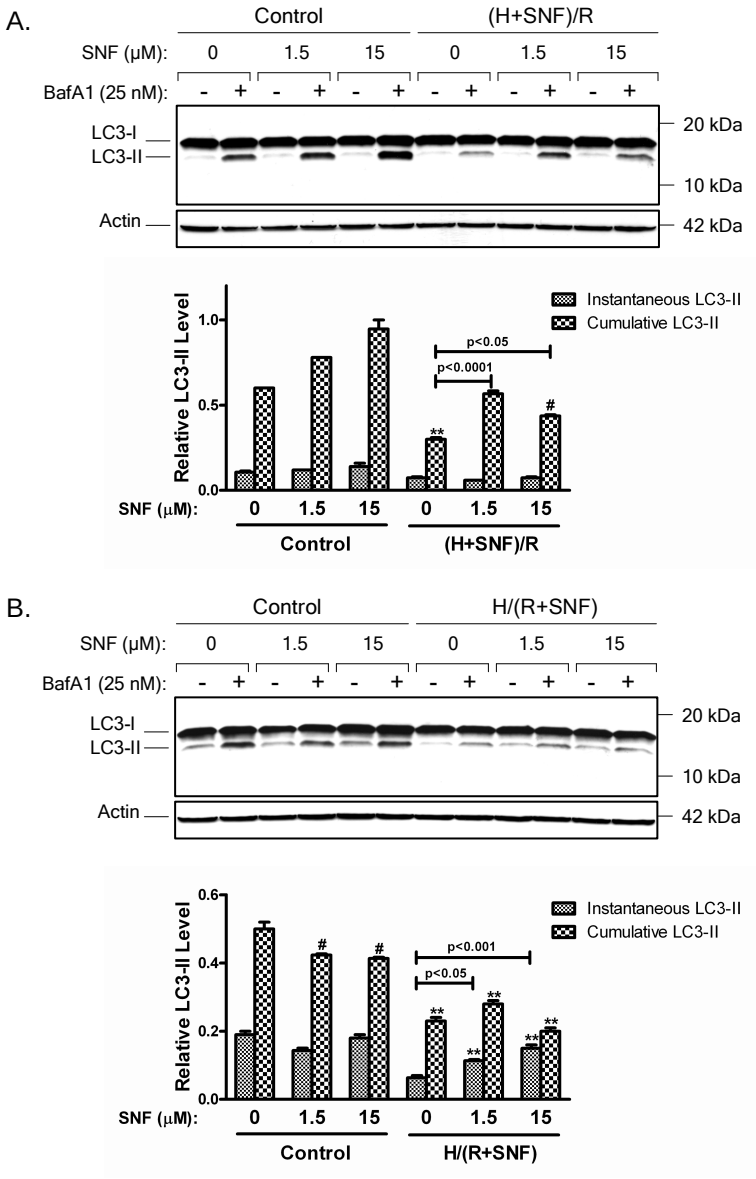

<u>Figure 27</u>: Effect of sildenafil on autophagy in cardiomyocytes exposed to hypoxia-reoxygenation. HL-1 cells were exposed to 2 hours of hypoxia (0.5% O_2) followed by 2 hours of reoxygenation. SNF (0, 1.5, 15 μM) was added at the onset of hypoxia [**A**, (H+SNF)/R] or reoxygenation [**B**, H/(R+SNF)]. Control cells were treated with similar doses of SNF and grown in normal conditions for identical periods of time. Baf A1 (25 nM) was absent (-) or present (+) throughout reoxygenation. Autophagy was assessed by LC3 Western blotting and actin was used as a loading control. The ratio LC3-II/Actin were determined by densitometry analysis of the immunoreactive bands and represented graphically as mean ± SEM from four independent experiments. $^{**}p<0.0001$, $^{\#}p<0.01$ (vs. Untreated Control) and p<0.001, 0.001, 0.05 (vs. Untreated H/R) by One-Way ANOVA.

of autophagy in reoxygenated HL-1 cells. Interestingly, the level of autophagy was also significantly decreased in healthy cells treated with SNF as judged by the reduced accumulation of LC3-II. Altogether, our results demonstrate that depending on its treatment regimen, SNF exerted antagonistic effects on autophagy in HL-1 cells during H/R. The administration of SNF during hypoxia induced autophagy during reoxygenation and this effect was maximal with a dose of 1.5 μM. In contrast, autophagy was further inhibited by SNF when added at the onset of reoxygenation. This effect was higher with a dose of 15 μM.

3.3.2. The effect of sildenafil on cardiac energetics during hypoxia-reoxygenation

To gain some insights into the mechanism employed by SNF to mediate its effects on cell death and autophagy during H/R, we sought to examine the effect of SNF on the bioenergetic status of cardiac cells during H/R. To this end, HL-1 cells were exposed to 2 hours of hypoxia in presence of graded concentrations of SNF (0, 1.5, 15 μM) and the ATP levels were measured. The results shown in Figure 28 indicate that SNF (15 μM) significantly limited the ATP depletion induced by hypoxia in HL-1 cells. The ATP levels in SNF-treated hypoxic cells reached approximately 30% of controls (vs. 10% of controls in hypoxic cells). This result suggests that SNF may partially protect cardiac cells from the deleterious metabolic effects of hypoxia. Next, we have examined the effect of SNF on the replenishment of the intracellular ATP stores during reoxygenation. Thus, HL-1 cells were exposed to 2 hours of hypoxia followed by 2 hours of reoxygenation, and SNF (0, 1.5, 15 μM) was added at the onset of hypoxia or reoxygenation. As previously shown, reoxygenation induced an increase in ATP in hypoxic cardiomyocytes as the ATP level reached 20% of controls. However, SNF had no significant

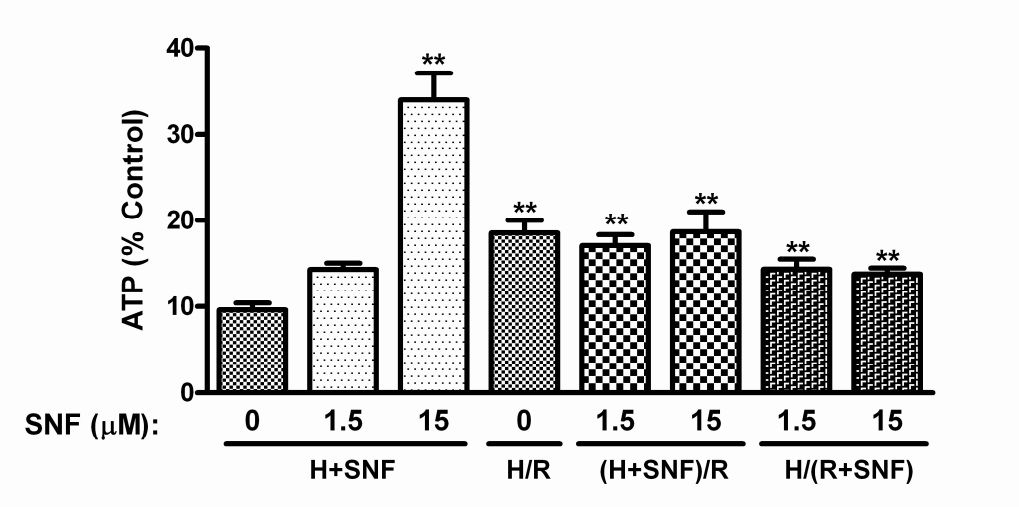

Figure 28: Modulation of the bioenergetic status of cardiac cells exposed to hypoxia-reoxygenation by Sildenafil. HL-1 cells were exposed to 2 hours of hypoxia (0.5% $O_{2,}$) alone (H) or followed by 2 hours of reoxygenation (H/R). SNF (0, 1.5, 15 μM) was added at the onset of hypoxia [H+SNF, (H+SNF)/R] or reoxygenation [H/(R+SNF)]. Control cells were treated with similar concentrations of SNF and grown under normal conditions for an identical period of time. The levels of ATP were measured and expressed as percentages relative to controls. Values are expressed as mean ± SEM from three independent experiments. **p<0.0001 (vs. Untreated Hypoxic cells) by One-Way ANOVA.

effect on the rate of ATP replenishment during reoxygenation, regardless of its concentration and time of application.

In summary, we have demonstrated the ability of SNF to protect cardiomyocytes against I/R injury in our model. The addition of SNF at the onset of hypoxia protected HL-1 cells against hypoxia-induced cell death and limited the occurrence of apoptosis during reoxygenation. These effects were maximal with a dose of 15 μM. In contrast, the administration of SNF at the onset of reoxygenation was detrimental to cardiac cells. Here, we report for the first time the effect of SNF on autophagy in a model of myocardial I/R injury. SNF (15 μM) limited the occurrence of autophagy in hypoxic cells. The presence of SNF during hypoxia attenuated the inhibition of autophagy in reoxygenated cells; this effect was maximal with a dose of 1.5 μM. In addition, the presence of SNF during reoxygenation further inhibited autophagy in a dose-dependent manner. While SNF significantly limited the ATP depletion induced by hypoxia, it has no effect on the rate of ATP repletion during reoxygenation.

CHAPTER 4 – DISCUSSION

The pathogenesis of myocardial ischemia-reperfusion (I/R) injury involves complex molecular and cellular mechanisms that have deleterious repercussions on the functional integrity of the heart [9]. The deprivation of nutrients and oxygen (ischemia) is accompanied by a drastic depletion in ATP, acidosis and dysregulation of ionic homeostasis, which leads to an overload of intracellular calcium. While these events lead to the demise of cardiomyocytes, the extent of irreversible damage depends on the severity of the ischemic insult and the onset of reperfusion. Paradoxically, reperfusion exacerbates the cellular instability induced by ischemia. While the reintroduction of oxygen promotes the production of ATP, it also induces the generation of reactive oxygen species by a dysfunctional electron transport chain. The opening of the mitochondrial permeability transition pore induced by oxidative stress and calcium overload further compromises cellular energetics and leads to cell death. The mechanisms of ischemic myocardial death are complex and may be determined by factors such as the location, severity and duration of the ischemic insult. In addition, the degree of ATP depletion, a hallmark of ischemia, is a major determinant in the mode of cell death injured myocytes will undergo. In the infarct core, which is completely deprived in oxygen and energy, myocardial death is marked predominantly by necrosis. On the other hand, cardiac myocytes present in the peri-infarct penumbra, which is hypoxic and undergoes oxidative injury, die mainly by apoptosis. In the remote myocardium cells remain viable, although delayed cell death can occur via both necrosis and apoptosis. The process of autophagy has also been associated with myocardial I/R injury. However, its significance and the nature of its role are unclear.

We have developed an *in vitro* model to study the process of autophagy in the experimental context of myocardial I/R injury. For our model to be relevant to the ischemic

conditions encountered *in vivo*, ischemia was induced with 0.5% and 2.0% O_2. In patients suffering from myocardial infarction, the occlusion of the coronary artery induces nearly complete ischemia in the risk area with subsequent irreversible damage. However, the peri-infarct penumbra of the myocardium still obtains low levels of oxygen from the adjacent area through diffusion. The validity of this model was established by assessing the bioenergetic status of HL-1 cardiac myocytes and the extent of cardiac injury during both hypoxia and reoxygenation. As previously mentioned, myocardial ischemia is characterized by a drastic depletion in ATP. Previous studies have shown that in the heart the ATP levels decrease by 65% and 90% by 15 and 40 minutes of ischemia, respectively [76]. The oxygen supply is completely and abruptly disrupted during myocardial ischemia *in vivo*, whereas in our model the oxygen concentration is progressively decreased as the medium in the dishes equilibrates with the oxygen level present in the chamber (0.5% or 2.0% O_2). Nonetheless, the level of ATP fell dramatically and was only 15% of normal by the end of the 2-hour hypoxic exposure irrespective of the oxygen concentration used (Figure 8A). While reperfusion promotes the replenishment of intracellular ATP stores, this process can be limited by damage caused to the mitochondria. Here, we report that the ATP content of hypoxic myocytes gradually increased during reoxygenation (Figure 8B). However, the restoration of ATP was not fully accomplished. In addition, the rate of ATP repletion was dependent on the degree of hypoxia. HL-1 cells exposed to hypoxia induced with 0.5% O_2 exhibited lower levels of ATP at all time points during reoxygenation than hypoxic myocytes incubated in presence of 2.0% O_2. The slow and incomplete re-energization of myocytes may be attributed to the presence of damaged mitochondria, which may be more prominent under lower hypoxic conditions.

AMPK acts as a sensor of energy and is activated in response to an elevated AMP to ATP ratio. AMPK is composed of three subunits, the catalytic α subunit and two regulatory subunits (β and γ). AMPK activity is regulated by several mechanisms [77-79]. In response to elevated intracellular AMP levels, AMPKα is activated by phosphorylation at Thr172 by the upstream family of AMPK kinases (AMPKK) such as LKB1. In addition, AMPK activity is regulated by conformational changes induced by the binding of AMP to the γ subunit. This interaction maintains AMPK in an activated state by preventing the dephosphorylation of Thr172 of AMPKα by protein phosphatases such as PP2C (protein phosphatase 2C). These regulatory mechanisms are antagonized by nanomolar concentrations of ATP [77-79]. In addition, phosphocreatinine was also shown to inhibit AMPK activity [80]. In our study, the activation status of AMPKα was examined by western blotting as an alternative and complementary indicator of the bioenergetic status of HL-1 cells during H/R. Our results demonstrated that the ATP depletion coincided with enhanced phosporylation of AMPKα phosphorylation in myocytes at all times during hypoxia (Figure 9A). In addition, the intracellular pool of AMPK present in hypoxic myocytes was fully activated. In turn, reoxygenation triggered a renormalization of AMPKα phosphorylation levels in HL-1 cells (Figure 9B). The temporal profile of AMPK activation in cardiomyocytes subjected to I/R has been previously described. Baron and colleagues have observed elevated levels of AMPKK and AMPK activity in isolated working rat hearts subjected to ischemia and in ischemic intact rat hearts. In perfused working rat hearts, AMPKK activity was increased by 3-fold after 1 minute and peaked by 5 to 20 minutes of low-flow ischemia. While the accumulation of phosphorylated AMPKα was less rapid during the first 2 minutes of ischemia, it reached a maximal level after 5 to 20 minutes of ischemia [81]. Furthermore, mouse hearts subjected to 30 minutes of ischemia exhibited elevated levels of

AMPKα activity, which were maintained during the first 30 minutes of reperfusion [82]. This effect was accompanied by a significant decrease in ATP and phosphocreatinine in the ischemic mouse heart. While the ATP level remained low during reperfusion, the phosphocreatinine content was renormalized. Cardiomyocytes rely on phosphocreatinine as a reserve for ATP. The levels of phosphocreatinine have not been evaluated in our model.

While the experimental approach used to mimic ischemia and reperfusion *in vitro* established a repressed energetic state in HL-1 myocytes, it resulted in a mild level of injury. The extent of cardiac injury was assessed by measuring the level of cell death and early apoptosis in HL-1 cells over a time course of several hours (0 to 16 hours post-hypoxia). Cell death was measured by two complementary techniques Trypan blue staining and flow cytometric analysis of AnnexinV-propidium iodide (PI) labeled myocytes. The results indicated that the levels of hypoxia that were used induced a moderate increase in cell death (Figure 10). While cells continued to die during the first hours of reoxygenation, cell death progressively decreased and the percentage of cells undergoing early apoptosis increased concomitantly (Figure 11). Importantly, the extent of cell death was highly dependent on the degree of hypoxia. Hypoxic cardiomyocytes exposed to 0.5% O_2 were more susceptible to death during both hypoxia and reoxygenation than cells exposed to 2.0% O_2. The population of cardiomyocytes pre-exposed to 0.5% O_2 that was undergoing early apoptosis was increased and peaked at a later time point during reoxygenation (4 hours) than cells pre-exposed to 2.0% O_2 (2 hours) (Figure 11B). Interestingly, the rate of ATP replenishment and the activation of early apoptosis occurred faster in HL-1 cells exposed to 2.0% than 0.5% O_2. These results suggest an association between the availability in ATP and the occurrence of apoptosis during H/R. While our studies have focused on early apoptosis, it would be of interest to examine the profile of biochemical or morphological

markers of late apoptosis in order to determine whether the ATP level present in HL-1 cells during reoxygenation is sufficient for the completion of the apoptotic program. The extent of injury to HL-1 cells exposed to I/R has been documented by several groups. For instance, Hamacher-Brady and colleagues have reported a 3-fold increase in Bax activation, a hallmark of apoptosis, in HL-1 cells expressing GFP-Bax exposed to 2 hours of simulated ischemia (anoxia) followed by 5 hours of reoxygenation [57]. In a subsequent study, 2 hours of simulated ischemia (anoxia) followed by 12 hours of reoxygenation resulted in a 5-fold increase in the percentage of apoptotic HL-1 cells with condensed chromatin labeled with Hoechst 33342 [40]. In addition, Yitzhaki and colleagues have demonstrated that the levels of LDH release from HL-1 cells subjected to 2 hours of simulated ischemia (anoxia) were increased by 5-fold in comparison to controls. Subsequent reoxygenation resulted in a 6-fold increase in cells that accumulated propidium iodide uptake by 3 hours [58]. These studies have yielded inconsistent data and the extent of the contribution of necrosis and apoptosis to each phase of I/R remains to be clearly established. In addition, the variability in the experimental context makes a comparison of the levels of cardiac injury elicited by I/R observed in the aforementioned studies and our study difficult. In the aforementioned studies, ischemia was induced in HL-1 cultures in absence of oxygen (anoxia). Therefore, the severity of the ischemic insult, the type of cell death (necrosis, apoptosis) and the methodology used to assess the occurrence of cell death may represent confounding factors in the extent of cell injury observed in these models. In our model, the extent of cardiac injury was confirmed by two different techniques (Trypan blue and PI staining). In addition, Annexin V staining allowed us to refine our analysis of cell death by evaluating the percentage of cells that were actively undergoing apoptosis. Our findings clearly indicated that H/R induced injury of cardiac cells resulting in two types of populations: (i) cells that have been

irreversibly damaged and died, and (ii) cells that had initiated apoptosis during reoxygenation and may still be salavaged. The ratio of these populations was dependent on the severity of the hypoxic insult. Thus, the presence of these populations indicates that our model recapitulated ischemic myocardial injury *in vivo*.

The *in vitro* model of I/R injury that has been described above was considered to be sufficiently faithful to the *in vivo* condition that the role of autophagy could be studied in cardiomyocytes. This model offers the advantage that it focuses on cardiac cells rather than a mixture of myocytes, endothelial cells, smooth muscle cells, fibroblasts and inflammatory cells. This is important because damage to cardiac muscle is the most crucial component of I/R injury. In addition, the use of two hypoxic conditions, rather than anoxia, should predict the response of tissue that surrounds the anoxic focus. The cardiomyocytes in this region are able to receive limited oxygen by diffusion and collateral circulation, and it seems probable that cells in this penumbra are most likely to recover, and understanding their response may lead to better therapies. Aside from facilitating the study of autophagy, the model can be used to evaluate therapeutic maneuvers that may preserve cardiomyocytes during I/R. As an example of this, the protective effect of sildenafil, an inhibitor of cGMP phosphodiesterase 5 (PDE5), has been studied.

Autophagy is involved in the turnover of organelles and cytoplasmic proteins that are in excess or dysfunctional. This multi-step process is initiated with the formation of the phagophore. The latter elongates while engulfing cytoplasmic material targeted for degradation to form the autophagosome. The fusion of the autophagosome with the lysosome leads to the degradation of the autophagic vacuole content by lysosomal hydrolases. The degradation products (amino acids, lipids and sugars) are recycled for ATP production (Figure 2). Autophagy

is an energy-dependent process. ATP is required for the completion of all steps but also for the synthesis and activation (by phosphorylation) of the molecular effectors that compose the autophagy machinery. Autophagy is a double-edge sword as it can promote cell survival and lead to cell death (Programmed Cell Death type 2). Autophagy has been extensively studied in the experimental setting of myocardial I/R injury [40,57]. However, these studies have yielded conflicting results with respect to the magnitude of autophagy and the nature of its role during cardiac I/R injury. In our study, autophagy was examined by assessing the endogenous level of LC3-II by Western blotting in presence of Baf A1, an inhibitor of autophagosomes maturation and lysosomal degradation of LC3-II. We have established the temporal profile of autophagy in HL-1 cells exposed to hypoxia alone or followed by reoxygenation. Our results demonstrated that autophagy was significantly influenced by the severity of the hypoxia. Cardiac cultures exposed to 2.0% O_2 exhibited a level of autophagy that was similar to healthy cells (Figure 12B). On the other hand, autophagy was partially inhibited in hypoxic myocytes exposed to 0.5% O_2 for 2 hours (Figure 12A). Autophagy is an energy-dependent process and surprisingly, hypoxic cells were able to sustain a basal level of autophagy despite the severe depletion of ATP. One role of autophagy is to provide the cell with new source of energy to survive periods of stress. Therefore, it is plausible that the process of autophagy was designed to unfold under drastic energetic constraints. However, the completion of autophagy may be impaired if the bioenergetic status of the cell is below a certain threshold. The modulation of autophagy in HL-1 myocytes during hypoxia appears to be oxygen-dependent. This notion is supported by the observation by Hamacher-Brady and colleagues [57] that autophagy was completely blocked in HL-1 cells subjected to 2 hours of simulated ischemia under anoxic conditions. ATP may also be a limiting factor for the successful completion of autophagy. The validity of this hypothesis was established

by introducing glucose instead of 2-deoxyglucose (2-DG, an inhibitor of glycolysis) in the ischemia buffer. This approach resulted in a significant attenuation of the ATP depletion induced by hypoxia (with 2-DG) (Figure 14) which coincided with an enhancement of autophagy in myocytes exposed to 1 and 2 hours of hypoxia induced with both, 0.5% and 2.0% O_2 (Figure 15). These results indicate that the lack of energy impaired the autophagic response early during hypoxia. The degree of hypoxia had some repercussions on the development of the autophagic response during reoxygenation as well. Severely hypoxic myocytes exhibited low level of autophagy by 2 hours of reoxygenation (Figure 13A). This effect was delayed in cells pre-exposed to 2.0% O_2 as autophagy declined later (4 hours of reoxygenation) (Figure 13B). These results indicate that reoxygenation elicited a partial blockade of autophagy with a timing that was oxygen-dependent. Interestingly, the introduction of glucose during hypoxia resulted in an up-regulation of autophagy, probably by promoting ATP production. However, the reintroduction of nutrients (glucose) to hypoxic cells should have increased the production of ATP and promoted autophagy during reoxygenation as well; however, it failed to do so. One possible explanation for the impairment of the autophagic response during both prolonged hypoxia (0.5% O_2) and reoxygenation is the presence of damaged mitochondria, a pathological hallmark of I/R injury. The damage to the mitochondria during I/R results from the generation of reactive oxygen species (ROS) and the activation of the mitochondrial permeability pore transition. All of these events are predominant during reperfusion. Mitochondria are a major site of ROS production. Ischemia was shown to lead to the production of ROS [83], which is rapidly enhanced by reperfusion. Studies have consistently reported an excessive burst of ROS at the onset of the reperfusion [84-88]. The damage to components of electron transport chain is thought to be responsible for the ROS production during I/R injury. The slow and incomplete recovery of ATP

production that occurs during reoxygenation may result from the presence of dysfunctional mitochondria. In addition, we observed that the re-energization of hypoxic cells occurred at a faster rate in HL-1 cells exposed to 2.0% than 0.5% O_2, suggesting that the extent of mitochondrial damage was greater under low hypoxic conditions (0.5% O_2). Further studies are required to examine the extent of ROS production as well as the integrity and function of mitochondria in HL-1 cells exposed to H/R. Oxidative stress was previously shown to be an inducer of autophagy [89], but we found that autophagy was progressively inhibited during reoxygenation. Considering the interplay between the mitochondria and autophagy, it is likely that the presence of damaged mitochondria can limit autophagy. A recent study has provided strong evidence that the outer membrane of mitochondria can be a source of autophagosomal membranes, at least during starvation [28]. Although it has not been demonstrated that the mitochondrial outer membrane has such a role during ischemia in cardiomyocytes, this possibility cannot be excluded. Cardiac muscle is an aerobic tissue and has a large number of mitochondria while the endoplasmic reticulum, another possible source of autophagosomal membranes, is specialized for the regulation of intracellular calcium concentration. It is possible that hypoxia (0.5% O_2) induces damage to the mitochondria and diminishes the ability of the outer membrane of mitochondria to spawn autophagosomal vesicles. This would ultimately impair the process of autophagy at the initiation step. In addition, cardiac myocytes have a high requirement in energy that is reflected by an abundant mitochondrial content. Therefore, myocytes certainly rely on mitophagy, a process whereby damaged mitochondria are targeted for degradation via autophagy, to maintain their functionality and viability. Hypoxic myocytes exposed to 0.5% O_2 exhibited low level of autophagy and may consequently be unable to eliminate damaged mitochondria through mitophagy. Severe hypoxia may cause a vicious circle

between mitochondria and autophagy where damaged mitochondria may limit the generation of autophagosomal membranes, which in turn, can lead to an inhibition of autophagy (mitophagy) and enhance the presence of damaged mitochondria.

While the lack of ATP and perhaps the increased presence of damaged mitochondria may limit autophagy during H/R, a dysregulation of signaling molecules that modulate autophagy may also contribute to this outcome. Thus, we have explored the activation and expression status of several key regulators of autophagy. Under conditions of nutrient and energy depletion, autophagy is stimulated through inactivation of mTOR, a negative modulator of autophagy. Our results showed that hypoxia induced a dramatic dephosphorylation of mTOR at Ser2448 with respect to control conditions (Figures 16a and 16b). The inhibition of mTOR in hypoxic cardiomyocytes could result from (i) the repression of the PI3-K/Akt pathway as indicated by the low level of Akt phosphorylation and/or (ii) the activation of AMPK in response to low ATP levels. The activation of AMPK was shown to protect cardiac cells against the injurious effect of ischemia and this effect was mediated by an induction of autophagy [46]. To our great surprise, the inhibition of mTOR did not coincide with an enhancement of autophagy in hypoxic cardiomyocytes, suggesting that other factors may thwart the action of mTOR and limit the occurrence of autophagy during hypoxia. The levels of phosphorylation of AMPKα, Akt and mTOR in hypoxic cells were differentially affected by reoxygenation. Western blotting analyses revealed that although reoxygenation induced a decrease in the degree of AMPKα phosphorylation, the latter remained elevated following 2 and 4 hours of reoxygenation (Figure 9B). In addition, the level of phosphorylated mTOR remained normal throughout reoxygenation. Whereas the level of phosphorylation of Akt was elevated during the first 2 hours of reoxygenation and declined to reach control levels by 4 hours of reoxygenation. The positive

regulators of autophagy include Beclin 1 and ERK1/2. Beclin 1 (a homologue of Atg6) is involved in the initiation step of autophagy through its interaction with other proteins (Vps34, Vps15, and Atg14) that compose the Class III PI3-K complex. The interaction of Beclin 1 with the anti-apoptotic protein Bcl-2 inhibits autophagy via disruption of the PI3-K complex. Our results indicated that H/R had no effect on the level of expression of Beclin 1 (Figures 16, 16-Bis, 17 and 17-Bis). However, it is possible that the activity of Beclin 1 on autophagy is inhibited through its interaction with Bcl-2. Further studies are required to test this hypothesis. The modulation of ERK1/2 activation in response to H/R was rather complex. The activation of ERK1/2 in response to amino acid depletion was shown to stimulate autophagy [32]. Surprisingly, the level of phosphorylated ERK1/2 was rapidly and drastically reduced during hypoxia (Figures 16a and 16b). When HL-1 cells were re-supplied with nutrients during reoxygenation, ERK1/2 phosphorylation was enhanced by 1 hour and declined thereafter to levels lower than controls (Figures 17a and 17b). This profile is consistent with a transient activation of ERK1/2 during reoxygenation. Studies have shown that ERK1/2 displayed a distinct temporal profile of activation according to its cellular function. The sustained activation of ERK1/2, which lasts more than 12 hours, is thought to be involved in cell differentiation and cell death. Whereas a transient activation of ERK1/2 is considered to lead to cell proliferation and cell survival. Therefore, the possibility that ERK1/2 could promote the survival of myocytes during reoxygenation cannot be excluded. Altogether, these results indicate a discrepancy between the activation status of these modulators of autophagy and the nature of the autophagic response elicited by reoxygenation as well. The renormalization of Akt and mTOR phosphorylation levels and the activation of AMPK triggered by reoxygenation did not coincide with the profile of autophagy. The disconnect between autophagy and the activation status of its

modulators may have several explanations. First, it is likely that these pathways were modulated to enhance autophagy during H/R but that this effect was countered by other events induced by hypoxia and/or reoxygenation such as the shortage of ATP and oxidative stress. Another possibility is that the lack of phosphorylation of Akt, mTOR and ERK1/2 was part of a chaotic response to ischemic ATP depletion and was not a regulatory event, but instead another form of injury. ATP may be a limiting factor for the activation of these kinases by their upstream effectors depending on their Km for ATP. Further studies are required to establish the profile of activation of upstream modulators and downstream effectors of Akt, mTOR and ERK1/2 in order to discriminate between these possibilities. In addition, it would be of interest to examine the activation profile of the hypoxia inducible factor 1α (HIF-1 α). Zhang and colleagues have shown that the activation of HIF-1 α by hypoxia induces mitophagy in mouse embryonic fibroblasts. In this case, mitophagy promoted cell survival by preventing the production of ROS [30].

Interestingly, the residual autophagic activity present in both, severely hypoxic and reoxygenated myocytes was necessary to maintain their viability. The significance of autophagy during both hypoxia and reoxygenation was demonstrated by a treatment with 3-MA, an inhibitor of PI3-K including the class III PI3-K which is involved in the initiation step of autophagy. The addition of 3-MA to HL-1 cardiac cultures exposed to 2 hours of hypoxia significantly inhibited autophagy (Figure 18) and enhanced hypoxia-induced cell death (Figure 19). The protective role of autophagy during hypoxia was further supported by the observation that the up-regulation of autophagy elicited by adding glucose instead of 2-DG in hypoxic HL-1 cultures coincided with a significant reduction in cell death that nearly reached the level of healthy cells (Figure 20). This approach appears to be a good alternative to the use of rapamcyin.

This drug is commonly used to stimulate autophagy through its inhibitory action on mTOR, a negative modulator of autophagy. However, our results showed that mTOR was completely inhibited in hypoxic cardiomyocytes, thus limiting the use of rapamycin. Interestingly, our results indicate that the up-regulation of autophagy was more beneficial to the most hypoxic cells (i.e. exposed to 0.5% rather than 2.0% O_2). So far, we have no explanation for this result. It is possible that besides the stimulation of autophagy, the introduction of glucose in HL-1 cells during hypoxia triggers additional molecular events that are protective and oxygen-dependent. While glucose limited hypoxia-induced cell death, it promoted the occurrence of early apoptosis in an oxygen-dependent manner. This result suggests that cardiomyocytes that were destined to die by necrosis entered the apoptotic program instead and thus may be salvaged. The presence of 3-MA during the first or last two hours of a 4-hour reoxygenation period induced a further increase in cell death while inhibiting autophagy (Figures 21 and 22). Moreover, the portion of early apoptotic cells during hypoxia was not affected by 3-MA. However, the presence of 3-MA during reoxygenation resulted in an increase or a decrease in the percentage of myocytes undergoing early apoptosis depending on whether cells were exposed to 0.5% or 2.0% O_2, respectively. This effect of 3-MA may be explained by the ability of 3-MA to accelerate the progression of the apoptotic program. In the case of 0.5% O_2, cells that were not apoptotic may have become early apoptotic while myocytes exposed to 2.0% O_2 were already in early apoptosis and progressed through a later stage. Complementary studies aiming at examining markers of late apoptotic stages are required to test this possibility. Altogether, these findings suggested that the autophagic response of HL-1 cells subjected to hypoxia alone or to H/R exerted a protective effect against injury. Given the lack of specificity of 3-MA, which can also inhibit the class I PI3-K, it is possible that the increase in cell death reported here may be due to adverse effects of

the drug. We have shown that under normal conditions 3-MA had very little effect on HL-1 cells viability. The possibility that this effect can be enhanced under stressful conditions cannot be excluded. Nevertheless, the validity of our findings can be partly supported by several studies that have demonstrated the effect of 3-MA on cardiac cell death in an *in vitro* model of I/R injury. Hamacher-Brady and colleagues have documented the cardioprotective effect of autophagy against sI/R on several occasions. They have demonstrated that pre-treatment with 3-MA of HL-1 cells exposed to 2 hours of simulated ischemia followed by 1.5 and 3 hours of reperfusion sensitized HL-1 cardiac cells to sI/R-induced apoptotic cell death [40,57]. In addition, the same effect was observed when autophagy was inhibited by wortmannin, down-regulation of Beclin 1 or over-expression of $Atg5^{K130R}$ (a dominant-negative mutant of Atg5). While these findings suggest that 3-MA may represent a reliable tool to inhibit autophagy, it is essential to confirm our findings by using complementary approaches that target specific effectors involved in the initiation step of autophagy.

Another objective of this project was to evaluate the protective effect of therapeutic agents in relationship to autophagy in our model. We chose to test Sildenafil citrate (SNF) as this inhibitor of PDE5 was shown to exhibit cardioprotective properties in various models of I/R injury. The administration of SNF as a pre-treatment was shown to reduce myocardial infarct size in rabbits [63,90], mice [61], dogs [91], and rats [92]. In addition, the effect of SNF on autophagy has never been reported. SNF is currently used to treat patients with erectile dysfunction and pulmonary hypertension. The inhibition of PDE5, an enzyme that catalyses the degradation of cyclic guanosine monophosphate (cGMP) leads to the accumulation of cGMP, which, in turn, causes vasodilatation. PDE5 is highly expressed in a large variety of tissues including platelets and smooth muscle of the systemic vasculature. The presence of PDE5 in

cardiomyocytes is controversial. However, the expression of PDE5 in the left ventricle and isolated cardiomyocytes from dog [93] and mouse [64] as well as hypertrophied human left and right ventricles [94] has been reported. HL-1 is a murine atrial cell line and we have demonstrated by western blotting that these cells express PDE5 (Figure 23A). Here, we highlighted the complexity of the cardioprotection afforded by SNF against cardiac I/R. To evaluate the therapeutic properties of SNF in our H/R model, we used different doses of the PDE5 inhibitor (1.5 and 15 μM) and different treatment regimens, where SNF was applied at the onset of hypoxia or reoxygenation. The rationale for this approach is that myocardial I/R injury is encountered during several situations including acute myocardial infarction and cardiac surgeries. Therefore, the time/phase of administration of an infarct-reducing drug will vary depending on the clinical context. In acute myocardial infarction patients, the only modality of treatment is to apply the cardioprotective agent at the onset of reperfusion. In contrast, in patients undergoing cardiac surgery, the damage elicited by I/R can be prevented or limited by applying the drug before or at the onset of ischemia (e.g. addition of the drug to the cardioplegic solution). Thus depending on its mechanism of action and dose, a drug may be more efficient in protecting the heart against I/R injury when administered before or at the onset of ischemia or at the onset of reperfusion. We showed that a high dose of sildenafil (15 μM) efficiently protects cardiomyocytes against necrosis following hypoxia as evidenced by the significant decrease in trypan blue positive cells (Figure 24). To our great surprise, no cardioprotection was observed with lower doses (0.15 and 1.5 μM). Paradoxically, SNF (15 μM) slightly induced cell death under normal conditions. These results suggest that the protection of hypoxic cells afforded by SNF may be associated to pathological events triggered by hypoxia. The absence of these events in healthy cells may result in an antagonistic effect of SNF. While we clearly demonstrated that

SNF was beneficial to cardiac cells during hypoxia, the effect of SNF against H/R injury was complex. The addition of SNF at the onset of hypoxia had no significant effect on the level of cell death during reoxygenation. However, it caused a dose-dependent reduction of the percentage of cells actively undergoing early apoptosis during reoxygenation (Figure 25). This result suggests that SNF may either prevent the activation of the apoptotic program and therefore protect cardiac cells against H/R-induced apoptosis, or induce a different type of cell death. The former possibility is more likely as our finding is, to a certain extent, consistent with previous observations made by Das and colleagues. They showed that SNF (1, 10 μM) pre-treatment of isolated mouse ventricular myocytes prior to 40 minutes of simulated ischemia (1.0-2.0% O_2) and 1 or 18 hours of reperfusion reduced both necrosis and apoptosis [64,65]. Here we report for the first time the effect of SNF administration at the onset of reperfusion in cardiac cultures. Strikingly, the addition of SNF at the onset of reoxygenation was detrimental to cardiac cells exposed to H/R. Indeed, SNF markedly enhanced H/R-induced cell death, irrespective of its dose (Figure 25). This effect was concomitant with a decrease in early apoptotic cells, presumably resulting from a rapid progression of the apoptotic program mediated by SNF. These findings clearly demonstrated and emphasized the importance of implementing different treatment regimens when evaluating the efficiency of a cardioprotective agent in the experimental context of I/R. Similar antagonistic effects of SNF, associated to its dose and time of application, on the autophagic response of HL-1 cells exposed to both H/R were observed in this study. We have demonstrated that autophagy was partially inhibited in hypoxic cells and that this effect was enhanced when a high dose of SNF (15 μM) was added at the onset of hypoxia (Figure 26). This effect may stem from two possible phenomena. We have shown a pro-survival role of autophagy during hypoxia. Consistent with this, the inhibition of autophagy mediated by 15 μM SNF should

consequently increase cell death. However, our results demonstrated that the same dose of SNF protected HL-1 cells against hypoxia-induced death. The second explanation, which is more likely, is that the presence of SNF at the onset of hypoxia may trigger a protective mechanism that limits the need of hypoxic cardiac cells to increase their autophagic response. In addition, the same dose of SNF limited the intracellular ATP depletion induced by hypoxia (Figure 28), suggesting that SNF protected cardiomyocytes against the metabolic stress elicited by hypoxia. Altogether, these findings strongly support a cardioprotective effect of SNF against the injurious effects of hypoxia and that this effect is mediated presumably by the ability of SNF to protect the mitochondria. We have also found that depending on the treatment regimen, SNF exerted opposite effects on autophagy in HL-1 cells during reoxygenation. When the drug was added during hypoxia, it increased autophagy and the maximal effect was observed with a dose of 1.5 μM (Figure 27A). In contrast, the addition of the drug at the onset of reoxygenation resulted in an inhibition of autophagy, which was maximal with 15 μM SNF (Figure 27B). We have shown that autophagy was protective during reoxygenation as well. Thus, it is likely that the induction of autophagy in reoxygenated HL-1 cells elicited by the presence of SNF during hypoxia may be beneficial as it coincided with a decrease in early apoptosis. However, the induction of autophagy did not result in an increase of ATP in reoxygenated cells. This is likely due to oxidative damage elicited by the restoration of oxygen. In contrast, the SNF-mediated inhibition of autophagy in reoxygenated cells is likely to be detrimental to cardiomyocytes. Indeed, the inhibition of autophagy coincided with an increase in cell death. These results suggest that SNF may, partly, mediate its effects on H/R injury via autophagy. However, a direct link between the effect of SNF on the association of H/R injury and autophagy remains to be established. This can be achieved by using a gene-based approach to inhibit the initiation of autophagy in HL-1 cells

(e.g. down-regulation of Atg5 or Atg12 expression) and study the effects of SNF on H/R injury in absence of autophagy. Here, we have also shown that SNF had no significant effect on the rate of ATP replenishment during reoxygenation, regardless of its concentration or time of application (Figure 28). Therefore, the cardioprotective and pro-autophagic effects of SNF during H/R may involve other mechanisms.

Our findings strongly indicate that the effects mediated by SNF in HL-1 cells exposed to H/R are highly dependent on its dose. Several groups reported a dose-dependent effect of SNF on I/R-induced cardiac cell death. For example, the administration of low concentrations of SNF (20-50 nM) in isolated heart of rat prior to 20 minutes of ischemia and 30 minutes of reperfusion reduced myocardial infarct size. The cardioprotection was lost with higher concentrations of SNF (200 nM) [95]. In the same line of evidence, isolated perfused mouse hearts subjected to 30 minutes of ischemia and 120 minutes of reperfusion were protected by 0.1 μM SNF when given for 10 minutes at reperfusion. However, lower (0.01 μM) or higher (1 or 10 μM) doses of SNF failed to reduce infarct size [67]. The aforementioned studies have been carried out in intact hearts. However, the presence of other cell types in the heart such as endothelial cells, which express PDE5 makes it difficult to assert that the cardioprotection resulted from the action of SNF in cardiomyocytes.

Importantly, it is likely that the effects of SNF on cardiac cell death, autophagy and cellular energetics in our model system are not PDE5-specific. Indeed, the concentrations used in our study are 10 to 100 times higher than the dose found in the serum of patients of 70 kg body weight after orally taking a 100 mg tablet of SNF (0.7 mg/kg, according to the drug manufacturer Pfizer). While this dose of SNF is known to specifically inhibit PDE5 activity, SNF may inhibit other classes of PDE at higher doses. The cardioprotective effect of SNF was shown to be

mediated by several pathways in cardiac cells (Figure 4). Thus, studies designed to explore these mechanisms are necessary to understand how SNF mediates its effects during cardiac I/R. The endpoint of PDE-5 inhibition is the increase in nitric oxide (NO) production. Although NO production was shown to occur during both ischemia and reperfusion, its role in the pathogenesis of cardiac I/R is highly controversial (for review [96]). Depending on its level of generation, NO can be either protective or detrimental to the heart during I/R. Excessive production of NO was shown to have deleterious effect during I/R as it can lead to mitochondrial dysfunction. Considering the mechanism of action of SNF, it would be of interest to evaluate the level of NO production in cardiomyocytes during I/R. In addition, the effect of SNF was shown to converge on the mitochondria, which plays a crucial role in the pathogenesis of I/R injury. Here, we demonstrated that high doses of SNF efficiently reduced cardiac cell death induced by hypoxia and reduced early apoptosis following H/R, provided the drug is administered at the onset of hypoxia. The administration of SNF at the onset of reoxygenation enhanced the injurious effect of reoxygenation. Therefore, we propose that SNF may represent a good therapeutic agent when as a cardioplegic solution component.

REFERENCES

1 Lloyd-Jones D, Adams RJ, Brown TM, Carnethon M, Dai S, De Simone G, Ferguson TB, Ford E, Furie K, Gillespie C, Go A, Greenlund K, Haase N, Hailpern S, Ho PM, Howard V, Kissela B, Kittner S, Lackland D, Lisabeth L, Marelli A, McDermott MM, Meigs J, Mozaffarian D, Mussolino M, Nichol G, Roger VL, Rosamond W, Sacco R, Sorlie P, Thom T, Wasserthiel-Smoller S, Wong ND, Wylie-Rosett J: Heart disease and stroke statistics--2010 update: A report from the american heart association. Circulation;121:e46-e215.

2 Hochman JS, Choo H: Limitation of myocardial infarct expansion by reperfusion independent of myocardial salvage. Circulation 1987;75:299-306.

3 Sutton MG, Sharpe N: Left ventricular remodeling after myocardial infarction: Pathophysiology and therapy. Circulation 2000;101:2981-2988.

4 Murry CE, Jennings RB, Reimer KA: Preconditioning with ischemia: A delay of lethal cell injury in ischemic myocardium. Circulation 1986;74:1124-1136.

5 Zhao ZQ, Corvera JS, Halkos ME, Kerendi F, Wang NP, Guyton RA, Vinten-Johansen J: Inhibition of myocardial injury by ischemic postconditioning during reperfusion: Comparison with ischemic preconditioning. Am J Physiol Heart Circ Physiol 2003;285:H579-588.

6 Kharbanda RK: Cardiac conditioning: A review of evolving strategies to reduce ischaemia-reperfusion injury. Heart;96:1179-1186.

7 Downey JM, Cohen MV: Why do we still not have cardioprotective drugs? Circ J 2009;73:1171-1177.

8 Moens AL, Claeys MJ, Timmermans JP, Vrints CJ: Myocardial ischemia/reperfusion-injury, a clinical view on a complex pathophysiological process. Int J Cardiol 2005;100:179-190.

9 Turer AT, Hill JA: Pathogenesis of myocardial ischemia-reperfusion injury and rationale for therapy. Am J Cardiol;106:360-368.

10 Ruiz-Meana M, Garcia-Dorado D: Translational cardiovascular medicine (ii). Pathophysiology of ischemia-reperfusion injury: New therapeutic options for acute myocardial infarction. Rev Esp Cardiol 2009;62:199-209.

11 Garcia-Dorado D, Inserte J, Ruiz-Meana M, Gonzalez MA, Solares J, Julia M, Barrabes JA, Soler-Soler J: Gap junction uncoupler heptanol prevents cell-to-cell progression of hypercontracture and limits necrosis during myocardial reperfusion. Circulation 1997;96:3579-3586.

12 Inserte J, Garcia-Dorado D, Hernando V, Barba I, Soler-Soler J: Ischemic preconditioning prevents calpain-mediated impairment of na+/k+-atpase activity during early reperfusion. Cardiovasc Res 2006;70:364-373.

13 Inserte J, Garcia-Dorado D, Hernando V, Soler-Soler J: Calpain-mediated impairment of na+/k+-atpase activity during early reperfusion contributes to cell death after myocardial ischemia. Circ Res 2005;97:465-473.

14 Searle J, Kerr JF, Bishop CJ: Necrosis and apoptosis: Distinct modes of cell death with fundamentally different significance. Pathol Annu 1982;17 Pt 2:229-259.

15 Leist M, Single B, Castoldi AF, Kuhnle S, Nicotera P: Intracellular adenosine triphosphate (atp) concentration: A switch in the decision between apoptosis and necrosis. J Exp Med 1997;185:1481-1486.

16 Anversa P, Cheng W, Liu Y, Leri A, Redaelli G, Kajstura J: Apoptosis and myocardial infarction. Basic Res Cardiol 1998;93 Suppl 3:8-12.

17 Kajstura J, Cheng W, Reiss K, Clark WA, Sonnenblick EH, Krajewski S, Reed JC, Olivetti G, Anversa P: Apoptotic and necrotic myocyte cell deaths are independent contributing variables of infarct size in rats. Lab Invest 1996;74:86-107.

18 Gottlieb RA, Burleson KO, Kloner RA, Babior BM, Engler RL: Reperfusion injury induces apoptosis in rabbit cardiomyocytes. J Clin Invest 1994;94:1621-1628.

19 Fliss H, Gattinger D: Apoptosis in ischemic and reperfused rat myocardium. Circ Res 1996;79:949-956.

20 Freude B, Masters TN, Kostin S, Robicsek F, Schaper J: Cardiomyocyte apoptosis in acute and chronic conditions. Basic Res Cardiol 1998;93:85-89.

21 Freude B, Masters TN, Robicsek F, Fokin A, Kostin S, Zimmermann R, Ullmann C, Lorenz-Meyer S, Schaper J: Apoptosis is initiated by myocardial ischemia and executed during reperfusion. J Mol Cell Cardiol 2000;32:197-208.

22 Scarabelli TM, Gottlieb RA: Functional and clinical repercussions of myocyte apoptosis in the multifaceted damage by ischemia/reperfusion injury: Old and new concepts after 10 years of contributions. Cell Death Differ 2004;11 Suppl 2:S144-152.

23 Cuervo AM: Autophagy: Many paths to the same end. Mol Cell Biochem 2004;263:55-72.

24 Scherz-Shouval R, Shvets E, Fass E, Shorer H, Gil L, Elazar Z: Reactive oxygen species are essential for autophagy and specifically regulate the activity of atg4. EMBO J 2007;26:1749-1760.

25 Bursch W: The autophagosomal-lysosomal compartment in programmed cell death. Cell Death Differ 2001;8:569-581.

26 Yang Z, Klionsky DJ: Eaten alive: A history of macroautophagy. Nat Cell Biol;12:814-822.

27 Hamasaki M, Yoshimori T: Where do they come from? Insights into autophagosome formation. FEBS Lett;584:1296-1301.

28 Hailey DW, Rambold AS, Satpute-Krishnan P, Mitra K, Sougrat R, Kim PK, Lippincott-Schwartz J: Mitochondria supply membranes for autophagosome biogenesis during starvation. Cell;141:656-667.

29 Glick D, Barth S, Macleod KF: Autophagy: Cellular and molecular mechanisms. J Pathol;221:3-12.

30 Zhang H, Bosch-Marce M, Shimoda LA, Tan YS, Baek JH, Wesley JB, Gonzalez FJ, Semenza GL: Mitochondrial autophagy is an hif-1-dependent adaptive metabolic response to hypoxia. J Biol Chem 2008;283:10892-10903.

31 Dou Z, Chattopadhyay M, Pan JA, Guerriero JL, Jiang YP, Ballou LM, Yue Z, Lin RZ, Zong WX: The class ia phosphatidylinositol 3-kinase p110-beta subunit is a positive regulator of autophagy. J Cell Biol;191:827-843.

32 Furuta S, Hidaka E, Ogata A, Yokota S, Kamata T: Ras is involved in the negative control of autophagy through the class i pi3-kinase. Oncogene 2004;23:3898-3904.

33 Pattingre S, Bauvy C, Codogno P: Amino acids interfere with the erk1/2-dependent control of macroautophagy by controlling the activation of raf-1 in human colon cancer ht-29 cells. J Biol Chem 2003;278:16667-16674.

34 Inbal B, Bialik S, Sabanay I, Shani G, Kimchi A: Dap kinase and drp-1 mediate membrane blebbing and the formation of autophagic vesicles during programmed cell death. J Cell Biol 2002;157:455-468.

35 Zalckvar E, Berissi H, Eisenstein M, Kimchi A: Phosphorylation of beclin 1 by dap-kinase promotes autophagy by weakening its interactions with bcl-2 and bcl-xl. Autophagy 2009;5:720-722.

36 Zalckvar E, Berissi H, Mizrachy L, Idelchuk Y, Koren I, Eisenstein M, Sabanay H, Pinkas-Kramarski R, Kimchi A: Dap-kinase-mediated phosphorylation on the bh3 domain of beclin 1 promotes dissociation of beclin 1 from bcl-xl and induction of autophagy. EMBO Rep 2009;10:285-292.

37 Nishida K, Kyoi S, Yamaguchi O, Sadoshima J, Otsu K: The role of autophagy in the heart. Cell Death Differ 2009;16:31-38.

38 Sybers HD, Ingwall J, DeLuca M: Autophagy in cardiac myocytes. Recent Adv Stud Cardiac Struct Metab 1976;12:453-463.

39 Decker RS, Wildenthal K: Lysosomal alterations in hypoxic and reoxygenated hearts. I. Ultrastructural and cytochemical changes. Am J Pathol 1980;98:425-444.

40 Hamacher-Brady A, Brady NR, Logue SE, Sayen MR, Jinno M, Kirshenbaum LA, Gottlieb RA, Gustafsson AB: Response to myocardial ischemia/reperfusion injury involves bnip3 and autophagy. Cell Death Differ 2007;14:146-157.

41 Nishino I, Fu J, Tanji K, Yamada T, Shimojo S, Koori T, Mora M, Riggs JE, Oh SJ, Koga Y, Sue CM, Yamamoto A, Murakami N, Shanske S, Byrne E, Bonilla E, Nonaka I, DiMauro S, Hirano M: Primary lamp-2 deficiency causes x-linked vacuolar cardiomyopathy and myopathy (danon disease). Nature 2000;406:906-910.

42 Tanaka Y, Guhde G, Suter A, Eskelinen EL, Hartmann D, Lullmann-Rauch R, Janssen PM, Blanz J, von Figura K, Saftig P: Accumulation of autophagic vacuoles and cardiomyopathy in lamp-2-deficient mice. Nature 2000;406:902-906.

43 Nakai A, Yamaguchi O, Takeda T, Higuchi Y, Hikoso S, Taniike M, Omiya S, Mizote I, Matsumura Y, Asahi M, Nishida K, Hori M, Mizushima N, Otsu K: The role of autophagy in cardiomyocytes in the basal state and in response to hemodynamic stress. Nat Med 2007;13:619-624.

44 Martinet W, Knaapen MW, Kockx MM, De Meyer GR: Autophagy in cardiovascular disease. Trends Mol Med 2007;13:482-491.

45 Yan L, Vatner DE, Kim SJ, Ge H, Masurekar M, Massover WH, Yang G, Matsui Y, Sadoshima J, Vatner SF: Autophagy in chronically ischemic myocardium. Proc Natl Acad Sci U S A 2005;102:13807-13812.

46 Matsui Y, Takagi H, Qu X, Abdellatif M, Sakoda H, Asano T, Levine B, Sadoshima J: Distinct roles of autophagy in the heart during ischemia and reperfusion: Roles of amp-activated protein kinase and beclin 1 in mediating autophagy. Circ Res 2007;100:914-922.

47 Noh HS, Shin IW, Ha JH, Hah YS, Baek SM, Kim DR: Propofol protects the autophagic cell death induced by the ischemia/reperfusion injury in rats. Mol Cells;30:455-460.

48 French CJ, Taatjes DJ, Sobel BE: Autophagy in myocardium of murine hearts subjected to ischemia followed by reperfusion. Histochem Cell Biol;134:519-526.

49 Osipov RM, Robich MP, Feng J, Liu Y, Clements RT, Glazer HP, Sodha NR, Szabo C, Bianchi C, Sellke FW: Effect of hydrogen sulfide in a porcine model of myocardial ischemia-reperfusion: Comparison of different administration regimens and characterization of the cellular mechanisms of protection. J Cardiovasc Pharmacol 2009;54:287-297.

50 Sala-Mercado JA, Wider J, Undyala VV, Jahania S, Yoo W, Mentzer RM, Jr., Gottlieb RA, Przyklenk K: Profound cardioprotection with chloramphenicol succinate in the swine model of myocardial ischemia-reperfusion injury. Circulation;122:S179-184.

51 Decker RS, Poole AR, Crie JS, Dingle JT, Wildenthal K: Lysosomal alterations in hypoxic and reoxygenated hearts. Ii. Immunohistochemical and biochemical changes in cathepsin d. Am J Pathol 1980;98:445-456.

52 Gurusamy N, Lekli I, Mukherjee S, Ray D, Ahsan MK, Gherghiceanu M, Popescu LM, Das DK: Cardioprotection by resveratrol: A novel mechanism via autophagy involving the mtorc2 pathway. Cardiovasc Res;86:103-112.

53 Lekli I, Ray D, Mukherjee S, Gurusamy N, Ahsan MK, Juhasz B, Bak I, Tosaki A, Gherghiceanu M, Popescu LM, Das DK: Co-ordinated autophagy with resveratrol and gamma-tocotrienol confers synergetic cardioprotection. J Cell Mol Med;14:2506-2518.

54 Mukherjee S, Ray D, Lekli I, Bak I, Tosaki A, Das DK: Effects of longevinex (modified resveratrol) on cardioprotection and its mechanisms of action. Can J Physiol Pharmacol;88:1017-1025.

55 Seglen PO, Gordon PB: 3-methyladenine: Specific inhibitor of autophagic/lysosomal protein degradation in isolated rat hepatocytes. Proc Natl Acad Sci U S A 1982;79:1889-1892.

56 Valentim L, Laurence KM, Townsend PA, Carroll CJ, Soond S, Scarabelli TM, Knight RA, Latchman DS, Stephanou A: Urocortin inhibits beclin1-mediated autophagic cell death in cardiac myocytes exposed to ischaemia/reperfusion injury. J Mol Cell Cardiol 2006;40:846-852.

57 Hamacher-Brady A, Brady NR, Gottlieb RA: Enhancing macroautophagy protects against ischemia/reperfusion injury in cardiac myocytes. J Biol Chem 2006;281:29776-29787.

58 Yitzhaki S, Huang C, Liu W, Lee Y, Gustafsson AB, Mentzer RM, Jr., Gottlieb RA: Autophagy is required for preconditioning by the adenosine a1 receptor-selective agonist ccpa. Basic Res Cardiol 2009;104:157-167.

59 Francis SH, Corbin JD: Molecular mechanisms and pharmacokinetics of phosphodiesterase-5 antagonists. Curr Urol Rep 2003;4:457-465.

60 Kukreja RC, Ockaili R, Salloum F, Yin C, Hawkins J, Das A, Xi L: Cardioprotection with phosphodiesterase-5 inhibition--a novel preconditioning strategy. J Mol Cell Cardiol 2004;36:165-173.

61 Salloum F, Yin C, Xi L, Kukreja RC: Sildenafil induces delayed preconditioning through inducible nitric oxide synthase-dependent pathway in mouse heart. Circ Res 2003;92:595-597.

62 Das A, Ockaili R, Salloum F, Kukreja RC: Protein kinase c plays an essential role in sildenafil-induced cardioprotection in rabbits. Am J Physiol Heart Circ Physiol 2004;286:H1455-1460.

63 Ockaili R, Salloum F, Hawkins J, Kukreja RC: Sildenafil (viagra) induces powerful cardioprotective effect via opening of mitochondrial k(atp) channels in rabbits. Am J Physiol Heart Circ Physiol 2002;283:H1263-1269.

64 Das A, Xi L, Kukreja RC: Phosphodiesterase-5 inhibitor sildenafil preconditions adult cardiac myocytes against necrosis and apoptosis. Essential role of nitric oxide signaling. J Biol Chem 2005;280:12944-12955.

65 Das A, Xi L, Kukreja RC: Protein kinase g-dependent cardioprotective mechanism of phosphodiesterase-5 inhibition involves phosphorylation of erk and gsk3beta. J Biol Chem 2008;283:29572-29585.

66 Das A, Salloum FN, Xi L, Rao YJ, Kukreja RC: Erk phosphorylation mediates sildenafil-induced myocardial protection against ischemia-reperfusion injury in mice. Am J Physiol Heart Circ Physiol 2009;296:H1236-1243.

67 Madhani M, Hall AR, Cuello F, Charles RL, Burgoyne JR, Fuller W, Hobbs AJ, Shattock MJ, Eaton P: Phospholemman ser69 phosphorylation contributes to sildenafil-induced cardioprotection against reperfusion injury. Am J Physiol Heart Circ Physiol;299:H827-836.

68 Claycomb WC, Lanson NA, Jr., Stallworth BS, Egeland DB, Delcarpio JB, Bahinski A, Izzo NJ, Jr.: Hl-1 cells: A cardiac muscle cell line that contracts and retains phenotypic characteristics of the adult cardiomyocyte. Proc Natl Acad Sci U S A 1998;95:2979-2984.

69 Esumi K, Nishida M, Shaw D, Smith TW, Marsh JD: Nadh measurements in adult rat myocytes during simulated ischemia. Am J Physiol 1991;260:H1743-1752.

70 Klionsky DJ, Abeliovich H, Agostinis P, Agrawal DK, Aliev G, Askew DS, Baba M, Baehrecke EH, Bahr BA, Ballabio A, Bamber BA, Bassham DC, Bergamini E, Bi X, Biard-Piechaczyk M, Blum JS, Bredesen DE, Brodsky JL, Brumell JH, Brunk UT, Bursch W, Camougrand N, Cebollero E, Cecconi F, Chen Y, Chin LS, Choi A, Chu CT, Chung J, Clarke PG, Clark RS, Clarke SG, Clave C, Cleveland JL, Codogno P, Colombo MI, Coto-Montes A, Cregg JM, Cuervo AM, Debnath J, Demarchi F, Dennis PB, Dennis PA, Deretic V, Devenish RJ, Di Sano F, Dice JF, Difiglia M, Dinesh-Kumar S, Distelhorst CW, Djavaheri-Mergny M, Dorsey FC, Droge W, Dron M, Dunn WA, Jr., Duszenko M, Eissa NT, Elazar Z, Esclatine A, Eskelinen EL, Fesus L, Finley KD, Fuentes JM, Fueyo J, Fujisaki K, Galliot B, Gao FB, Gewirtz DA, Gibson SB, Gohla A, Goldberg AL, Gonzalez R, Gonzalez-Estevez C, Gorski S, Gottlieb RA, Haussinger D, He YW, Heidenreich K, Hill JA, Hoyer-Hansen M, Hu X, Huang WP, Iwasaki A, Jaattela M, Jackson WT, Jiang X, Jin S, Johansen T, Jung JU, Kadowaki M, Kang C, Kelekar A, Kessel DH, Kiel JA, Kim HP, Kimchi A, Kinsella TJ, Kiselyov K, Kitamoto K, Knecht E, Komatsu M, Kominami E, Kondo S, Kovacs AL, Kroemer G, Kuan CY, Kumar R, Kundu M, Landry J, Laporte M, Le W, Lei HY, Lenardo MJ, Levine B, Lieberman A, Lim KL, Lin FC,

Liou W, Liu LF, Lopez-Berestein G, Lopez-Otin C, Lu B, Macleod KF, Malorni W, Martinet W, Matsuoka K, Mautner J, Meijer AJ, Melendez A, Michels P, Miotto G, Mistiaen WP, Mizushima N, Mograbi B, Monastyrska I, Moore MN, Moreira PI, Moriyasu Y, Motyl T, Munz C, Murphy LO, Naqvi NI, Neufeld TP, Nishino I, Nixon RA, Noda T, Nurnberg B, Ogawa M, Oleinick NL, Olsen LJ, Ozpolat B, Paglin S, Palmer GE, Papassideri I, Parkes M, Perlmutter DH, Perry G, Piacentini M, Pinkas-Kramarski R, Prescott M, Proikas-Cezanne T, Raben N, Rami A, Reggiori F, Rohrer B, Rubinsztein DC, Ryan KM, Sadoshima J, Sakagami H, Sakai Y, Sandri M, Sasakawa C, Sass M, Schneider C, Seglen PO, Seleverstov O, Settleman J, Shacka JJ, Shapiro IM, Sibirny A, Silva-Zacarin EC, Simon HU, Simone C, Simonsen A, Smith MA, Spanel-Borowski K, Srinivas V, Steeves M, Stenmark H, Stromhaug PE, Subauste CS, Sugimoto S, Sulzer D, Suzuki T, Swanson MS, Tabas I, Takeshita F, Talbot NJ, Talloczy Z, Tanaka K, Tanida I, Taylor GS, Taylor JP, Terman A, Tettamanti G, Thompson CB, Thumm M, Tolkovsky AM, Tooze SA, Truant R, Tumanovska LV, Uchiyama Y, Ueno T, Uzcategui NL, van der Klei I, Vaquero EC, Vellai T, Vogel MW, Wang HG, Webster P, Wiley JW, Xi Z, Xiao G, Yahalom J, Yang JM, Yap G, Yin XM, Yoshimori T, Yu L, Yue Z, Yuzaki M, Zabirnyk O, Zheng X, Zhu X, Deter RL: Guidelines for the use and interpretation of assays for monitoring autophagy in higher eukaryotes. Autophagy 2008;4:151-175.

71 Mizushima N, Yoshimori T: How to interpret lc3 immunoblotting. Autophagy 2007;3:542-545.

72 Rubinsztein DC, Cuervo AM, Ravikumar B, Sarkar S, Korolchuk V, Kaushik S, Klionsky DJ: In search of an "Autophagomometer". Autophagy 2009;5:585-589.

73 White SM, Constantin PE, Claycomb WC: Cardiac physiology at the cellular level: Use of cultured hl-1 cardiomyocytes for studies of cardiac muscle cell structure and function. Am J Physiol Heart Circ Physiol 2004;286:H823-829.

74 Russell R, 3rd: Stress signaling in the heart by amp-activated protein kinase. Curr Hypertens Rep 2006;8:446-450.

75 Sekulic A, Hudson CC, Homme JL, Yin P, Otterness DM, Karnitz LM, Abraham RT: A direct linkage between the phosphoinositide 3-kinase-akt signaling pathway and the mammalian target of rapamycin in mitogen-stimulated and transformed cells. Cancer Res 2000;60:3504-3513.

76 Jennings RB, Hawkins HK, Lowe JE, Hill ML, Klotman S, Reimer KA: Relation between high energy phosphate and lethal injury in myocardial ischemia in the dog. Am J Pathol 1978;92:187-214.

77 Corton JM, Gillespie JG, Hawley SA, Hardie DG: 5-aminoimidazole-4-carboxamide ribonucleoside. A specific method for activating amp-activated protein kinase in intact cells? Eur J Biochem 1995;229:558-565.

78 Davies SP, Helps NR, Cohen PT, Hardie DG: 5'-amp inhibits dephosphorylation, as well as promoting phosphorylation, of the amp-activated protein kinase. Studies using bacterially expressed human protein phosphatase-2c alpha and native bovine protein phosphatase-2ac. FEBS Lett 1995;377:421-425.

79 Hawley SA, Selbert MA, Goldstein EG, Edelman AM, Carling D, Hardie DG: 5'-amp activates the amp-activated protein kinase cascade, and ca2+/calmodulin activates the calmodulin-dependent protein kinase i cascade, via three independent mechanisms. J Biol Chem 1995;270:27186-27191.

80 Ponticos M, Lu QL, Morgan JE, Hardie DG, Partridge TA, Carling D: Dual regulation of the amp-activated protein kinase provides a novel mechanism for the control of creatine kinase in skeletal muscle. EMBO J 1998;17:1688-1699.

81 Baron SJ, Li J, Russell RR, 3rd, Neumann D, Miller EJ, Tuerk R, Wallimann T, Hurley RL, Witters LA, Young LH: Dual mechanisms regulating ampk kinase action in the ischemic heart. Circ Res 2005;96:337-345.

82 Russell RR, 3rd, Li J, Coven DL, Pypaert M, Zechner C, Palmeri M, Giordano FJ, Mu J, Birnbaum MJ, Young LH: Amp-activated protein kinase mediates ischemic glucose uptake and prevents postischemic cardiac dysfunction, apoptosis, and injury. J Clin Invest 2004;114:495-503.

83 Becker LB, vanden Hoek TL, Shao ZH, Li CQ, Schumacker PT: Generation of superoxide in cardiomyocytes during ischemia before reperfusion. Am J Physiol 1999;277:H2240-2246.

84 Arroyo CM, Kramer JH, Dickens BF, Weglicki WB: Identification of free radicals in myocardial ischemia/reperfusion by spin trapping with nitrone dmpo. FEBS Lett 1987;221:101-104.

85 Garlick PB, Davies MJ, Hearse DJ, Slater TF: Direct detection of free radicals in the reperfused rat heart using electron spin resonance spectroscopy. Circ Res 1987;61:757-760.

86 Vanden Hoek TL, Shao Z, Li C, Zak R, Schumacker PT, Becker LB: Reperfusion injury on cardiac myocytes after simulated ischemia. Am J Physiol 1996;270:H1334-1341.

87 Zweier JL: Measurement of superoxide-derived free radicals in the reperfused heart. Evidence for a free radical mechanism of reperfusion injury. J Biol Chem 1988;263:1353-1357.

88 Zweier JL, Flaherty JT, Weisfeldt ML: Direct measurement of free radical generation following reperfusion of ischemic myocardium. Proc Natl Acad Sci U S A 1987;84:1404-1407.

89 Scherz-Shouval R, Elazar Z: Ros, mitochondria and the regulation of autophagy. Trends Cell Biol 2007;17:422-427.

90 Bremer YA, Salloum F, Ockaili R, Chou E, Moskowitz WB, Kukreja RC: Sildenafil citrate (viagra) induces cardioprotective effects after ischemia/reperfusion injury in infant rabbits. Pediatr Res 2005;57:22-27.

91 Jamnicki-Abegg M, Weihrauch D, Chiari PC, Krolikowski JG, Pagel PS, Warltier DC, Kersten JR: Diabetes abolishes sildenafil-induced cgmp-dependent protein kinase-i expression and cardioprotection. J Cardiovasc Pharmacol 2007;50:670-676.

92 Das S, Maulik N, Das DK, Kadowitz PJ, Bivalacqua TJ: Cardioprotection with sildenafil, a selective inhibitor of cyclic 3',5'-monophosphate-specific phosphodiesterase 5. Drugs Exp Clin Res 2002;28:213-219.

93 Senzaki H, Smith CJ, Juang GJ, Isoda T, Mayer SP, Ohler A, Paolocci N, Tomaselli GF, Hare JM, Kass DA: Cardiac phosphodiesterase 5 (cgmp-specific) modulates beta-adrenergic signaling in vivo and is down-regulated in heart failure. FASEB J 2001;15:1718-1726.

94 Nagendran J, Archer SL, Soliman D, Gurtu V, Moudgil R, Haromy A, St Aubin C, Webster L, Rebeyka IM, Ross DB, Light PE, Dyck JR, Michelakis ED: Phosphodiesterase type 5 is highly expressed in the hypertrophied human right ventricle, and acute inhibition of phosphodiesterase type 5 improves contractility. Circulation 2007;116:238-248.

95 du Toit EF, Rossouw E, Salie R, Opie LH, Lochner A: Effect of sildenafil on reperfusion function, infarct size, and cyclic nucleotide levels in the isolated rat heart model. Cardiovasc Drugs Ther 2005;19:23-31.

96 Bolli R: Cardioprotective function of inducible nitric oxide synthase and role of nitric oxide in myocardial ischemia and preconditioning: An overview of a decade of research. J Mol Cell Cardiol 2001;33:1897-1918.

ABSTRACT

THE PROCESS OF AUTOPHAGY IN AN *IN VITRO* MODEL OF MYOCARDIAL ISCHEMIA-REPERFUSION INJURY

by

KADIJA ABOUNIT

December 2011

Advisor: Dr. Roy B. McCauley

Major: Pharmacology

Degree: Doctor of Philosophy

Autophagy has been implicated in the pathogenesis of myocardial ischemia-reperfusion (I/R) injury; however, it is not clear whether autophagy is beneficial or detrimental to cell survival. We hypothesized that autophagy is beneficial to cardiomyocytes during I/R and that the paucity of ATP may limit its occurrence. To test this hypothesis, we developed a model of ischemia (hypoxia) involving exposure of HL-1 murine atrial cardiomyocytes to two concentrations of oxygen (0.5% and 2.0%) and 2-deoxyglucose.

Hypoxia, irrespective of the oxygen concentration, caused a dramatic drop in cellular ATP and an increase in the phosphorylation of AMPK (an indication of energy starvation),. The activation of the pro-autophagic AMPK coincided with an inactivation of mTOR and Akt in hypoxic myocytes. While these molecular events would be expected to lead to a stimulation of autophagy, we found that the level of autophagy remained at or near control levels under both conditions of ischemia. Autophagy was limited by the shortage in ATP as the presence of glucose instead of 2-deoxyglucose in the ischemia buffer increased ATP content and stimulated autophagy in hypoxic cells. In addition, cardiac cell death was significantly increased by 2 hours

of hypoxia, to a higher extent with 0.5% oxygen. Importantly, inhibition of autophagy by 3-methyladenine increased hypoxia-induced cell death. In contrast, the stimulation of autophagy mediated by glucose coincided with a significant reduction in cardiac cell death following hypoxia. These results suggest that autophagy is beneficial to HL-1 cells during ischemia, but that the marked reduction in ATP limits the autophagic response. In turn, reoxygenation of hypoxic cells exposed to 0.5% or 2.0% oxygen caused a partial restoration of ATP levels, which coincided with an activation of apoptosis. Importantly, the rates of these events were dependent on the degree of hypoxia. Interestingly, the levels of phosphorylation/activation of AMPK, Akt and mTOR returned to basal levels in reoxygenated cells. However, autophagy was greatly compromised as cells pre-exposed to 0.5% and 2.0% oxygen exhibited low levels of autophagy after 2 and 4 hours of reoxygenation, respectively. As under ischemic conditions, the presence of 3-methyladenine during reoxygenation enhanced cardiac cell death.

In conclusion, we found that autophagy was differentially affected by the degree of hypoxia during both hypoxia and reoxygenation. The residual level of autophagy was essential to protect cardiomyocytes against the injurious effects of both hypoxia and reoxygenation, further validating our hypothesis.

AUTOBIOGRAPHICAL STATEMENT

KADIJA ABOUNIT

EDUCATION

University Denis Diderot, Paris, France
Master of Science, Cell Biology and Physiology (2002)

Wayne State University School of Medicine
Doctor of Philosophy, Pharmacology (2011)

PUBLICATIONS

1. Anagli J, Abounit K, Stemmer P, Han Y, Allred L, Weinsheimer S, Movsisyan A, Seyfried D. Effects of cathepsins B and L inhibition on postischemic protein alterations in the brain. Biochem Biophys Res Commun. 2008 Feb 1; 366(1):86-91.

2. Kuizon E, Pearce EG, Bailey SG, Chen-Scarabelli C, Yuan Z, Abounit K, McCauley RB, Saravolatz L, Faggian G, Mazzucco A, Townsend PA, Scarabelli TM. Mechanisms of action and clinical implications of cardiac urocortin: a journey from the heart to the systemic circulation, with a stopover in the mitochondria. Int J Cardiol. 2009 Nov 12; 137(3):189-94.

3. Anagli J, Han Y, Stewart L, Yang D, Movsisyan A, Abounit K, Seyfried D. A novel calpastatin-based inhibitor improves postischemic neurological recovery. Biochem Biophys Res Commun. 2009 Jul 17; 385(1):94-9.

4. Chen-Scarabelli C, Faggian G, Yuan Z, Tessari M, Rungatscher A, Di Rezze J, Scarabelli GM, Abounit K, McCauley R, Saravolatz L, Mazzucco A, Scarabelli TM. Warm-blood cardioplegic arrest induces selective mitochondrial translocation of protein kinase C epsilon followed by interaction with 6.1 inwardly rectifying potassium channel subunit in viable myocytes overexpressing urocortin. J Thorac Cardiovasc Surg. 2009 Nov; 138(5):1213-21.

5. Yuan, Z., McCauley, R., Chen-Scarabelli, C., Abounit, K., Stephanou, A., Knight, R., Saravolatz, S. F., Saravolatz, L. D., Ulgen, B. O., Scarabelli, G. M., Faggian, G., Mazzucco, A., Saravolatz, L., Scarabelli, T. M., and Barry, S. Activation of Src protein tyrosine kinase plays an essential role in urocortin-mediated cardioprotection. Mol Cell Endocrinol 2010 Aug 30; 325(1-2):1-7.